MODEL DEVELOPMENT FOR LIQUID RESISTANCE-

CONTROLLED REACTIVE ION EXCHANGE AT

LOW SOLUTION CONCENTRATIONS WITH

APPLICATION TO MIXED BED

ION EXCHANGE

By

CARL EUGENE HAUB

Bachelor of Science

Oklahoma State University

Stillwater, Oklahoma

1982

Submitted to the Faculty of the
Graduate College of the
Oklahoma State University
in partial fulfillment of
the requirements for
the Degree of
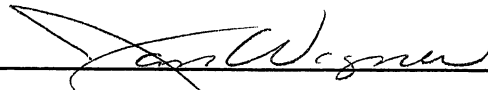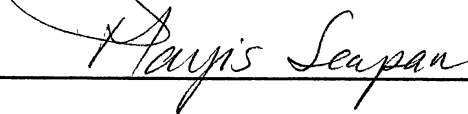MASTER OF SCIENCE
May, 1984

Thesis
1984
H368m
Cop.2

MODEL DEVELOPMENT FOR LIQUID RESISTANCE-
CONTROLLED REACTIVE ION EXCHANGE AT
LOW SOLUTION CONCENTRATIONS WITH
APPLICATION TO MIXED BED
ION EXCHANGE

Thesis Approved:

_____
Thesis Adviser

_____

_____

_____
Dean of Graduate College

1184151

PREFACE

This study involved the extension of current liquid resistance-controlled reactive ion exchange theory to low concentration levels. This necessitated accounting for the effects of water dissociation and electric potential gradients on the rate of exchange. The model was particularly developed for application to mixed bed ion exchange involving more than one type of exchange resin and a neutralization reaction. The ease of utility and applicability to a variety of systems were priorities in the model development.

I would like to express my deepest appreciation to my major adviser, Dr. Gary L. Foutch, for his guidance and helpfulness throughout this study. Grateful acknowledgement is also extended to Dr. Mayis Seapan and Dr. Jan Wagner for serving on the advisory committee and for their technical assistance.

Financial support for this study was gratefully received from the Amoco Foundation. Particular thanks is due Dr. Billy L. Crynes for the assistantship which enabled me to pursue this study.

I would like to express a special thanks to Lynda Mullins for her assistance in preparing this manuscript. I am also grateful for the loving encouragement from my parents, Mr. and Mrs. Fred Haub. Finally, I owe a deep debt

of gratitude to my wife, Rene´, for her encouragement, patience, and understanding throughout the course of this study.

TABLE OF CONTENTS

LIST OF TABLES

LIST OF FIGURES

NOMENCLATURE

a_s	specific surface area, cm^2 area/cm^3 resin
$\bar{C}$	total concentration of fixed ionic groups in resin, meq/cm^3
C_i	concentration of species i, meq/cm^3
$<\bar{C}_i>$	average concentration of species i in resin, meq/cm^3
C_t	total counterion concentration, meq/cm^3
d_p	particle diameter, cm
D	effective system diffusivity, cm^2/s
D_e	effective liquid phase diffusivity, cm^2/s
D_i	diffusion coefficient of species i, cm^2/s
e	fractional pore volume
f_c	volume cation resin/total resin volume
F	Faraday's constant, coulombs/mole
F_1	volumetric flow rate, cm^3/s
h	reaction plane position, δ/δ_r, Equation III-69
I_o	modified Bessel's function of the first order
J_i	ionic flux of species i, meq/s cm^2
k	second order rate constant, cm^3/meq s
k_1	nonionic liquid phase mass transfer coefficient, cm/s
k_1'	ionic liquid phase mass transfer coefficient, cm/s

K_A^B selectivity coefficient for ion B in the solution replacing ion A in the resin phase

$(K_A^B)^m$ corrected selectivity coefficient, Equation II-8

$K_{t,B/A}$ thermodynamic equilibrium constant for ion B replacing ion A, Equation II-7

K_w dissociation constant of water

m_i molality of species i

n total number of exchanging species

N number of mass transfer units, Equation II-53

q column cross-sectional area

q_i mean resin phase concentration of species i, meq/cm^3

Q total resin exchange capacity, meq/cm^3

r radial distance

r_o particle radius, cm

R universal gas constant

R_e particle Reynolds number, $\rho d_p \mu / ((1-\epsilon/\nu))$, dimensionless

R_i ratio of electrolyte to nonelectrolyte mass transfer coefficients

Sc Schmidt number, dimensionless

Sh Sherwood number, dimensionless

t time, s

T absolute temperature, K

T_p throughput parameter, Equation II-59

T_r throughput ratio, Equation II-53

V volume of solution having passed a given column layer, cm^3

V_b bed volume, cm^3

V_f volume of solution fed to column, cm^3

V_s solution volume which is stoichiometrically equivalent to bed capacity, $(V_b\bar{X}/C_t)$, Equation II-53

x_i equivalent fraction of species i in solution

x_i' equivalent fraction of species i based on the column feed concentration, C_i/C_i^f

$\bar{X}$ total ion concentration in resin phase per unit volume of bed, meq/cm^3

$\bar{X}_i$ concentration of species i in resin phase per unit volume of bed, meq/cm^3

y distance normal to solid-liquid interface, cm

y_i equivalent fraction of species i in resin phase

Z distance from column inlet, cm

Z_i ionic charge of species i

Z' column length, cm

Greek Letters

α ratio of exiting to entering ion diffusivities

$\alpha_{B/A}$ separation factor, Equation II-3

γ_i activity coefficient of species i

γ bulk phase concentration ratio

δ liquid film thickness, cm

ε bed void fraction

μ superficial liquid velocity, cm/s

ν	solution viscosity, cp
ξ	dimensionless distance, Equation III-77
ρ_b	bulk density of resin, g/cm^3
τ	dimensionless time, Equation III-78
ϕ	electric potential, ergs/coulomb

Superscripts

bar	refers to resin phase
*	interfacial equilibrium condition
1	cation exchange parameter
2	anion exchange parameter
f	column feed condition
o	bulk phase condition
r	reaction plan condition

Subscript

A	ion exiting the resin phase
B	ion entering the resin phase
c	chloride ion
h	hydrogen ion
i	species i
n	sodium ion
o	hydroxide ion
r	at the reaction plane

CHAPTER I

INTRODUCTION

Mixed bed deionization serves as an economical and convenient way to produce high purity water. In particular, mixed bed ion exchange units have found widespread applications in the power generation and electronic component industries (2,16,20,81,84). However, technological advances in equipment design have necessitated continual reductions in the quantities of corrosion products and dissolved solids allowed in industrial water. In certain cases, current water standards limit the concentrations of dissolved solids to less than one part per billion (84,13). These low impurity requirements have placed stringent demands upon the performance of mixed bed ion exchange units.

Mixed bed deionization requires the use of an intimate mixture of cation and anion exchange resins. Water with the lowest impurity levels is produced in the hydrogen-hydroxide mode of operation (13). The cation resin replaces cations with hydrogen ions, while the anion resin replaces anions with hydroxide ions. The hydrogen and hydroxide ions then combine to form water. This reaction guarantees extremely favorable equilibria of cation and anion exchange throughout the column as the reverse exchange is eliminated. Due to

the strongly favorable equilibria, a high degree of resin utilization and very pure product is obtained (16).

Early investigations of mixed bed column performance in typical deionization systems, having high flow rates and low solution concentrations, concluded that the exchange kinetics were controlled by film diffusion through the liquid layer surrounding the resin bead (9,22,61,62,84). The assumptions of a completely stagnant film surrounding the particle and constant ionic diffusion coefficients were generally made for ion exchange rate investigations. Also, exchange kinetics were assumed to be governed by a linear driving force due to concentration differences across the liquid film. In mixed bed units, the mixture of cation and anion resins was considered as a single salt removing resin. Other assumptions particularly applicable to mixed bed processes included irreversible exchange, no water dissociation, and equal rates of cation and anion exchange.

When these investigations were made, the lowest effluent ion concentrations considered were on the order of several hundred parts per million. For effluent concentrations less than one part per billion, the mixed bed exchange process can no longer be considered irreversible, as the desired effluent ion concentations are the same order of magnitude as the dissociated water ions. With respect to the applied kinetics, Helfferich (32,33) and Kataoka (42) have shown that a neutralization reaction following ion exchange has a pronounced effect on the exchange kinetics.

In this case, the exchange rate may be partially controlled by the diffusion of ions to the reaction front which are not involved in the exchange process. Ionic diffusion coefficients have also been shown to be concentration dependent and vary as the exchange proceeds.

Ion exchange is now modeled using rigorous equations which account for the effect of electric fields induced by diffusing ions. Calculations with these equations have been primarily focused on describing rates of binary ion exchange for single particle or shallow bed systems having simplified boundary conditions. Inherent difficulties also arise due to various authors defining new ion diffusion coefficients or using different reference solutions. These diffusion coefficients are normally supported by a small amount of data, and experimental measurements must be obtained before a variety of systems can be modeled.

Limits of water purity obtainable from mixed bed ion exchange units are established by experimental equilibrium. A model which approaches these limits for mixed bed units has not been established. The purpose of this thesis is to extend the current theory of liquid resistance-controlled reactive ion exchange to low solution concentrations and to develop a practical model for mixed bed ion exchange. For the first time, cation and anion resins in a mixed bed are treated separately. This permits the study of parameters never before modeled for a mixed bed. These parameters include variation of the cation to anion resin ratio,

different exchange rates, and different capacities for the cation and anion resins. Effluent impurity concentrations on the order of one part per billion, accounting for reversible exchange and the dissociation of water molecules, are also modeled. Finally, neutralization reactions occurring at the resin-film interface, within the film, or in the bulk fluid are automatically accounted for based on ion ratios in the bulk liquid phase.

CHAPTER II

LITERATURE REVIEW

Four major topics will be presented here. These topics include ion exchange fundamentals, rate laws, column models, and mixed bed modeling. The first section reviews basic definitions and principles of ion exchange. The material in this section is common among the many articles and books on ion exchange and is presented as discussed by Helfferich (32,34), Kunin (52), and Grimshaw (29), unless otherwise noted. The second section reviews the kinetic theories which have been used to describe rates of ion exchange. These theories are required as rate equations in the column models which are discussed in the third section. The fourth section discusses the status of mixed bed modeling with respect to current ion exchange theory.

Fundamentals of Ion Exchange

Structure and Preparation

Synthetic ion exchange resins are typical gels. Their framework consists of a three-dimensional, cross-linked, hydrocarbon matrix. The matrix contains a surplus charge due to functional groups incorporated into the matrix structure. Cation resins incorporate such functional groups

as sulphonic acid ($-SO_3H$), carboxylic acid ($-CO_2H$), phosphonic acid ($-PO_3H_2$), and arsenic acid ($-AsO_3H_2$) into the matrix. Anion resins incorporate quaternary ammonium, quaternary phosphonium, or tertiary sulphonium groups as the fixed charges within the matrix. The respective major functional groups most widely used in cation and anion resins are the sulphonic acid and quaternary ammonia groups.

The hydrocarbon structure is most often made by copolymerizing styrene and divinylbenzene to produce a hydrocarbon matrix consisting of styrene polymer chains interconnected by divinylbenzene (DVB) molecules (Figure 1).
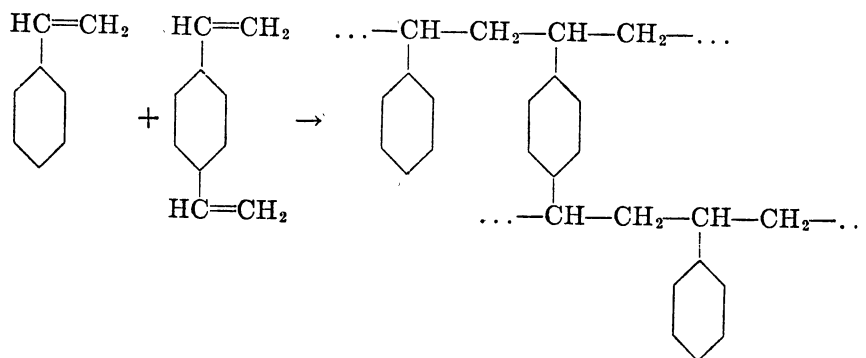
Figure 1. Copolymerization of Styrene
and Divinylbenzene (32)

The amount of DVB in the reaction mixture controls the number of cross-links between the styrene polymer chains. The resin product is often classified by its DVB content.

This classification denotes the mole percent of DVB used in the polymerization reaction mixture instead of the actual mole percent of DVB in the resin product.

During polymerization, the diameters of the resin beads are controlled to close tolerances by using pearl or more recently by jet polymerization techniques (29,32,53). In pearl polymerization, the styrene, DVB, and organic peroxide catalyst are thoroughly mixed and then introduced into a water-stabilizer solution. The organic solution is dispersed into droplets throughout the aqueous phase, and the bead diameters are controlled by regulating the amount of agitation. In jet polymerization, the organic phase is introduced into a static aqueous solution through orifices in the bottom of the tank. This permits much more uniform control of the particle diameters.

Cation and anion resins are then prepared by the respective introduction of acid and base functional groups into matrix (1,70,71,95). Cation resins are prepared by heating the copolymer beads in concentrated sulfuric acid or other sulfonating agents (Figure 2). The preparation of anion resins normally requires more than one step. A typical procedure is to produce a chloromethylated intermediate using a Friedel Crafts reaction followed by amination with trimethylamine (Figure 3).

...—CH—CH₂—CH—CH₂—...
    | |

$\xrightarrow{\text{H}_2\text{SO}_4}$

...—CH—CH₂—CH—CH₂—...
    | |

SO₃⁻H⁺   SO₃⁻H⁺
    ...—CH—CH₂—...
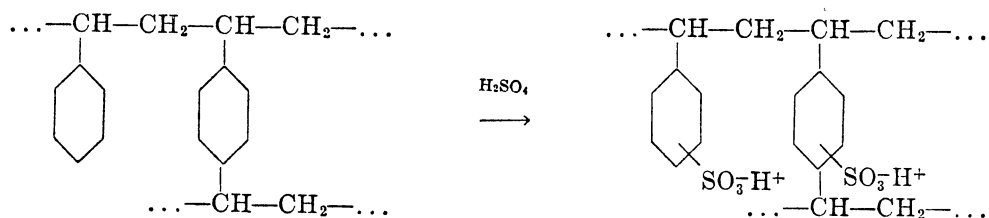
Figure 2.   Typical Production of Cation
            Resin Through Sulfonation (32)

...—CH—CH₂—...
    |

$\downarrow$ ClCH₂OCH₃
             ZnCl₂

...—CH—CH₂—...
    |

          CH₂Cl

N(CH₃)₃ ↙   NH₃ ↘

...—CH—CH₂—...   ...—CH—CH₂—...
    | |

         CH₃
CH₂N⁺—CH₃Cl⁻   CH₂NH₃⁺Cl⁻
         CH₃
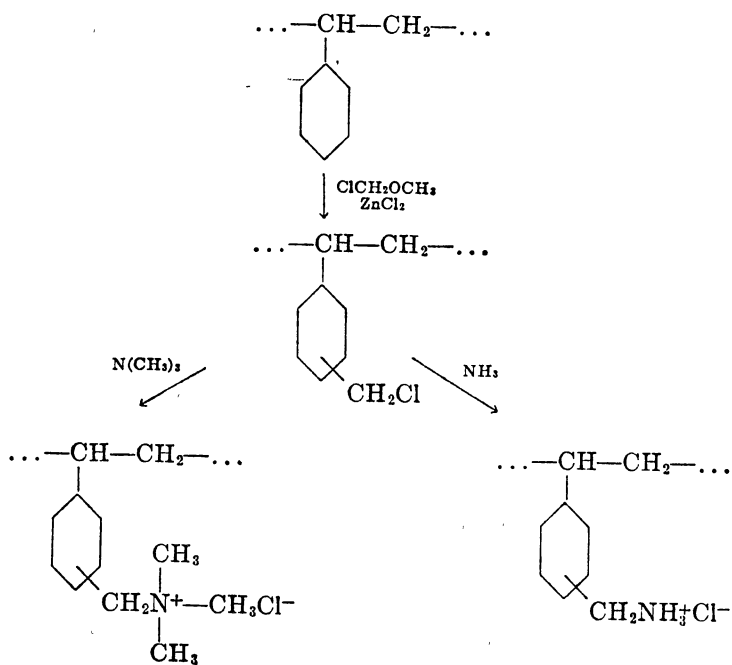
Figure 3.   Typical Production of Anion
            Resin through Amination (32)

Elementary Principles

The characteristic properties of ion exchangers are determined by their unique structure. Due to the preservation of electroneutrality within the exchanger, the positive or negative surplus charge of the matrix structure must be compensated for by a stoichiometrically equivalent number of ions of the opposite charge, called counterions. The counterions are the exchangeable species, as they are free to move about within the exchanger. When one counterion leaves the exchanger, another ion must enter simultaneously to compensate for the potential difference. Thus, ion exchange is a stoichiometric process. Since the number of fixed ions in the matrix determines the exchange capacity, the capacity is generally independent of the nature of the exchanging ions.

When an ion exchange resin is placed in an aqueous solution, sorption or solvent uptake will occur due to the affinity between polar water molecules and fixed changes within the resin matrix. Unlike the matrix of zeolites and other natural crystalline ion exchangers, the resin matrix is flexible, and swelling of the resin will occur with solvent uptake. The amount of swelling is governed by the degree of cross-linking within the resin. Uptake of electrolytes with the solvent increases the number of counterions within the exchanger. However, each counterion sorbed by the exchanger must be accompanied by an ion of the opposite charge called coions. The coions have the same

charge as the matrix of the exchanger and maintain electroneutrality in the system.

Electrostatic forces also play an important role in ion exchange. When a cation exchanger is initially placed in an electrolyte solution, there are large concentration differences between ions in the solid and liquid phases. The initial migration of counterions (cations) into the solution and coions (anions) into the exchanger results in a potential difference between the two phases. This "Donnan potential" repels coions from entering in the exchanger and pulls counterions back into the exchanger. Thus, coions are almost completely excluded from the exchanger while counterion exchange takes place.

Equilibria and Selectivity

When an ion exchanger is placed in an electrolyte solution, equilibrium will be obtained after a certain time. At this point, the ion exchanger and solution contain both of the exchanging ions. However, the concentration ratio of the two ions will not be the same in both phases. This preference for one ion over another is known as selectivity. Selectivity is affected by the nature of the counterion, the nature of the fixed charges in the matrix, the degree of ion exchanger saturation, the total solution concentration, and external forces such as temperature and pressure. As discussed by Helfferich (32), the ion exchanger prefers the counterion that has the higher valence, smaller equivalent

volume, greater polarity, and the stronger association with fixed ionic groups in the matrix.

Ion exchange equilibria and selectivity for exchange between two ions (binary exchange) at a given temperature and total solution concentration can be conveniently expressed by the ion exchange isotherm. A typical isotherm for the exchange of ion A in the resin phase for ion B in the solution phase is shown in Figure 4. Curve 1 represents a preference for ion B (favorable equilibrium), and Curve 2 represents a preference for ion A (unfavorable equilibrium). Normally, the compositions in the solution phase (x_i) and resin phase (y_i) are represented by equivalent fractions defined by

$$x_B = \frac{z_B \, m_B}{\Sigma z_i \, m_i} \qquad \text{(II-1)}$$

and

$$y_B = \frac{z_B \, \bar{m}_B}{\Sigma z_i \, \bar{m}_i} \qquad \text{(II-2)}$$

where

z_i = ionic charge of species i

m_i = molality of species i in the solution phase

$\bar{m}_i$ = molality of species i in the resin phase
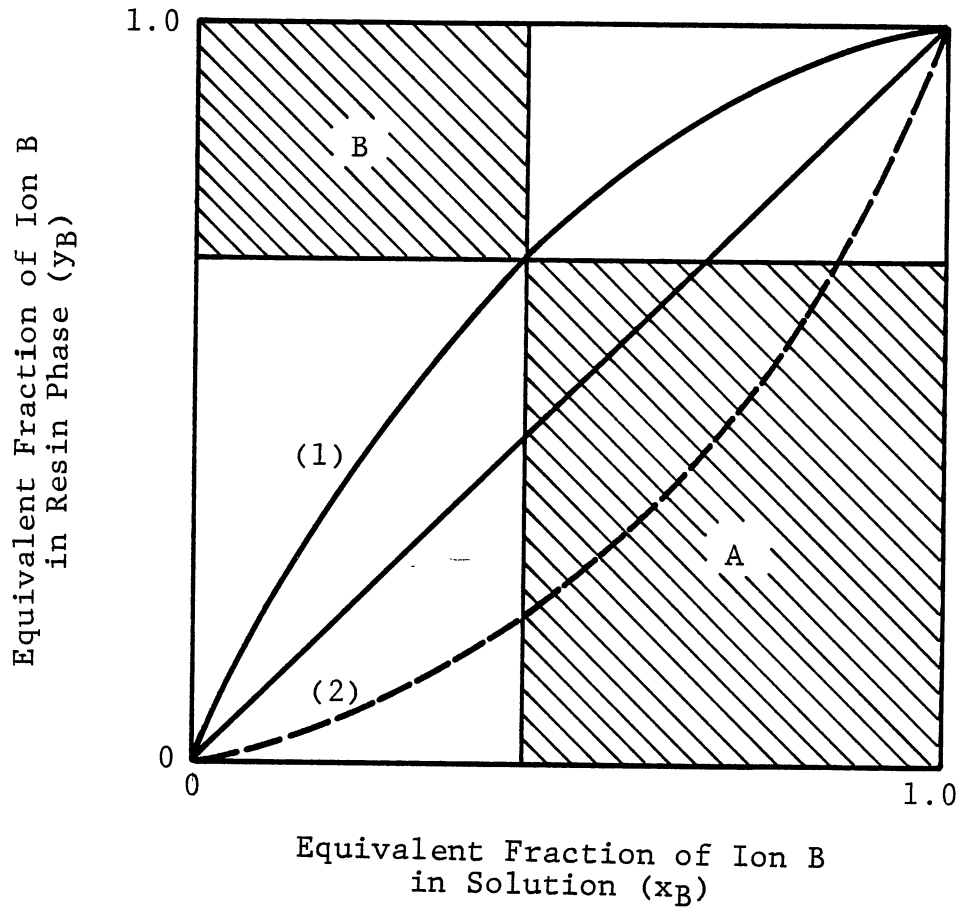
Figure 4. Typical Ion Exchange Isotherm

The summations are carried out over all counterion species. If an ion exchanger does not favor one ion over the other, then the isotherm is linear and is shown by the diagonal in Figure 4.

Selectivity is also expressed by the separation factor. The separation factor ($\alpha_{B/A}$) is the quotient of the concentration, molality, or equivalent ion fraction ratios of the exchanging ions in the resin and solution phases.

$$\alpha_{B/A} = \frac{\bar{C}_B/\bar{C}_A}{C_B/C_A} = \frac{\bar{C}_B}{\bar{C}_A}\frac{C_A}{C_B} = \frac{\bar{m}_B}{\bar{m}_A}\frac{m_A}{m_B} = \frac{y_B}{y_A}\frac{x_A}{x_B} \qquad \text{(II-3)}$$

where

C_i = concentration of species i in the solution phase, meq/cm^3

$\bar{C}_i$ = concentration of species i in the resin phase, meq/cm^3

The separation factor can be directly obtained from the ion exchange isotherm. The separation factor for any solution and resin phase composition is given by the ratio of Area B to Area A, as shown in Figure 4.

The stoichiometric exchange between the counterions A in the resin phase and B in the solution phase may be written as

$$z_B(\overline{A})^{z_A} + z_A(B)^{z_B} \rightleftharpoons z_A(\overline{B})^{z_B} + z_B(A)^{z_A} \qquad \text{(II-4)}$$
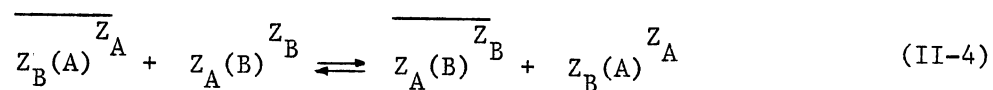
for both cation and anion exchange. The selectivity coefficient (K_A^B) is the mass action relationship written for the preceding reaction according to a particular choice of concentration units. For molar units of concentration

$$K_A^B = \frac{(\bar{c}_B)^{z_A}(c_A)^{z_B}}{(\bar{c}_A)^{z_B}(c_B)^{z_A}} \tag{II-5}$$

For exchange of ions of equal valence, the selectivity coefficients written in terms of molality (m), molarity (c), and equivalent ionic fractions (x) are equal and related to the separation factor by

$$(K_A^B)_m = (K_A^B)_c = (K_A^B)_x = (\alpha_{B/A})^{z_A} \tag{II-6}$$

The selectivity coefficient is often nearly constant at a given total ion concentration for binary exchange (34,65,89).

The thermodynamic equilibrium constant for Equation II-4 includes resin and solution phase activity coefficients. The selectivity coefficient and thermodynamic equilibrium constant are related by

$$K_{t,B/A} = K_A^B \frac{(\bar{\gamma}_B)^{z_A}(\gamma_A)^{z_B}}{(\bar{\gamma}_A)^{z_B}(\gamma_B)^{z_A}} \tag{II-7}$$

where

$K_{t,B/A}$ = thermodynamic equilibrium constant

γ_i = activity coefficient of species i

$K_{t,B/A}$ is difficult to obtain because an estimation method for resin phase activity coefficients has not been established (47). A corrected selectivity coefficient which does not contain the effect of the resin phase activity coefficient is defined as

$$(K_A^B)^m = K_{t,B/A} \frac{(\bar{\gamma}_A)^{z_B}}{(\bar{\gamma}_B)^{z_A}} = \frac{(\bar{C}_B)^{z_A}(C_A)^{z_B}}{(\bar{C}_A)^{z_B}(C_B)^{z_A}} \frac{(\gamma_A)^{z_B}}{(\gamma_B)^{z_A}} \qquad \text{(II-8)}$$

The liquid phase activity coefficients may be evaluated with the Debye-Hückel equation. For dilute solutions, the liquid phase activity coefficients are assumed to be unity, and the selectivity coefficient is used in ion exchange calculations (34,49,65).

Several methods have been reported to express the equilibrium relations for ternary ion exchange. Dranoff et al. (17,73) assumed that the influence of the third ion was negligible and expressed the equilibrium relationships by three binary pairs. The effect of the third ion has also been accounted for by graphical procedures on ternary diagrams (81). These calculations cannot be extended to systems with more than three exchanging ions. Kataoka et al. (47) showed that equilibrium relations in multicomponent systems could be evaluated by using the corrected selectivity coefficients for each of the binary ion pairs (Equation II-8). This method must be used cautiously for if any one of the corrected selectivity coefficients for the

binary pairs is not constant, then this method cannot be used.

The selectivity coefficients, or separation factors as described above are used to determine interfacial concentrations and to set boundary conditions in the ion exchange rate expressions. These relations do not appear explicity in the rate expressions unless large gradients of activity coefficients exist during the exchange process. If these gradients do exist, then the partial of the selectivity coefficient with respect to the concentration of the counterion leaving the exchanger is required in the flux equations.

Capacity

Capacities of ion exchangers are defined in numerous ways. Thus, one must be certain of the definition of a particular capacity before using that value. The nature of the fixed ionic groups within the matrix affects the capacity of an exchanger as well as the total number of functional groups. If the functional groups are weak acids or bases, then these groups will not be ionized and will contribute to the surplus framework charge in high and low pH solutions respectively.

The scientific or weight capacity is defined as the number of equivalents of fixed matrix ions per unit weight of the exchanger and is used primarily for resin characterization. This capacity is determined for dry resin in a

particular ionic form. The hydrogen form is used for cation resins, and the chloride form is used for anion resins. Typical values for exchange resins are approximately 55 milliequivalents per gram (15).

The volume capacity is much more useful for design applications. This capacity is the number of equivalents of fixed ions per liter of packed bed with the resin in a fully swollen state and a particular ionic form. Typical values for resins are approximately 0.5-1.5 equivalents per liter of bed.

The apparent capacity refers to the number of ions which can be exchanged from a solution with an exchange resin in a particular form. This capacity includes effects due to solution and electrolyte sorption, ionic association, solution pH, and any other interactions. When electrolyte sorption is negligible and the fixed functional groups are completely ionized, the apparent capacity approaches the scientific or weight capacity, and the apparent capacity is essentially constant.

Rate Laws of Ion Exchange

Rate Controlling Step

Theoretical ion exchange kinetic rate laws are difficult to apply to other than simple ideal systems with constant or well behaved boundary conditions. Proposed rate theories have been confirmed using single particle batch studies. Assumptions made in the derivation of the

following rate laws include isothermal systems and uniform spherical particles of equal size. Also, the effects due to particle swelling and activity coefficient gradients are neglected (6,32,34,92).

Boyd et al. (6) were the first to show that the two major rate controlling steps of ion exchange are particle and film diffusion. Since these two steps occur in series, the slower of the two will be the controlling resistance to exchange. The following criterion for determining the controlling resistance has been theoretically derived based on half lives of exchange particles (32). For

$$\frac{\bar{C}_t \, \bar{D} \, \delta}{C_t \, D \, r_o} \, (5 + 2 \, \alpha_{A/B}) \ll 1 \qquad \qquad (II-9)$$

where

C_t = total counterion concentration (meq/cm^3)

D = effective system diffusivity (cm^2/s)

δ = film thickness (cm)

r_o = particle radius (cm)

Bar superscript denotes resin phase

particle diffusion is the controlling resistance. For

$$\frac{\bar{C}_t \, \bar{D} \, \delta}{C_t \, D \, r_o} \, (5 + 2 \, \alpha_{A/B}) \gg 1 \qquad \qquad (II-10)$$

film diffusion is the controlling resistance.

The diffusion coefficient within the exchange particle ($\bar{D}$) must be known to use Equations II-10 and II-11. The rate of

diffusion within ion exchangers is not as fast as in solutions due to framework hinderance, tortuous paths, impedance of large ions, and ionic interactions with fixed functional groups (55,58,63). Internal diffusion coefficients have not been predicted theoretically but have been related to diffusion coefficients in aqueous solutions. Mackie et al. (59) derived the following relationship

$$\bar{D} = D(e/(2-e))^2 \tag{II-11}$$

where

e = fractional pore volume

by assuming no blocked or dead end pores. Equation II-11 is not accurate for quantitative work. Recently, Kataoka et al. (41) have published a much more accurate correlation based on the degree of resin cross-linking, external solution concentration, gram equivalent weight of the resin, and the ion diffusion coefficients at infinite dilution in water. Precise internal diffusion coefficients may only be obtained by tracer analysis (32,34).

In the following discussion of rate theories, a binary exchange between counterions A and B will be considered. The counterion moving from the exchanger will be designated as species A and the counterion moving into the exchanger as species B. The coion in solution will be designated as species Y (Figure 5).
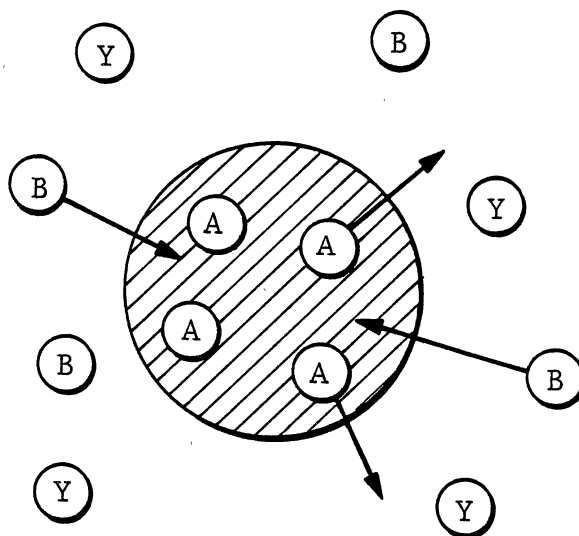
Figure 5. Typical Binary Ion
Exchange System

Particle-Diffusion Control

Due to the preservation of electroneutrality within the particle, the fluxes of ions A and B are rigidly coupled and the total counterion concentration (in equivalents) must remain constant and equal to the concentration of fixed ionic groups (32).

$$z_A \ \bar{C}_A \ + \ z_B \ \bar{C}_B \ = \ \bar{C} \qquad\qquad (II-12)$$

where

$\bar{C}$ = total concentration of fixed ionic groups in resin
    (meq/cm^3)

and

$$Z_A \ \bar{J}_A + Z_B \ \bar{J}_B = 0 \qquad \text{(II-13)}$$

where

$$J_i = \text{flux of species i (meg/sec cm}^2)$$

Early exchange theories used Fick's first law with a constant diffusion coefficient as the flux equation with the same $\bar{D}$ in both $\bar{J}_A$ and $\bar{J}_B$ equations (6,36,48).

$$\bar{J}_B = -\bar{D} \ \text{grad}(\bar{C}_B) \qquad \text{(II-14)}$$

Helfferich first introduced the Nernst-Plank equation for ion exchange applications (30,74). He included an additional term in Fick's first law to account for the ionic effect on the exchange rate

$$\bar{J}_B = -\bar{D}_B \ \text{grad} \ \bar{C}_B - \bar{D}_B \bar{C}_B (Z_B F/RT) \text{grad}(\phi) \qquad \text{(II-15)}$$

where

F = Faraday's constant (coulombs/mole)

R = universal gas constant (ergs/mole K)

ϕ = electrical potential (ergs/coulomb)

D_i = diffusion coefficient of ionic species (cm^2/s)

T = absolute temperature, K

The combination of Equations II-12 and II-13 with the
Nernst-Plank equation for both species A and B and the
elimination of $\bar{J}_A$ yields

$$\bar{J}_B = -\bar{D} \text{ grad } \bar{C}_B \tag{II-16}$$

where

$$\bar{D} = \bar{D}_A \bar{D}_B (z_A^2 \bar{C}_A + z_B^2 \bar{C}_B)/(z_A^2 \bar{C}_A \bar{D}_A + z_B^2 \bar{C}_B \bar{D}_B) \tag{II-17}$$

Thus, the effective diffusion coefficient ($\bar{D}$) is not
constant but depends on the concentrations of A and B within
the exchanger which vary during the exchange process. As
the concentration of either ion becomes negligible, the
interdiffusion coefficient approaches the diffusion
coefficient of that ion.

Combination of Equations II-16 and II-17 with the
continuity equation

$$\partial \bar{C}_B / \partial t = -\text{div } \bar{J}_B \tag{II-18}$$

where

t = time (sec)

allows calculation of the concentration profile and exchange
rate within the exchanger upon integration with the proper
boundary conditions (34). Tabulated solutions of Equations
II-16 and II-18 with the most simple boundary conditions can
be found as referenced by Helfferich (32). Due to the
difficulty of solving Equation II-18 for complex boundary

conditions such as exist in exchange columns, simplified differential rate equations of the general form

$$- \partial \langle \bar{C}_B \rangle / \partial t = f(C_A, C_B, \langle \bar{C}_A \rangle, \langle \bar{C}_B \rangle \ldots) \tag{II-19}$$

where

$$\langle \bar{C}_i \rangle = \text{average resin phase concentration of species i}$$
$$(\text{meq}/\text{cm}^3)$$

have continued to be used since they can be easily integrated. Two forms of Equation II-19 are common. These are the second order rate law (27,31,82,92)

$$- \partial \langle \bar{C}_B \rangle / \partial t = k(C_A \langle \bar{C}_B \rangle - \alpha_{B/A} C_B \langle \bar{C}_A \rangle) \tag{II-20}$$

where

$$k = \text{second order rate constant}$$

and the quadratic driving force (90)

$$\frac{\partial \langle \bar{C}_B \rangle}{\partial t} = \frac{\bar{D} \pi^2}{r_o} \frac{\bar{C}_B^{*2} - \langle C_B \rangle^2}{2 \langle \bar{C}_B \rangle} \tag{II-21}$$

where

$$* = \text{interface equilibrium condition}$$

As discussed by Helfferich (32,34), equations of the form of Equation II-19 are fundamentally wrong, as they suggest that the momentary rate of exchange is a function of the bulk solution concentrations and the average

concentrations within the particle. However, the rate of exchange is actually dependent upon the concentration profiles within the particle and thus the history of the exchange particle. No matter how complex, rate equations of the type of Equation II-19 will never be able to account for variations in the exchange rate due to actions such as interruption of a column feed or removal of an exchanger from its surrounding solution. In these instances, concentration profiles within the exchanger may level out while the average concentration within the exchanger remains constant.

Film Diffusion

Film diffusion is more complex than particle diffusion as the effects of coions within the film and hydrodynamic models must be considered. The theoretical models for film diffusion have been developed using the Nernst film concept (64). The particle is assumed to have a completely stagnant film of thickness δ surrounding it with a sharp boundary separating the film layer and bulk solution. Curvature of the film is neglected, and the film thickness is based on the Sherwood number

$$\delta = 2 \, r_o / Sh \qquad (II-22)$$

where

Sh = Sherwood number

The flux across the film is assumed to be determined as a function of the boundary concentrations (32). The coion Y must also be considered in the conditions of electroneutrality and coupled exchange rates.

$$C_A + C_B = C_Y \qquad\qquad (II-23)$$

and

$$J_A + J_B = J_Y = 0 \qquad\qquad (II-24)$$

Three basic theoretical approaches have been widely used to determine the ionic fluxes. Boyd et al. (6) again applied Fick's first law of diffusion with a constant diffusion coefficient as they did for particle diffusion. Adamson (4) suggested that each ion obey Fick's first law of diffusion but with each ion having its own diffusion coefficient. This theory leads to a coion flux into the exchanger, which is incompatible with experimental results and theory (34). Helfferich again suggested application of the Nernst-Plank equation (32). All three of the above approaches have been used to match particular experimental results with theory (32).

Application of the Nernst-Plank equation to film diffusion has shown excellent qualitative agreement with experimental data. However, the quantitative agreement has not always been good (42,68,79,87). The film diffusion application of the Nernst-Plank equation, as suggested by Schlögl and Helfferich (75), was originally proposed to

demonstrate the effects of the ionic potential in film diffusion. An accurate description of film diffusion-controlled exchange with the Nernst-Plank equations requires the use of a hydrodynamic film model other than the Nernst film concept to account for the effect of velocity gradients in the film (34).

David et al. (68,87,88) and Kataoka et al. (38,40) have investigated the Nernst (64), Danckwert penetration (12), Acrivos boundary layer (3), and hydraulic radius (39,40) film models in conjunction with the Nernst-Plank equations. Both authors used the correlations of Carberry (10) and Kataoka (40) to obtain packed bed mass transfer coefficients excluding ionic effects. These coefficients account for the bed geometry and flow field effects on the mass transfer rate.

Carberry's equation,

$$k_1 = 1.15 \frac{\mu}{\varepsilon} (S_c)^{-2/3} (R_e)^{-1/2} \qquad (II-25)$$

where

k_1 = nonionic liquid phase mass transfer coefficient (cm/s)

ε = bed void fraction

μ = superficial liquid velocity (cm/s)

S_c = Schmidt number

R_e = Reynolds number

was developed by the application of boundary layer theory for a flat plate to a fixed bed under the assumption that

the boundary layer develops and collapses over a distance approximately equal to one particle diameter. Predicted values and experimental data deviate significantly for Reynolds numbers below 10. Kataoka's equation,

$$k_1 = 1.85 \frac{\mu}{\epsilon} \left(\frac{\epsilon}{1 - \epsilon}\right)^{+1/3} (S_c)^{-2/3} (R_e)^{-2/3} \qquad \text{(II-26)}$$

is based on the hydraulic radius model. In this model, the mass transfer is assumed to take place between liquid flowing through a pipe and the inner surface of the pipe. The steady laminar flow velocity profile within the pipe is instantly formed and collapsed over a distance equivalent to twice the hydraulic radius of a particle. Kataoka's equation was developed for the low Reynolds number region. Pan and David (67) used Kataoka's correlation for Reynolds numbers below 20 and Carberry's equation otherwise.

The effects of ionic interactions were accounted for by defining a ratio of electrolyte to nonelectrolyte mass transfer coefficients, or by a similarly defined effective diffusivity. David et al. compared the Nernst, Danckwert penetration, and boundary layer film models. In the various studies, an R_i factor was defined as the ratio of electrolyte to nonelectrolyte mass transfer with equations II-14 and II-15 as the respective constitutive equations.

$$R_i = \frac{-D_i \left\{\frac{\partial C_i}{\partial y} + \frac{Z_i C_i F}{RT} \frac{\partial \Phi}{\partial y}\right\} \; y=0}{-D_i \left\{\frac{\partial C_i}{\partial y}\right\} \; y=0} = \frac{k_1'}{k_1} \qquad \text{(II-27)}$$

where

y = distance normal to solid liquid interface (cm)

k_1 = ionic liquid phase mass transfer coefficient (cm/s)

Since the numerator and denominator of Equation II-27 give the respective ionic fluxes, R_i is equal to the ratio of the electrolyte to nonelectrolyte mass transfer coefficients. Once k_1 and R_i are known, the rate of exchange accounting for ionic effects can be determined using Equation II-28.

$$\frac{\partial q_i}{\partial t} = k_1 R_i a_s C_t (x_i^o - x_i^*)$$

(II-28)

where

q_i = mean resin phase concentration of species i (meq/cm^3 resin)

a_s = specific surface area, cm^2 area/cm^3 resin

o = superscipt denotes value in bulk phase

The R_i factor is determined by integrating the respective film model equations with the appropriate boundary conditions. Only the case using the Nernst film model has an analytical solution. The resulting R_i factor is dependent on the concentrations of species i at the solution-resin interface and in the bulk solution phase. For experiments with a single exchange particle, the bulk solution concentration is normally held constant and the R_i factor for the process is a single curve. For column operations, both concentration variables continually change, and a

series of R_i curves, as shown in Figure 6, are required to describe the exchange rate.

Kataoka compared the hydraulic radius and Nernst film models (40). Ionic effects were accounted for by defining an effective ionic liquid phase diffusivity (D_e). This effective diffusivity is related to the ratio of ionic to nonionic mass transfer coefficients by

$$\left\{\frac{D_e}{D_B}\right\}^{2/3} = \frac{k_1'}{k_1} \tag{II-29}$$

The relationship between R_i, as defined by David, and D_e, as defined by Kataoka, is obtained from equations II-27 and II-29.

$$R_i = \left\{\frac{D_e}{D_B}\right\}^{2/3} \tag{II-30}$$

With D_e known, the rate of exchange can be determined using Equation II-31.

$$\frac{\partial q_i}{\partial t} = k_1 \left\{\frac{D_e}{D_B}\right\}^{2/3} a_s \, C_t \, (x_i^o - x_i^*) \tag{II-31}$$

Similar to the R_i factor, D_e has the same dependent variables and has an analytical solution for the Nernst film case only. Diagrams showing the relationship between D_e and the ion solution concentrations have the same form as Figure 6. Both R_i and D_e are reduced as the ion concentrations in the bulk phase approach zero.
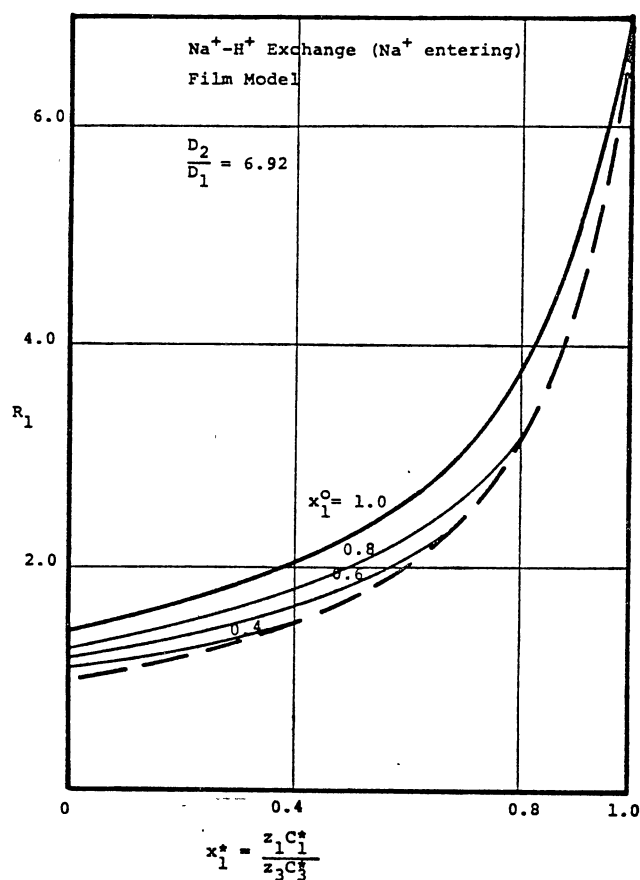
Figure 6. Variation of R_i as Ion
Exchange Progresses (88)

David and Kataoka obtained very similar experimental results. David claimed that the boundary layer model was the correct model for packed beds, whereas Kataoka suggested the hydraulic radius model to be the most appropriate model. From respective published figures, both models have differences between experimental and predicted values of less than two percent. Results from these models showed errors in studies based on the static (Nernst) film model to be in the

range of 20-30 percent (67,38). However, the ionic mass transfer coefficients in these studies were calculated by

$$k_1^{'} = D_e/\delta \qquad \text{(II-32)}$$

which required an estimate of the liquid film thickness and did not account for any effects on the mass transfer due to fluid flow around the particles. Only during the rigorous derivation of the hydraulic radius model did Kataoka (40) develop the relationship given in Equation II-29. This allowed the use of packed bed mass transfer coefficient correlations (Equations II-25 and II-26) to account for fluid flow effects on the exchange rate. Ion exchange rate predictions, using the film model, were now found to differ from experimental results by less than five percent for exchange systems of ions having equal valence and a favorable exchange equilibrium (40). The maximum error found was approximately 16 percent for unfavorable exchange systems.

Simplified differential equations have once again continued in use due to their simplicity of integration (84). In particular, the simple linear driving force concept has often been used (25,35,92).

$$\frac{\partial \bar{C}_B}{\partial t} = k_1^{'} a_s (C_B^o - C_B^*) \qquad \text{(II-33)}$$

and

$$k_1^{'} = D/\delta \qquad \text{(II-34)}$$

Some type of average system diffusivity (D), which is between the diffusion coefficients for the two exchanging species, is normally used. In some cases, the linear driving force model has given quantitative results comparable to those given by the Nernst-Plank equation (42,68,79). For two cases, the linear driving force concept gives the identical flux equations as the Nernst-Plank equation combined with the stagnant liquid film model if the proper average system diffusivity is used. These cases include isotopic exchange ($D_A = D_B = D$, no selectivity) and ion exchange accompanied by a reaction which completely consumes the counterion released by the ion exchanger at the exchanger-fluid interface (34). For isotopic exchange, the exchanging counterions have the same mobility and diffuse at equal rates. Thus, a potential difference which would affect the rate of exchange is not created between the exchanging ions. The case for ion exchange accompanied by a reaction is explained in the next section.

Ion Exchange Accompanied by Reaction

In the theories presented previously, the ion exchange process has essentially been a redistribution of counterions with the ions retaining their identity. This is no longer the case when the ions exiting from the exchanger are consumed by a reaction and removed from the solution. As discussed by Helfferich (32,33,34), a reaction accompanying

ion exchange can greatly influence the flux equations depending on the rate controlling step.

A cation exchanger in the hydrogen form being contacted with a sodium hydroxide solution will be accompanied by a neutralization reaction. As the hydrogen exits from the exchanger, it will immediately react with the hydroxide coion at the particle surface. For exchange rates controlled by particle diffusion, the reaction will not affect the diffusion or rate of exchange within the particle, and Equations II-16 and II-17 are valid. However, the boundary condition at the particle surface will be affected. Solutions have been tabulated for particle diffusion control and $C_A = 0$ at the exchanger interface (32,33,74).

When the exchange rate is controlled by film diffusion, an accompanying reaction has a significant effect on the flux equations. For the example above, electroneutrality requires that

$$C_H + C_{Na} = C_{OH}.$$

(II-35)

Thus,

$$C_H \leq C_{OH}$$

(II-36)

in the film. Since the hydrogen and hydroxide ions are also linked by the dissociation equilibrium,

$$C_H C_{OH} = K_w = 10^{-14} \text{ mole}^2/\text{lit}^2$$

(II-37)

Equations II-35 and II-36 indicate that the hydrogen ion concentration is less than 10^{-7} mol/lit if the sodium hydroxide concentration in the bulk solution is higher than 10^{-7} M. Thus, the hydrogen ion does not diffuse past the particle surface, and the exchange rate is actually controlled by film diffusion of the counterion (Na) and coion (OH) from the solution to the exchanger interface.

For negligible flux of hydrogen ions past the particle interface

$$J_{Na} = J_{OH} \tag{II-38}$$

Application of Equation II-15 and elimination of J_{OH} gives

$$J_{Na} = - D \text{ grad } C_{Na} \tag{II-39}$$

where

$$D = 2 D_{Na} D_{OH}/(D_{Na} + D_{OH}) \tag{II-40}$$

Since the effective system diffusivity (D) is constant, analytical solutions for various batch systems with constant bulk solution conditions have been readily derived (33). These solutions all incorporate the assumption that the hydrogen concentration is zero at the exchanger-film interface. Experimental data of Kataoka (43) for strong acid or base binary systems with feed concentrations as low as 0.001 N agreed with the analytical solutions within the experimental error except for the exhaustion region. Exchange in

the exhaustion region was most likely influenced by particle diffusion resistance which was not taken into account.

Film diffusion-controlled exchange accompanied by chemical reaction has received very little attention outside of that concerned with verifying the previously discussed analysis of ion exchange accompanied by neutralization with a strong base. Wagner and Dranoff (93) studied ion exchange with a weak base in which the dissociation equilibrium and flux of the undissociated base were additional considerations. The solution was greatly simplified by assuming that the reaction took place at the resin-film interface and was irreversible. The concentrations of all ions involved in the reaction were also assumed to be negligible at the reaction front.

Kataoka (42) has been the only person to consider film diffusion-controlled ion exchange with a chemical reaction occurring at various distances across the film. Kataoka made single particle studies to model the recovery or purification of acids and bases using ion exchange. This system consists of a neutral salt (E^{n+} - B^{n-}) coexisting with an acid or a base (D^{n+} - B^{n-}) in contact with a resin containing A^{n-} type ions. The ion exchange, accompanied by chemical reaction, is shown by the following equations:

$$\overline{A^{n-}} + B^{n-} \rightleftharpoons \overline{B^{n-}} + A^{n-} \qquad (II\text{-}41)$$

and

$$A^{n-} + D^{n+} \longrightarrow (AD)_{Product} \qquad (II\text{-}42)$$

Figure 7 shows the liquid phase concentration diagram for this case.
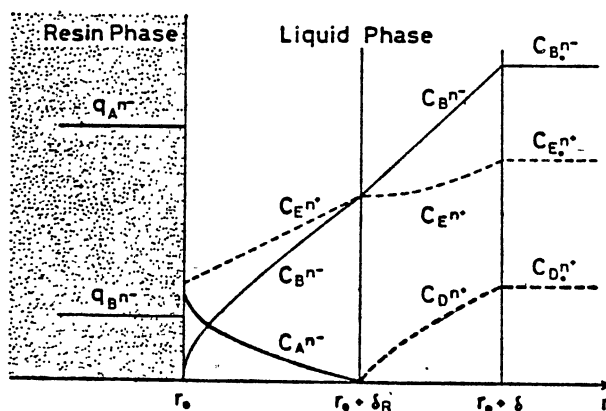
Figure 7. Concentration Profiles for Ion
Exchange with Chemical Reaction
in the Liquid Film (42)

The A^{n-} ion in the resin phase exchanges with the B^{n-} ion in the liquid phase and then reacts with coion D^{n+} at the reaction plane $r_o + \delta_r$. The coion E^{n+} does not take part in the reaction. The conditions of electroneutrality and no net current flow are described with the following equations:

$$C_A + C_B = C_E, \quad r_o \leq r \leq r_o + \delta_r \tag{II-43}$$

$$C_D + C_E = C_B, \quad r_o + \delta_r \leq r \leq r_o + \delta \tag{II-44}$$

$$J_A + J_B = J_E, \quad r_o \leq r \leq r_o + \delta_r \tag{II-45}$$

$$J_D + J_E = J_B, \quad r_o + \delta_r \leq r \leq r_o + \delta \tag{II-46}$$

$$J_E = 0, \quad r_o \leq r \leq r_o + \delta \tag{II-47}$$

The mathematics of this system were simplified with the assumptions that the reaction was irreversible and the concentrations of ions A^{n-} and D^{n-} were negligible after the reaction. With these assumptions, the flux equations of only three ions instead of five ions had to be solved simultaneously. Kataoka was able to analytically solve for the flux expression of any ion with the reaction front at any position in the film by writing the Nernst-Planck equation for each ionic flux (Equation II-15) and integrating these expressions with the above relationships and boundary conditions. Experimental results and predicted values agreed within experimental error until the resin was approximately 80 percent exhausted. The resin phase resistance was no longer negligible past this point for the solution concentrations that were studied (0.0025 meq/cm^3).

Column Models

Qualitative Aspects

The desired result from a column calculation is the effluent volume and concentration as a function of time. As discussed by Helfferich (31,32), a universal theory of

column performance does not exist. Instead, there have been a multitude of column performance equation derivations with individual sets of negligible terms and simplifications. Depending upon the case study at hand, it is of vital importance that the proper assumptions and simplifications are made.

An ion exchange column begins an exchange cycle in a regenerated state. As the column is contacted with solution, the bed is exhausted or converted to another form as the exchange process continues. The exchange wave or boundary between unconverted and exhausted resins is not ideally sharp. Thus, when breakthrough occurs, the layers of resin at the bottom of the bed are not fully utilized. The degree of column utilization is the ratio of the capacity at breakthrough to the total resin capacity in the column.

The selectivity of the resin towards the exchanging ions determines the sharpness of the exchange wave (31,32). For a column exchanging ions A in the resin phase for ions B in the solution phase, the separation factor, Equation II-3, is greater than one when ion B is preferred in the resin phase. In this case, the equilibrium is favorable. Ions A lagging behind the exchange wave are preferentially displaced into the solution by ions B, and the ions A catch up with the exchange wave. Ions B, which are ahead of the exchange wave, are preferentially held until the wave catches them. Thus, the wave does not spread out but remains sharp. In this case, the wave maintains a steady

state "constant pattern" form where sharpening effects due to favorable equilibrium and spreading effects due to finite exchange rates, longitudinal diffusion, and hydrodynamic effects are in equilibrium with each other. When the separation factor is less than one, the exchanger prefers ion A which is already in the resin, and the equilibrium is said to be unfavorable. In this case, the wave continues to spread with distance through the column.

Mathematical Solutions

Modeling of an ion exchange column requires the simultaneous solution of rate laws which are nonlinear differential equations, equilibrium expressions which are functions of the total solution concentration and fractional attainment of equilibrium, and material balances for each species in the column. Simplifications are normally made so that a solution may be readily obtained.

The various theories of column performance are divided into equilibrium and rate theories (31,32). Equilibrium theories assume local equilibrium exists between the bulk solution and exchanger particle. Rate theories are based on the assumption that finite exchange rates can be calculated and their effect on column performance taken into account. Both equilibrium theories and rate theories may have similar equation constants such as effective plate heights. For equilibrium theories, these constant will be strictly empirical whereas they will be defined functions of operating

or controlled parameters for rate theories. Numerical solutions are essentially extensions of the various rate theories.

Equilibrium Theories. Equilibrium theories were developed in the 1940's. Mayer and Tompkins (60) applied basic distillation theory with discontinuous effective plates to ion exchange chromatography. Deviations from local equilibrium were accounted for by a suitable choice of the plate height. De Vault and other authors (11,14,94) assumed that local equilibrium between the exchanger and bulk solution existed throughout the bed and developed column models based on a differential material balance

$$q \frac{\partial (\bar{X}_i + \varepsilon C_i)}{\partial V} + \frac{\partial C_i}{\partial Z} = 0 \qquad \text{(II-48)}$$

where

q = column cross-sectional area (cm^2)

Z = downstream space coordinate (cm)

V = volume of solution having passed layer (cm^3)

$\bar{X}_i$ = concentration of species i in resin phase per unit volume of bed

The relationship between X_i and C_i was given by the exchange isotherm. The effects of longitudinal diffusion and finite particle size were neglected, and plug flow was assumed.

Equilibrium theories do not apply if the exchange wave is affected by the rate of exchange. This is normally the

case when equilibrium is favorable (31). Thus, equilibrium theories are not strictly applicable to most ion exchange processes. However, this theory is especially useful in the area of multicomponent ion exchange. From the equilibrium data, feed composition, and initial composition of the exchanger, the ideal process performance may be predicted. On this basis, the economic feasibility or qualitative effects of any change in operating conditions may be estimated. Excellent reviews of the application of equilibrium theory to practical multicomponent ion exchange problems are given by Klein and Tondeur (49,84).

Rate Theories. In general, the rate theories solve the following set of equations:

$$q \frac{\partial (\bar{X}_i + \epsilon C_i)}{\partial V} + \frac{\partial C_i}{\partial Z} \quad \text{Material Balance} \tag{II-49}$$

$$\bar{X}_i^* = f(C_i) \quad \text{Isotherm} \tag{II-50}$$

$$\frac{\partial \bar{X}_i}{\partial t} = f(\bar{X}_i^*, \bar{X}_i, C_i^*, C_i) \quad \text{Rate Law} \tag{II-51}$$

The various rate theories use the same material balance but use different isotherm and rate law expressions.

Although not exact (31), the most general theory was developed by H. C. Thomas (82). His theory was the first solution of Equation II-49 for nonequilibrium conditions and a nonlinear isotherm. He assumes a constant separation

factor and a rate law corresponding to a second order
kinetic reaction

$$\frac{\partial \bar{X}_B}{\partial t} = kC_B(\bar{X} - X_B) - k\alpha_{A/B} \bar{X}_B(C_t - C_B) \qquad (II-52)$$

where

$\bar{X}$ = total counterion concentration in exchanger per unit
volume of bed (meq/cm^3)

The general solution for the effluent of a column in the A
form with B ions as feed can be written as

$$X_B = \frac{J(\alpha_{A/B} N, T_r N)}{J(\alpha_{A/B}N, T_r N) + [1-J(N,\alpha_{A/B}T_r N)]\exp[(\alpha_{A/B}^{-1})n(T_r^{-1})]} \qquad (II-53)$$

where

N = $k\bar{X}Z/u$; number of mass transfer units

T_r = $(V - \epsilon V_b)/V_s$; throughput ratio

$J_{(x,y)}$ = $1 - \int_o^x \exp(-x-\epsilon)I_o(2\sqrt{y\epsilon})d\epsilon$

V_s = volume of bulk solution equivalent to exchange capacity of
bed $(V_b\bar{X}/C_t)$

V_b = bed volume (cm^3)

Z' = column length (cm)

I_o = modified Bessel function of the first order

Stanford Research Institute has tabulated the solution of
Equation II-53 for a large number of sets of the parameters
$\alpha_{A/B}$, N, and T_r (66). The Thomas theory is general in that,

for limiting cases, it reduces to results which have been previously derived for simple systems (23,26,27,35).

The main theoretical problem with Thomas' solution is his use of a second order kinetic expression for the exchange rate when ion exchange is known to be controlled by ionic diffusion rather than a chemical reaction. Because of this dilemma, Vermeulen and Hiester (35,91) expanded Thomas' solution to consider exchange rates given by the more appropriate linear driving force equations. They also developed generalized plots of column and breakthrough profiles. These profiles are now commonly used for sorption column design and evaluation (72).

For constant pattern exchange (very favorable equilibrium), the mathematics are greatly simplified by using a moving reference frame stationed at the center of the exchanger wave. As the constant exchange pattern is attained, the concentration of the counterion B in the solution becomes a function of the space coordinate only and not of time. Using Thomas' theory and the linear driving force rate laws for film diffusion control, Glueckauf (79) obtained the following expression for the effluent volume at which the concentration X_B emerges

$$V_{x_B} = V_b \frac{\bar{X}}{C_t} + \varepsilon \left[1 - \left\{ \frac{\bar{X}/C_t}{\bar{X}/C_t + \varepsilon} \right\}^2 \cdot \frac{\mu}{k_1 Z} \left\{ \frac{\alpha_{A/B}}{1-\alpha_{A/B}} \ln(1-x_B) - \frac{1}{1-\alpha_{A/B}} \ln x_B - 1 \right\} \right]$$

$$(II-54)$$

A similar expression was also derived for particle diffusion control. Unlike Thomas' solution with a second order rate law, Equation II-54 displays a finite amount of ion leakage through the column.

For $0 < \alpha_{A/B} << 1$ (very favorable equilibrium) and $\bar{X}/C_t >> \epsilon$, film diffusion control leads to the simplification of Equation II-54 to

$$x_B = \exp[N(T_r-1)-1] \qquad \text{(II-55)}$$

as long as $X_B << 1$.

In the previous rate theories, the rate of exchange, Equation II-51, was given as a function of the momentary solution concentration (C_i) and average ion concentration within the exchanger $(\bar{X}_i)$. As discussed earlier in particle diffusion kinetics, the rate of exchange actually depends on the history of the exchanger particles or the concentration profiles within the particle (31,32).

Wicke (96), Rosen (77), and Amundson (5,37) have used a more rigorous rate model (for spherical particles) which accounts for the effects of concentration profiles within the exchanger (31).

$$\frac{\partial \bar{C}_i}{\partial t} = \frac{1}{r_o^2} \frac{\partial}{\partial r} (r^2 \bar{D} \frac{\partial \bar{C}_i}{\partial r}) \qquad \text{(II-56)}$$

$$\bar{X}_i = \frac{3}{r_o^3(1-\epsilon)} \int_o^r \bar{C}_i \, r^2 \, dr \qquad \text{(II-57)}$$

where

$\bar{C}_i$ = local concentration in the resin per unit volume resin

However, solutions with the above expressions were derived using a linear isotherm and constant intraparticle diffusion coefficient. Rosen's solution is the most general in that he gives extensions for various entrance conditions and a solution for film diffusion using a rate law of the type of Equation II-33 (31,77).

The assumption of a linear isotherm restricts the practical application of Rosen's theory as even slight deviations from linearity of the exchange isotherm greatly affect the performance of an exchange column (31,32). The assumption of a constant intraparticle diffusion coefficient is a less serious idealization and may be approximately correct, depending on the exchange case. Wicke (31,96) solved the limiting case of irreversible exchange, but his solution has not been applied to mixed bed processes due to the assumption of a linear isotherm which is not applicable.

Numerical Solutions. Solutions of the more complex analytical equations, such as those of Thomas, are so tedious that they have been tabulated for large sets of parameters using computers (66). A more important application of numerical methods is that of complicated systems for which analytical solutions are not available (31). General analytical solutions are not available for processes having more than two exchanging ions, for beds with nonuniform

initial composition, and for variable flow rate and feed composition.

Simultaneous material balances for all species must be integrated when more than two exchanging ions are considered. Dranoff et al. (18,19) and Omatete et al. (65) studied column dynamics of ternary ion exchange. The studies by Dranoff extended Thomas' analytical solution and were among the early developments in numerical analysis of ion exchange. The studies by Omatete were recent applications of multicomponent diffusion equations based on irreversible thermodynamics to ion exchange. The numerical programming used in both studies is typical of ion exchange column calculations, although the rate expressions and equilibrium relationships are completely different.

For numerical computations, the material balance on each ionic species is written in terms of ionic equivalents;

$$F_1 \left\{ \frac{\partial x_i}{\partial Z} \right\}_t + \frac{Q\rho_b}{C_{tn}} \left\{ \frac{\partial y_i}{\partial t} \right\}_Z + \varepsilon \left\{ \frac{\partial x_i}{\partial t} \right\}_Z = 0 \qquad \text{(II-58)}$$

$$i = 1,\ldots,n-1$$

where

F_1 = volumetric flow rate

Q = total exchange capacity (equivalents)

n = total number of exchanging ions

The effects of longitudinal diffusion and finite particle size are normally neglected, and plug flow is assumed. The

material balance equation is simplified by defining dimensionless time and distance coordinates, or more often, a throughput parameter

$$T_p = \frac{C_t (V_B - \varepsilon Z)}{Q \rho_b Z} \qquad (II-59)$$

where

V_B = volume of solution fed to the column $(F_1 t)$

Using the throughput parameter, Equation II-58 is transformed to Equation II-60.

$$\left\{ \frac{\partial x_i}{\partial Z} \right\}_{(T_p Z)} + \left\{ \frac{\partial y_i}{\partial T_p Z} \right\}_{Z} = 0 \qquad (II-60)$$

$$i = 1,\ldots,n-1$$

In addition to the material balance equation, an independent equation for the rate of exchange of each species must be specified,

$$\left\{ \frac{\partial y_i}{\partial t} \right\}_{Z} = R_{t,i} \qquad (II-61)$$

$$i = 1,\ldots,n-1$$

where

$R_{t,i}$ = rate expression for component i

Equilibrium relationships are required to determine interfacial concentrations used in the rate expressions. The

combination of Equations II-60 and II-61 at a given column cross-section yield

$$-\left\{\frac{\partial X_i}{\partial Z}\right\}_{(T_p Z)} = \left\{\frac{\partial y_i}{\partial (T_p Z)}\right\}_Z = \frac{Q\rho_b}{C_t F}(R_{t,i})$$ (II-62)

$$i = 1,\ldots,n-1$$

Because of overall material balance considerations, it is only necessary to write equations for $n-1$ ionic species.

Equation II-62 is readily adapted to computer solution by the method of characteristics (18,19,31,56,65). The ion exchange column is considered to be a grid defined by lines of constant $T_p \cdot Z$ and of constant Z, as shown in Figure 8. The concentrations at grid points along the lines $T_p \cdot Z = 0$ (initial bed composition) and $Z = 0$ (feed composition as a function of time) are given as initial and boundary conditions. The rate expression for each component, Equation II-61, is represented by a finite difference equation. Using the equilibrium relationships and finite difference rate expressions, the concentration of each component at a mesh point $(Z + \Delta Z, T_p \cdot Z + \Delta T_p \cdot Z)$ can be calculated from the concentrations at the points $(Z + \Delta Z, T_p \cdot Z)$ and $(Z, T_p \cdot Z + \Delta T_p \cdot Z)$. Thus, the calculations proceed from left to right across an entire grid row before $T_p \cdot Z$ is incremented. The calculations continue until $T_p \cdot Z = T_p \cdot Z_{end}$ (feed is discontinued). The effluent concentration history is given by the concentrations along the line $Z = Z'$.
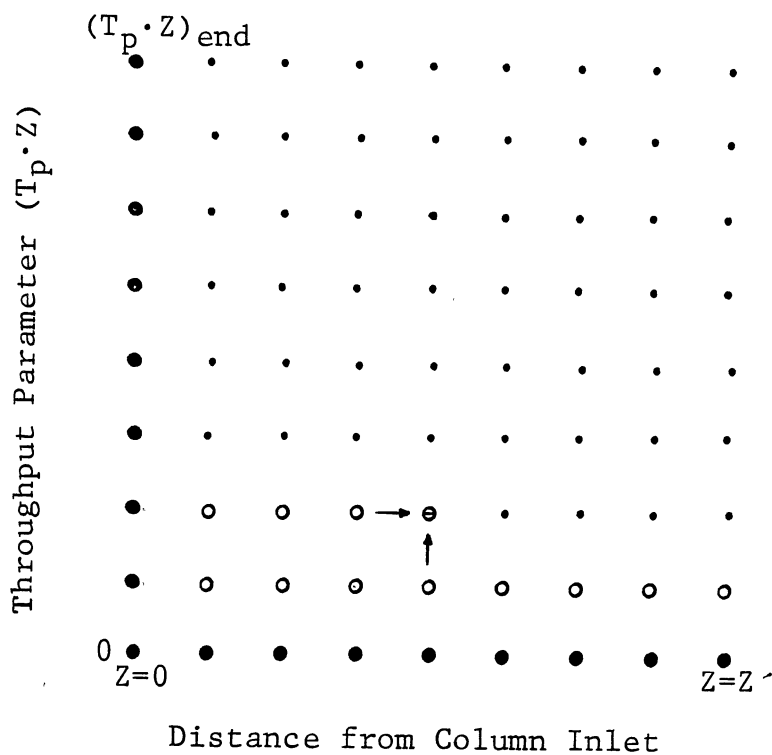
Figure 8.   Function Grid for Numerical
            Calculations by the
            Method of Characteristics

Numerical calculations allow the use of rigorous rate
laws of the type of Equations II-56 and II-57 which account
for concentration gradients within the resin particles.
However, the use of these rate laws significantly increases
the calculation time and memory-capacity requirements. At
each mesh point, an array of intraparticle concentrations
for a series of radius values must be computed and stored
for each ionic species. As many as 15 zones (concentric
spherical shells) have been used to simulate concentration

gradients in particles with diameters of approximately 1 mm (67).

Pan and David (67,68,69) studied the effect of liquid phase ionic migration on ion exchange operations by simulating a moving packed bed process for sodium-hydrogen ion exchange. A moving bed process was studied as steady state can be assumed and the process is time independent. The sodium-hydrogen exchange system was selected because it has significant ionic-migration effects due to the large difference between ionic diffusivities of the exchanging ions.

The ionic migration effect in the liquid film was accounted for by the inclusion of an R_i factor based on the laminar boundary layer model as discussed earlier. The effect of the potential gradient on diffusion within the particle was included by the use of the Nernst-Plank flux equation which leads to a composition dependent internal diffusivity for each ion species.

Pan and David were able to make a complete mathematical analysis of ionic migration effects in binary sodium-hydrogen ion exchange. The corrections due to ionic effects were most limited for favorable exchange with low solution concentrations. Exchange systems with ions having similar diffusion coefficients and the aforementioned conditions may be modeled within the error of the mass transfer coefficients by using a constant diffusivity model for the liquid phase and constant average diffusivity model

for the resin phase. The effective system diffusivity for the liquid phase should be based on the diffusion coefficient of the entering ion instead of the average of the exchanging ion diffusion coefficients. The ionic migration effects were very significant for exchange with slightly favorable or unfavorable equilibrium, high percentage saturation of the exchange, and high percentage removal of the incoming ion in the solution.

Kataoka et al. (44,45,46) also studied the effects of ionic interactions on column breakthrough curves for several binary systems including sodium-hydrogen exchange. Separate studies were made for particle diffusion control and liquid phase diffusion control. The study of ionic effects during particle diffusion control was analogous to that of Pan and David (67). The Nernst-Plank equation with a composition dependent internal diffusivity accounted for the ionic effects. The governing equations were written in finite difference form, and the numerical solution was accelerated by using a variable mesh spacing in the radial direction.

The study of ionic effects during liquid phase diffusion control was based on the hydraulic radius model as discussed earlier. Low feed solution concentrations of 0.005 N were used to make the liquid phase mass transfer dominant. The typical finite difference technique described earlier in this section was used to obtain a numerical solution. Based on published figures, experimental and theoretical results for the breakthrough curves of the

hydrogen-sodium system agreed within approximately two percent, except for the exhaustion region. This region began at an equivalent ionic fraction of the entering ion in the resin of 0.75. The deviation arises due to the effect of resin diffusion, which was not accounted for in the model. The results concerning the conditions for significant ionic effects were the same as those given in the studies by Pan and David (67,69).

Mixed Bed Modeling

Mixed bed deionization technology and industrial practice has been well ahead of the corresponding theory of ion exchange accompanied by chemical reaction ever since the introduction of mixed bed units. The majority of articles on mixed bed ion exchange have been concerned with proper mechanical design, operation, and maintenance of these units instead of the ion exchange theory. Of the articles dealing with mixed bed theory, most of these have been oriented towards the development of correlations relating breakthrough time with fluid flow rates, inlet concentrations, resin capacities, etc (51,76,83). The actual modeling of mixed bed units has primarily been left in the hands of resin manufacturers.

The current status of published mixed bed modeling theory is at best very crude. These models do not represent the actual ion exchange-reaction process occurring in a mixed bed. The ideal of mixed bed ion exchange was conceived

by Kunin (50). The purpose of mixing cation and anion resins was to obtain a neutralization reaction which would make the exchange process irreversible. This was a giant step in water treatment capabilities, as it enabled the obtainment of extremely low impurity levels with a neutralized effluent.

There have been two major systematic studies on the ion exchange theory and modeling of mixed bed units (9,22). Based on earlier ion exchange investigations, it was known that the exchange kinetics of mixed bed units were controlled by film diffusion resistance and that the cation and anion resins in mixed beds normally exchanged ions at equivalent rates. Thus, the simple linear driving force concept (Equation II-33) was used as the constituitive flux equation, and the mixture of cation and anion resins was treated as a single salt removing resin. For all of the concentrations studied, the exchange isotherm was found not only to be strongly concentration dependent but also strongly irreversible. Consequently, the equilibrium was described by:

$$c_B^* = 0, \quad q_B < Q \qquad\qquad \text{(II-63)}$$

$$c_B^* > 0, \quad q_B = Q \qquad\qquad \text{(II-64)}$$

The above flux equation with the corresponding equilibrium conditions was integrated using the column balance given by Equation II-49 to yield the expression for the

effluent ion concentration as given by Equation II-55. This equation predicted mixed bed breakthrough curves for effluent ion concentrations as low as several hundred parts per million ($\approx$ 0.001 M). The most appropriate effective system diffusivity was found to be that given by Helfferich (33) for ion exchange followed by a strong neutralization reaction (Equation II-39). Helfferich's theoretical development for ion exchange followed by a strong reaction was published shortly after the major mixed bed investigations. Helfferich's derivations were thought to support the use of a constant effective system diffusivity for mixed bed exchange. Articles published as recently as 1981 still contain mixed bed models which are based on flux equations using a constant system diffusivity (84).

The strong agreement between predicted and experimental data by the previously discussed model must be understood in light of current ion exchange theory before the conclusion can be made that this model is erroneous. For the cation resin exchanging hydrogen for sodium in mixed beds, the hydrogen ion will not accumulate at the resin-film interface due to very low hydrogen concentrations in the bulk phase and a strong concentration gradient across the film. The sodium interfacial concentration will be reduced along with the reduction in the hydrogen concentration due to the resin phase equilibrium relationship (Equation II-5). Thus, the interfacial sodium concentration was reduced below the

desired effluent concentration levels for early mixed bed studies and could be considered as negligible.

As previously discussed, mixed bed ion exchange equilibrium is strongly favorable at effluent concentrations for which these units were initially developed. The use of a constant system diffusivity can be explained by a favorable equilibrium curve (a) - operating line (b) diagram (69).

Equivalent Fraction in Solution
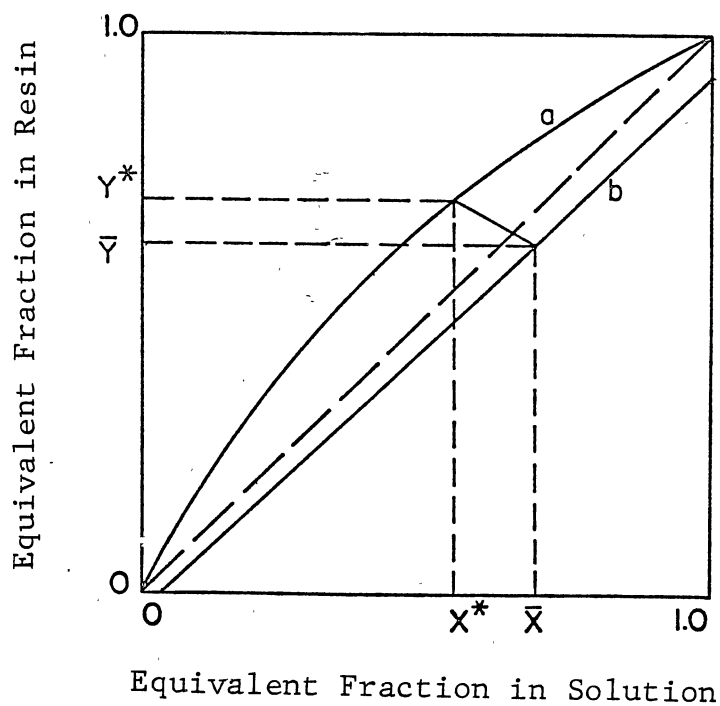
Figure 9. Equilibrium Curve-
Operating Line
Diagram for Favor-
able Ion Exchange
(69)

The driving force for mass transfer in the liquid phase is represented by the quantity $x_B^o - x_B^*$, which is the largest in the middle of the diagram and decreases towards the ends of the operating line. For mixed bed ion exchange, it is desired to reduce the exiting solution concentration (x_B^o) to a low value. Thus, a considerable portion of the bed size is required by the small driving force at the lower end of the operating line. As discussed under models for film diffusion, the R_i factor (Figure 6) or the ratio of ionic to nonionic mass transfer coefficients is closest to unity in this region. The elimination of ionic effects in the Nernst-Planck flux equation (Equation II-15) produces a flux equation with the constant system diffusivity, as used by early experimenters in modeling fixed bed ion exchange columns.

CHAPTER III

MODEL DEVELOPMENT

Basis and Assumptions

The rate laws and column models discussed in Chapter II
were a small fraction of the voluminous amount of material
available for modeling ion exchange columns. Deciding which
correlation best represents a certain exchange case or the
amount of modeling detail required for a desired accuracy of
results can be difficult to determine. These decisions must
be made by considering the relative errors and mathematical
complexities imposed by the assumptions made in the various
exchange models. The following model development was an
attempt to optimize model accuracy, considering the amount
of calculational effort required. The applicability of the
resulting model to a variety of systems with a minimum
amount of experimental data required was also a high
priority in this development. Several more recently
published ion exchange models and theory developments were
not discussed in the Literature Review and were not used in
this study because they use newly defined diffusion
coefficients which are not supported by a substantial amount

of data, are not applicable to the conditions of mixed bed exchange, or require lengthy modeling programs which are not practical for everyday calculations (7,21,28,86).

The model development was based on the desire to simulate certain desired column variables and exchange conditions which are not considered in current mixed bed ion exchange models. These requirements include consideration of the following effects: variation of the cation and anion resin ratio; differing cation and anion exchange rates, exchange capacities, and particle sizes; reversibility of exchange at low concentrations; neutralization reactions within the film and bulk liquid phases; and effluent ion concentrations on the order of one part per billion $(1 \times 10^{-7}$ M). All of the above considerations were included in the mixed bed model by accounting for the position of the neutralization reaction front and the water dissociation constant in separate flux equations for the cation and anion resins. These flux equations were based on the Nernst-Planck theory (Equation II-15) in conjunction with the static film hydrodynamic model and nonionic mass transfer coefficient correlations for packed beds (Equations II-25 and II-26).

As discussed in Chapter II, the conditions of favorable equilibrium and low effluent concentrations are prevalent in mixed bed ion exchange. The effects of the electric potential gradient on the ion fluxes are greatly reduced for conditions of strongly favorable equilibrium and low ion

concentrations. Electric potential effects increase rapidly as equilibrium becomes unfavorable. The electric potential effects are in between these two extremes for the low ion concentrations simulated in this model. The most accurate ion flux would be obtained by combining the Nernst-Planck theory with the boundary layer or hydraulic radius hydrodynamic models. The improvement in the predicted ion fluxes by using the more rigorous hydrodynamic models over the static film model would be approximately five percent for the slightly favorable equilibrium conditions at extremely low ion concentration levels. This additional accuracy is not merited, since the overall electric potential effect is still at a reduced level for the case under consideration. The use of the static film model also allows part of the flux equations to be analytically integrated. This reduces the computing time and memory requirements, since the ion concentration gradients must be calculated at each mesh point in a numerical column model.

The derived ion flux expressions do not account for the exchange resistance due to particle diffusion within the exchange resins. As fluid flow rates increase and ion concentrations decrease, the percent of resin exhausted before particle diffusion resistance becomes important increases. This value was found to be approximately 80 percent for systems with Reynolds numbers up to 15 and ion concentrations of only 0.0025 M (42). Thus, the fraction of resin exhausted before particle diffusion affects the

exchange rate should be quite high for ion concentrations on the order of one part per billion. Considering that the breakthough curve is controlled by the pinch zone at the lower end of the operating curve (Figure 9), where ions are contacting fresh resin, particle diffusion should have a negligible effect on all but the tail end of the break-through curve.

Other assumptions used in the model development include the following: uniform bulk liquid and surface compositions exist for a given exchange particle, equilibrium at the particle-film interface and neutralization reactions are instantaneous compared to the rate of exchange, activity coefficients are unity for the concentrations studied, mass transfer is pseudo steady state across the film layer, the system is isothermal, and dispersion may be neglected in the mixed bed. The assumptions of instantaneous neutralization reactions and equilibrium establishment at the particle-fluid interface were necessary for modeling purposes. To the author's knowledge, no experimental evidence has been presented which would indicate that these assumptions are not valid. The assumptions of an isothermal system and activity coefficients of unity are good for mixed bed systems due to the extremely low solution concentrations encountered.

In a packed column, the assumption of uniform surface conditions and bulk phase concentrations for each exchange particle may not be totally accurate. Concentration

gradients are present near each exchanging particle and in the bulk liquid phase. Thus, the fluid contacting a given particle may not be of uniform concentration. This situation was not considered due to the lack of modeling methods and the complexity which would be introduced. The consideration of longitudinal diffusion adds an additional term to the column material balance. This term involves the solution flow rate in the denominator and has been shown to be important only for exchange systems at very low flow rates (31). Mixed bed systems are typically operated at high flow rates; and thus, the longitudinal diffusion effects have been disregarded.

Ion Flux Expressions

A mixed bed ion exchange unit produces a neutral effluent when operating at optimum conditions. This effluent may also be slightly acidic or basic, depending on the ratio of cation to anion resins or selective fouling of one of the resin types. The neutralization reaction within a mixed bed may occur in the bulk liquid, film, or particle-film interface due to this variation in the solution ionic composition. The ion flux equation must account for all of these cases. For simplicity in mathematical equations and diagrams, ion species will be represented as follows:

Sodium   = n   Hydrogen = h
Chloride = c   Hydroxide = o

Helfferich (33), Kataoka (38), and Smith et al. (79) have used the Nernst-Planck equation to determine ion fluxes in film diffusion-controlled binary exchange systems having a single coion. These flux equations were solved for single particle systems with the concentration of the ion exiting from the exchanger set equal to zero in the bulk phase. One such system is represented in Figure 10.
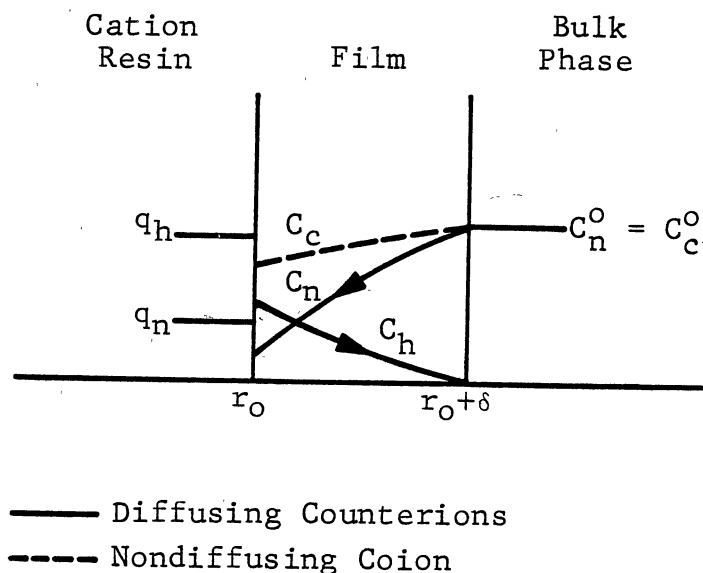
Figure 10. Concentration Profiles for a Single Particle Experimental Study of Binary Exchange

Only the final equation results with very few of the intermediate details are given in the published literature. The integrated flux equations for even the most simple system,

as shown in Figure 10, are not easily obtained. Thus, the
flux equations for the above system were first derived to
establish a solution procedure for more difficult systems.
This derivation is given in Appendix A.

Bulk Phase Neutralization

The first case considered for mixed bed ion exchange is
that of neutralization occurring in the bulk phase. Ion
concentration profiles are shown in Figure 11. These
concentration profiles are exaggerated for clarification.

Figure 11. Concentration Profiles for Mixed Bed
Ion Exchange with Neutralization
in the Bulk Phase

The conditions of electroneutrality and no net current flow are described as follows:

$$C_n + C_h = C_c + C_o, \quad r_o \leq r \leq r_o + \delta \qquad \text{(III-1)}$$

$$J_n + J_h = J_c + J_o, \quad r_o \leq r \leq r_o + \delta \qquad \text{(III-2)}$$

Since there is no net flux of the coions, Equations III-3 and III-4 are respectively obtained for the cation and anion exchanges.

$$J_c = J_o = 0 \qquad \text{(III-3)}$$

$$J_n = J_h = 0 \qquad \text{(III-4)}$$

The derivation of the ion fluxes for the anion exchange system is identical to that for the cation system. Only the derivation of the cation flux equations is shown here.

Applying the Nernst-Planck equation for the flux of each ion, and assuming that curvature in the film is negligible, Equations III-5 through III-8 are obtained.

$$J_h = -D_h \left\{ \frac{\partial C_h}{\partial r} + \frac{C_h F}{RT} \frac{\partial \phi}{\partial r} \right\} \qquad \text{(III-5)}$$

$$J_n = -D_n \left\{ \frac{\partial C_n}{\partial r} + \frac{C_n F}{RT} \frac{\partial \phi}{\partial r} \right\} \qquad \text{(III-6)}$$

$$J_c = -D_c \left\{ \frac{\partial C_c}{\partial r} + \frac{C_c F}{RT} \frac{\partial \phi}{\partial r} \right\} \qquad \text{(III-7)}$$

$$J_o = -D_o \left\{ \frac{\partial C_o}{\partial r} + \frac{C_o F}{RT} \frac{\partial \phi}{\partial r} \right\} \qquad \text{(III-8)}$$

The potential gradient is first expressed in terms of diffusing ion concentrations by elimination of the nondiffusing ion (coion) terms. Equations III-7 and III-8 are each solved for the potential gradient using Equation III-3.

$$\frac{\partial \phi}{\partial r} = \frac{RT}{C_c F} \frac{\partial C_c}{\partial r} \qquad \text{(III-9)}$$

$$\frac{\partial \phi}{\partial r} = \frac{RT}{C_o F} \frac{\partial C_o}{\partial r} \qquad \text{(III-10)}$$

The concentration gradient relationship between the hydroxide and chloride ions is expressed by equating Equations III-9 and III-10.

$$\frac{\partial C_o}{\partial r} = \frac{C_o}{C_c} \frac{\partial C_c}{\partial r} \qquad \text{(III-11)}$$

Using the water dissociation equilibrium, C_o is eliminated from Equation III-11.

$$C_o = 10^{-14}/C_h \qquad \text{(III-12)}$$

Thus,

$$\frac{\partial C_o}{\partial r} = \left\{\frac{10^{-14}}{C_c C_h}\right\} \frac{\partial C_c}{\partial r} \qquad \text{(III-13)}$$

The following expression for $\partial C_c/\partial r$ is obtained by differentiating Equation III-1 with respect to r, eliminating $\partial C_o/\partial r$ using Equation III-13, and rearranging.

$$\frac{\partial C_c}{\partial r} = \left\{\frac{C_c C_h}{C_c C_h + 10^{-14}}\right\}\left\{\frac{\partial C_h}{\partial r} + \frac{\partial C_n}{\partial r}\right\} \qquad \text{(III-14)}$$

From Equations III-1 and 12,

$$C_c C_h + 10^{-14} = C_h(C_h + C_n) \qquad \text{(III-15)}$$

and Equation III-14 reduces to

$$\frac{\partial C_c}{\partial r} = \left\{\frac{C_c}{C_h + C_n}\right\}\left\{\frac{\partial C_h}{\partial r} + \frac{\partial C_n}{\partial r}\right\} \qquad \text{(III-16)}$$

The final expression for the potential gradient in terms of the diffusing ion concentrations is found by substituting $\partial C_c/\partial r$ from Equation III-16 into Equation III-9.

$$\frac{\partial \phi}{\partial r} = \frac{RT}{F} \frac{1}{(C_n + C_h)} \left\{\frac{\partial C_h}{\partial r} + \frac{\partial C_n}{\partial r}\right\} \qquad \text{(III-17)}$$

Substituting Equation III-17 into Equations III-5 and III-6 yields flux equations in terms of diffusing ion concentrations and concentration gradients only.

$$J_n = -D_n\left[\frac{\partial C_n}{\partial r} + \frac{C_n}{C_n + C_h}\left\{\frac{\partial C_n}{\partial r} + \frac{\partial C_h}{\partial r}\right\}\right] \qquad \text{(III-18)}$$

$$J_h = -D_h\left[\frac{\partial C_h}{\partial r} + \frac{C_h}{C_n + C_h}\left\{\frac{\partial C_n}{\partial r} + \frac{\partial C_h}{\partial r}\right\}\right] \qquad \text{(III-19)}$$

Equations III-18 and III-19 are the same as Equations A-10 and A-11 in Appendix A. The flux relationship obtained from Equations III-2 and III-3,

$$J_n = -J_h \qquad \text{(III-20)}$$

is also the same as is used in Appendix A (Equations A-12 through A-18) to obtain the relationships between the diffusing ion concentrations and concentration gradients. The concentration relationship between sodium and hydrogen in the film to that in the bulk phase is determined by integrating Equation III-21 (Equation A-18).

$$\frac{dx}{x} = - \frac{dy}{y} \qquad \text{(III-21)}$$

where

$$x = \frac{D_h}{D_n} C_h + C_n$$

$$y = C_h + C_n$$

The boundary conditions as shown in Figure 11 are

$$C_h = C_h, \; C_n = C_n \text{ for } r_o \le r \le r_o + \delta \qquad \text{(III-22)}$$

$$C_h = C_h^o, \; C_n = C_n^o \text{ for } r = r_o + \delta \qquad \text{(III-23)}$$

Integration of Equation III-20 with these boundary conditions yields

$$\left\{ \frac{D_h}{D_n} C_h + C_n \right\} \left\{ C_h + C_n \right\} = \left\{ \frac{D_h}{D_n} C_h^o + C_n^o \right\} \left\{ C_h^o + C_n^o \right\} \qquad \text{(III-24)}$$

Equation III-24 is valid at any position in the film.

The derivation of the flux expressions for sodium and hydrogen follow directly from Appendix A, beginning with Equation A-23, if the expression

$$\left\{ \frac{D_h}{D_n} C_h^o + C_n^o \right\} \left\{ C_h^o + C_n^o \right\} \tag{III-25}$$

is substituted for $(C_n^o)^2$ in each applicable equation. The final flux equations contain an additional term not included in the flux equations derived in Appendix A.

$$J_n = \frac{2 D_h D_n (C_h^o + C_n^o - C_h^* - C_n^*)}{(D_n - D_h)\delta} \tag{III-26}$$

and

$$J_h = \frac{2 D_h D_n (C_h^o + C_n^o - C_h^* - C_n^*)}{(D_h - D_n)\delta} \tag{III-27}$$

The coion concentrations at any point in the film are given by

$$C_o = 10^{-14}/C_h \tag{III-12}$$

and

$$C_c = C_n + C_h - 10^{-14}/C_h \tag{III-15}$$

Applying the static film model for liquid phase mass transfer in ion exchange, the diffusion rate, excluding fluid flow effects, is defined by Equation III-28.

$$\frac{\partial \langle \bar{C}_n \rangle}{\partial t} = k_1' \, a_s (C_n^o - C_n^*) = -(J_n) a_s \qquad \text{(III-28)}$$

where

$$k_1' = D_e / \delta$$

The negative of J_n is required in Equation III-28, since the positive direction used in the integration to obtain J_n was from the resin particle towards the bulk solution. Substituting for J_n from Equation III-26 and solving for the effective diffusivity yields

$$D_e = \frac{2 \, D_h D_n \, (C_h^* + C_n^* - C_h^o - C_n^o)}{(D_n - D_h)(C_n^o - C_n^*)} \qquad \text{(III-29)}$$

A more convenient form of Equation III-29 is

$$D_e = \frac{2\alpha \, D_n}{(1 - \alpha)(1 - C_n^*/C_n^o)} \left\{ \frac{C_h^*}{C_n^o} + \frac{C_n^*}{C_n^o} - \frac{C_h^o}{C_n^o} - 1 \right\} \qquad \text{(III-30)}$$

where

α = ratio of exiting to entering ion diffusivities (D_h/D_n)

Noting that

$$\langle \bar{C}_n \rangle = y_n \cdot Q \qquad \text{(III-31)}$$

and that Q is constant, the rate of exchange in terms of equivalent fractions is expressed as

$$\frac{\partial y_n}{\partial t} = \frac{D_e}{\delta} a_s \frac{C_n^o}{Q} \left\{ 1 - \frac{C_n^*}{C_n^o} \right\} \tag{III-32}$$

where D_e is given by Equation III-30.

The relationship between interfacial and resin phase concentrations is given by the selectivity coefficient (Equation II-5). The selectivity coefficient arranged in a form similar to Equations III-30 and III-32 is expressed as

$$K_h^n = \frac{(C_h^*/C_n^o)}{(C_n^*/C_n^o)} \frac{y_n}{1 - y_n} \tag{III-33}$$

The interface and bulk liquid concentration relationship given by Equation III-24 may also be expressed in terms of concentration ratios.

$$\left\{ \alpha \frac{C_h^*}{C_n^o} + \frac{C_n^*}{C_n^o} \right\} \left\{ \frac{C_h^*}{C_n^o} + \frac{C_n^*}{C_n^o} \right\} = \left\{ \alpha \frac{C_h^o}{C_n^o} + 1 \right\} \left\{ \frac{C_h^o}{C_n^o} + 1 \right\} \tag{III-34}$$

Combining Equations III-30, III-33, and III-34, the effective system diffusivity (D_e) depends on α, D_n, K_h^n, y_n, and C_h^o/C_n^o as shown in Equation III-35.

$$D_e = \frac{2\alpha D_n}{(1 - \alpha)(1 - X)} (SX + X - Y - 1) \tag{III-35}$$

where

$$X = \frac{C_n^*}{C_n^o} = \left\{ \frac{(\alpha Y + 1)(Y + 1)}{(\alpha S + 1)(S + 1)} \right\}^{1/2}$$

$$S = K_h^n \frac{1 - y_n}{y_n}$$

$$Y = C_h^o / C_n^o$$

Finally, Equation III-32 is written in terms of a nonionic mass transfer coefficient, using Equation II-30, so that fluid flow effects will be incorporated into the exchange rate:

$$R_i = \left(\frac{D_e}{D_n} \right)^{2/3} = \frac{k_i'}{k_i}$$

$$\frac{\partial y_n}{\partial t} = k_1 \left\{ \frac{D_e}{D_n} \right\}^{2/3} a_s \frac{C_n^o}{Q} (1 - X) \qquad \text{(III-36)}$$

where X is defined in Equation III-35 and k_1 is determined using Equation II-25 or II-26.

At the start of exchange, y_n and C_n^*/C_n^o are equal to zero. Using Equations III-30 and III-34, Equation III-35 reduces to

$$D_e = \frac{2\alpha \, D_n}{(1 - \alpha)} \left\{ Y' - \frac{C_h^o}{C_n^o} - 1 \right\} \qquad \text{(III-37)}$$

where

$$Y' = \frac{C_h^*}{C_n^o} = \left[\left\{ \frac{C_h^o}{C_n^o} + \frac{1}{\alpha} \right\} \left\{ \frac{C_h^o}{C_n^o} + 1 \right\} \right]^{1/2}$$

The effective diffusivity expressed by Equation III-37 is readily obtained and may be a good approximation of the average diffusivity for exchange systems where D_e is fairly constant. At the end of exchange, y_n is equal to one. Using Equations III-30, III-33, and III-34, Equation III-35 reduces to

$$D_e \approx \frac{2\alpha\, D_n}{(1 - \alpha)(1 - Y'')} \left\{ Y'' - \frac{C_h^o}{C_n^o} - 1 \right\} \qquad \text{(III-38)}$$

where

$$Y'' = \frac{C_h^*}{C_n^o} = \left[\left\{ \alpha\, \frac{C_n^o}{C_n^o} + 1 \right\} \left\{ \frac{C_h^o}{C_n^o} + 1 \right\} \right]^{1/2}$$

Equations III-35 through III-38 also describe the anion system exchange rate when all terms involving sodium (n) and hydrogen (h) are respectively replaced with equivalent chloride (c) and hydroxide (o) terms.

Liquid Film Neutralization

Mixed bed ion exchange units produce a fairly neutral effluent over a broad range of operating conditions. This resistance to produce a nonneutral effluent is contributed

to the "irreversible" exchange and electronic coupling due to the neutralization reaction. A substantial explanation of the coupling effect between the cation and anion exchange rates, along with any type of attempt to predict or model systems with slightly nonneutral effluents, have not been published.

Simple experiments based on generally known information for cation and anion resins and mixed bed units, having liquid film diffusion-controlled exchange rates, support a flux equation model accounting for neutralization within the liquid film surrounding the exchange particles. Anion and cation resins exchange ions at different rates in separate shallow bed or single particle studies, even though the exchange rates are determined with resins of equal diameters and salt solutions of the same concentrations. The exchange rates for the separated resins are not equivalent because of different diffusivities of the exchanging ions. In these studies, the bulk phase remains neutral (infinite dilution), and the concentration profiles of the exchanging ions should be identical to the concentration profiles during mixed bed exchange with a neutralized bulk phase. Thus, the explanations using irreversible exchange and equivalent cation and anion concentration driving forces do not truly account for nearly equal cation and anion exchange rates in mixed bed units.

The ion exchange-film reaction model, as studied by Kataoka (42), provides an explanation for the mixed bed

phenomenon. Hydrogen ions will begin to diffuse into the liquid film surrounding the anion resin as the acidity of the bulk solution increases due to faster cation than anion exchange. Concurrent with this, the neutralization reaction front will move from the bulk liquid phase into the liquid film. The movement of the reaction front towards the particle surface will decrease the effective film thickness and thus increase the concentration gradient of the hydroxide ion diffusing away from the anion resin-liquid interface. Buildup of the hydrogen concentration in the bulk phase is also prevented, since hydrogen ions are removed from the bulk phase to the reaction front.

Typical ion concentration profiles for neutralization occurring in the anion liquid film are shown in Figure 12. The overall rate of exchange is controlled by the diffusion of hydrogen and chloride to the reaction front as well as the respective diffusion of chloride and hydroxide ions to and from the resin. The conditions of electroneutrality and no net current flow are described as follows:

$$C_n + C_h = C_c + C_o, \quad r_o \leq r \leq r_o + \delta \tag{III-39}$$

$$J_n + J_h = J_c + J_o, \quad r_o \leq r \leq r_o + \delta \tag{III-40}$$
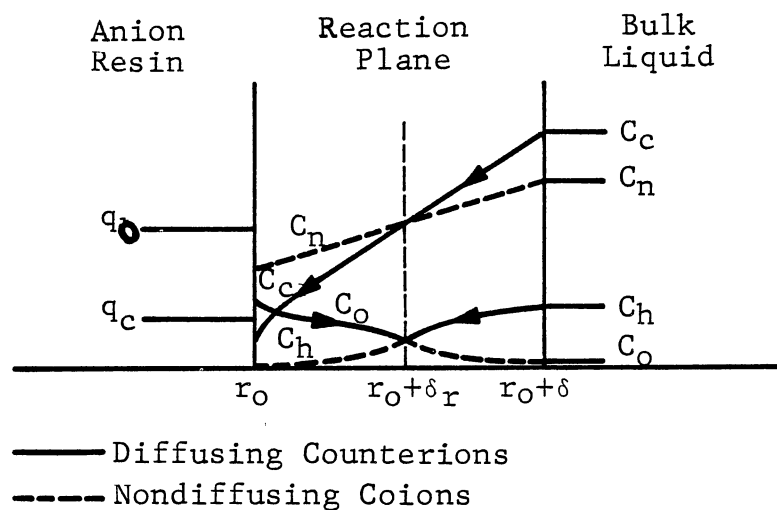
Figure 12. Concentration Profiles for Anion
Exchanger with Neutralization
in the Liquid Film

The neutralization reaction and no net coion flux between
the resin surface and reaction plane introduce additional
system restraints:

$$J_n = 0, \quad r_o \leq r \leq r_o + \delta_r \tag{III-41}$$

$$J_n = 0, \quad r_o \leq r \leq r_o + \delta_r \tag{III-42}$$

$$C_o = C_h = 10^{-7} \ M, \quad r = r_o + \delta_r \tag{III-43}$$

Additional system restraints for ionic diffusion in the film between the reaction plane and the bulk liquid must be carefully considered. For strong acid systems, the hydroxide ion flux is negligible compared to the hydrogen ion flux as discussed under rate laws for ion exchange accompanied by reaction. The assumption of negligible hydroxide ion flux should still be valid at the low concentrations considered in mixed bed ion exchange units because hydroxide ions coming from the resin are consumed in the neutralization occurring at the reaction front. Thus, the hydroxide ions in the film region between the reaction front and the bulk phase are produced from the water dissociation and hydrogen ion equilibrium. Also, the concentration driving force for the diffusion of hydroxide ions is one-tenth to one-hundredth of that for hydrogen ions having respective concentrations of 10^{-6} M and 10^{-5} M due to the water dissociation equilibrium. With this assumption of negligible hydroxide ion flux after the reaction phase, additional system restraints are

$$J_n = 0, \quad r_o + \delta_r \leq r \leq r_o + \delta \tag{III-44}$$

$$J_o = 0, \quad r_o + \delta_r \leq r \leq r_o + \delta \tag{III-45}$$

The ion flux expressions for this system are obtained by combining flux expressions for each of the two film sections. Solving the flux expressions for the inner film region relates ion concentrations in the resin to those at

the neutralization reaction plane. The solution of ion flux equations for the outer film region then relates the ion concentrations at the reaction front to ion concentrations in the bulk phase.

Comparing Figures 11 and 12, the anion exchange system between the resin surface and reaction plane is the same system used for mixed bed exchange with neutralization occurring in the bulk phase, except that δ must be replaced by δ_r. Thus, rewriting Equations III-26, III-33, and III-34 for the anion system yield:

$$J_c = \frac{2\,D_o\,D_c\,C_c^o}{(D_c - D_o)\delta_r}\left\{\frac{C_o^r}{C_c^o} + \frac{C_c^r}{C_c^o} - \frac{C_o^*}{C_c^o} - \frac{C_c^*}{C_c^o}\right\} \tag{III-46}$$

where

C_i^r = concentration of species i at the reaction plane

$$K_o^c = \frac{(C_o^*/C_c^o)}{(C_c^*/C_c^o)}\;\frac{y_c}{(1 - y_c)} \tag{III-47}$$

and

$$\left\{\alpha\,\frac{C_o^*}{C_c^o} + \frac{C_c^*}{C_c^o}\right\}\left\{\frac{C_o^*}{C_c^o} + \frac{C_c^*}{C_c^o}\right\} = A \tag{III-48}$$

where

$$A = \left\{ \alpha \frac{C_o^r}{C_c^o} + \frac{C_c^r}{C_c^o} \right\} \left\{ \frac{C_o^r}{C_c^o} + \frac{C_c^r}{C_c^o} \right\}$$

$$\alpha = D_o/D_c$$

Combining Equations III-47 and III-48, the interfacial equilibrium concentrations for the chloride and hydroxide ions may be expressed in terms of equivalent fractions in the resin phase and concentrations at the reaction plane.

$$\frac{C_o^*}{C_c^o} = \frac{(1 - y_c)(K_o^c)(A)^{1/2}}{[(\alpha(1 - y_c)K_o^c + y_c)((1 - y_c)K_o^c + y_c)]^{1/2}} \qquad \text{(III-49)}$$

$$\frac{C_c^*}{C_c^o} = \frac{y_c(A)^{1/2}}{[(\alpha(1 - y_c)K_o^c + y_c)((1 - y_c)K_o^c + y_c)]^{1/2}} \qquad \text{(III-50)}$$

Substitution of Equations III-49 and III-50 into III-46 gives the chloride ion flux in terms of concentrations in the resin phase and at the reaction plane.

$$J_c = \frac{2 D_c \left(D_c \right) C_c^o}{(D_c - D_o)\delta_r} \left\{ \frac{C_o^r}{C_c^o} + \frac{C_c^r}{C_c^o} - Y \right\} \qquad \text{(III-51)}$$

where

$$Y = (A)^{1/2} \left\{ \frac{(1 - y_c)K_o^c + y_c}{\alpha(1 - y_c)K_o^c + y_c} \right\}^{1/2}$$

and A is given in Equation III-48.

The diffusion rate equations for the ionic fluxes through the film layer between the reaction plane and bulk phase must consider diffusion of the hydrogen coion. The constituitive equations are the Nernst-Planck equation for each ion flux (Equations III-5 through III-8) along with the electroneutrality and system constraints given by Equations III-39, III-40, III-44, and III-45. Again, the potential gradient is first expressed in terms of diffusion ion concentrations by elimination of the nondiffusing ion terms. Equations III-6 and III-8 are each solved for the potential gradient using Equations III-44 and III-45, respectively.

$$\frac{\partial \phi}{\partial r} = - \frac{RT}{C_n F} \frac{\partial C_n}{\partial r} \tag{III-52}$$

$$\frac{\partial \phi}{\partial r} = + \frac{RT}{C_o F} \frac{\partial C_o}{\partial r} \tag{III-53}$$

The relationship between the sodium and hydrogen concentration gradients is determined by equating the potential gradients.

$$\frac{\partial C_o}{\partial r} = - \frac{C_o}{C_n} \frac{\partial C_n}{\partial r} \tag{III-54}$$

Differentiating Equation III-39 with respect to r, substituting for $\partial C_o/\partial r$ from Equation III-54, eliminating C_o with Equation III-12, and solving for $\partial C_n/\partial r$ yields

$$\frac{\partial C_n}{\partial r} = \left\{\frac{C_h C_n}{C_h C_n + 10^{-14}}\right\}\left\{\frac{\partial C_c}{\partial r} - \frac{\partial C_h}{\partial r}\right\} \qquad (III-55)$$

The potential gradient can now be expressed in terms of diffusing ion concentrations by combining Equations III-55 and III-52 and eliminating C_n with Equations III-39 and III-12.

$$\frac{\partial \phi}{\partial r} = -\frac{RT}{F}\frac{C_h}{(C_h C_c - (C_h)^2 + 2\cdot10^{-14})}\left\{\frac{\partial C_c}{\partial r} - \frac{\partial C_h}{\partial r}\right\} \qquad (III-56)$$

Substitution of Equation III-56 into Equations III-5 and III-7 yields flux equations for the diffusion ions in terms of diffusing ion concentrations only.

$$J_c = -D_c\left[\frac{\partial C_c}{\partial V} + \frac{C_c C_h}{(C_h C_c - (C_h)^2 + 2\cdot10^{-14})}\left\{\frac{\partial C_c}{\partial r} - \frac{\partial C_h}{\partial r}\right\}\right] \qquad (III-57)$$

$$J_h = -D_h\left[\frac{\partial C_h}{\partial V} - \frac{(C_h)^2}{(C_h C_c - (C_h)^2 + 2\cdot10^{-14})}\left\{\frac{\partial C_c}{\partial r} - \frac{\partial C_h}{\partial r}\right\}\right] \qquad (III-58)$$

To integrate Equation III-57, the concentration and concentration gradient relationships between chloride and hydrogen must be determined. Substituting Equations III-57 and III-58 along with the constraints of Equations III-44

and III-45 into Equation III-40 and simplifying gives the following concentration gradient and concentration relationships:

$$\frac{\partial C_h}{\partial r} = \frac{\partial C_c}{\partial r} \left\{ \frac{2D_c \, 10^{-14} + 2D_c C_c C_h - D_c (C_h)^2 + D_h (C_h)^2}{2D_h \, 10^{-14} + D_h C_c C_h + D_c C_c C_h} \right\} \qquad \text{(III-59)}$$

or

$$\frac{\partial C_h}{\partial C_c} = \left\{ \frac{2D_c \, 10^{-14} + 2D_c C_c C_h - D_c (C_h)^2 + D_h (C_h)^2}{2D_h \, 10^{-14} + D_h C_c C_h + D_c C_c C_h} \right\} \qquad \text{(III-60)}$$

Eliminating $\partial C_h / \partial r$ from Equation III-57 using Equation III-59 gives

$$J_c = - \frac{\partial C_c}{\partial r} \left\{ \frac{2D_c D_h (C_c C_h + 10^{-14})}{2D_h \, 10^{-14} + D_h C_c C_h + D_c C_c C_h} \right\} \qquad \text{(III-61)}$$

after proper factoring and simplification. The concentration relationship between the hydrogen and chloride ions is determined numerically. Known values include chloride and hydrogen ion concentrations in the bulk phase as well as the hydrogen concentration at the reaction plane $(C_h = 10^{-7} \text{ M})$. Thus, the chloride ion concentration across the film is readily determined using the Quartic Runge-Kutta method for solving the differential equation (Equation III-60).

Assuming pseudo-steady state exchange ($\partial J_c / \partial r = 0$), and integrating with respect to the radial distance, Equation III-62 is obtained.

$$J_c = K'$$

<div align="right">(III-62)</div>

where

$$K' = \text{constant of integration}$$

Substituting Equation III-61 for J_c and integrating yields

$$\int_{C_c^r}^{C_c^o} \left\{ \frac{2D_c D_h (C_c C_h + 10^{-14})}{2D_h 10^{-14} + D_h C_c C_h + D_c C_c C_h} \right\} dC_c = \int_{r_o + \delta_r}^{r_o + \delta} (-K' dr)$$

<div align="right">(III-63)</div>

The left side of Equation III-63 is numerically integrated using Simpson's method combined with an interpolating routine for the numerical results relating the hydrogen and chloride ion concentrations. The solution of Equation III-60 is determined using constant increments of the hydrogen concentration, but Equation III-63 is integrated using constant increments of the previously determined chloride ion concentration. Thus, the interpolation routine is required to relate values for the hydrogen and chloride ion concentrations which are between incremental values previously used in the solution of Equation III-60.

For simplicity, let the numerical integration results of Equation III-63 be represented by I. Equation III-63 now becomes

$$- \frac{I}{(\delta - \delta_r)} = K' = J_c \qquad \text{(III-64)}$$

At the reaction plane,

$$J_o = -J_h \qquad \text{(III-65)}$$

From Equations III-40, III-41, and III-42,

$$J_c = -J_o, \quad r_o \leq r \leq r_o + \delta_r \qquad \text{(III-66)}$$

and from Equations III-44, III-45, and III-40,

$$J_n = J_c, \quad r_o + \delta_r \leq r \leq r_o + \delta \qquad \text{(III-67)}$$

Substituting Equation III-65 for J_o in Equation III-66 and comparing the resulting equation with Equation III-67 gives the result:

$$J_{c_{r_o \leq r \leq r_o + \delta_r}} = J_{c_{r_o + \delta_r \leq r \leq r_o + \delta}} \qquad \text{(III-68)}$$

Substituting the derived chloride ion flux expressions for each film region (Equations III-51 and III-64) into Equation III-68 and rearranging gives the relative position of the reaction plane to the total film thickness:

$$h = \frac{\delta_r}{\delta} = \frac{2 D_o D_c C_c^o (C_o^r/C_c^o + C_c^n/C_c^o - Y)}{(-I)(D_c - D_o) + 2D_o D_c C_c (C_o^r/C_c^o + C_c^r/C_c^o - Y)} \qquad \text{(III-69)}$$

where Y is defined in Equation III-51.

The overall effective liquid phase diffusivity for this system can now be determined using Equations III-64 and III-69. Applying the static film model for liquid phase mass transfer

$$\frac{\partial \langle C_c \rangle}{\partial t} = \frac{D_e}{\delta} a_s C_c^o \left\{ 1 - \frac{C_c}{C_c^o} \right\} = (-J_c) a_s = \frac{I}{\delta - \delta_r} a_s \quad \text{(III-70)}$$

The negative of J_c is used in Equation III-70, since the positive direction during integration was defined to be away from the resin. Substituting for h (Equation III-69) and rearranging yields the final expression for the effective system diffusivity:

$$D_e = \frac{(I)}{(1 - h)(C_c^o)(1 - C_c^*/C_c^o)} \quad \text{(III-71)}$$

where

$$h = \frac{2 \, D_o D_c C_c^o (C_o^r/C_c^o + C_c^r/C_c^o - Y)}{(-I)(D_c - D_o) + 2 \, D_o D_c C_c^o (C_o^r/C_c^o + C_c^r/C_c^o - Y)}$$

$$C_c^*/C_c^o = \frac{y_c (A)^{1/2}}{[(\alpha(1 - y_c)K_o^c + y_c)((1 - y_c)K_o^c + y_c)]^{1/2}}$$

$$Y = (A)^{1/2} \left\{ \frac{(1 - y_c)K_o^c + y_c}{\alpha(1 - y_c)K_o^c + y_c} \right\}^{1/2}$$

$$A = \left\{ \alpha \frac{C_o^r}{C_c^o} + \frac{C_c^r}{C_c^o} \right\} \left\{ \frac{C_o^r}{C_c^o} + \frac{C_c^r}{C_c^o} \right\}$$

$$\alpha = D_o/D_c$$

I = numerical integral result for the left side of Equation III-63

Finally, the rate of exchange is given by

$$\frac{\partial y_c}{\partial t} = k_1 \left\{ \frac{D_e}{D_c} \right\}^{2/3} a_s \frac{C_c^o}{Q} \left\{ 1 - \frac{C_c^*}{C_c^o} \right\} \qquad \text{(III-72)}$$

where D_e and C_c^*/C_c^o are given in Equation III-71 and k_1 is evaluated using Equations II-25 or II-26.

From Equations III-71 and III-72, the rate of exchange depends upon the following variables: α, K_o^c, C_o^r/C_c^o, C_c^r/C_c^o, C_c^o, C_h^o, and y_c. The first two variables are properties of the exchange system. The third and fourth variables are calculated from the last three variables which must be specified. The instantaneous solution of Equation III-72 can be readily calculated once D_e is known. The following procedure is used to calculate D_e:

1. Specify C_c^o, y_c, and C_h^o or C_h^o/C_c^o.

2. Numerically solve Equation III-60 to obtain the ion concentration profiles between the bulk phase and reaction plane.

3. Numerically integrate equation III-63 to obtain I.

4. Respectively calculate A, Y, C_c^*/C_i^o, h, and D_e as defined in Equation III-71.

This development will be referred to as the simplified film reaction model due to the assumption of negligible hydrogen and hydroxide ion fluxes after the reaction plane.

The simplified model was developed in hopes that the numerical differentiation and integration of Equations III-60 and III-61, respectively, could be done using analytical methods. Since analytical solutions were not obtained, the use of rigorous equations accounting for the hydrogen and hydroxide fluxes after the reaction plane may be substituted for Equations III-61 and III-63 with a minimal amount of extra computational effort once the proper relationships have been developed. These relationships are derived in Appendix B and are given by Equations III-73 and III-74.

$$\frac{\partial C_h}{\partial C_c} = \frac{(A)(C_h)^2}{(B)} \tag{III-73}$$

and

$$J_c = -D_c \frac{\partial C_c}{\partial r}\left\{\frac{C_n(B) + C_c(B) - C_c(A)\,10^{-14} - C_c(A)(C_h)^2}{C_n(B)}\right\} \tag{III-74}$$

where

$$A = D_h(C_h)^2 - D_c(C_h)^2 + 2 D_c C_c (C_h) + D_o 10^{-14} + D_c 10^{-14}$$

$$B = D_h C_c (C_h)^3 + 2 D_h (C_h)^2 10^{-14} + D_o C_c C_h 10^{-14} + 2 D_o 10^{-28} +$$

$$D_c C_c C_h 10^{-14} + D_c C_c (C_h)^3$$

The model development using Equations III-73 and III-74 will be referred to as the rigorous film reaction model, since the flux effects of all ionic species on the rate of exchange are considered.

Column Material Balance

The column material balance developed here assumes plug flow and neglects the effects of longitudinal diffusion and finite particle size as previously discussed. This material balance is slightly different from that discussed along with Equations II-58 through II-62 in that dimensionless time and distance coordinates are used instead of the throughput parameter as defined by Equation II-59. A separate material balance is required for the cation and the anion resins. Because of this, a new variable accounting for the volume fractions of the respective resins is introduced.

The general material balance for a sodium cation exchange column corresponding to Equation II-58 is written as

$$\frac{u}{\varepsilon} \frac{\partial C_n}{\partial Z} + \frac{\partial C_n}{\partial t} + \frac{(1 - \varepsilon)}{\varepsilon} \frac{\partial q_n}{\partial t} = 0 \qquad \text{(III-75)}$$

Equation III-75 is written for the cation exchanger in a mixed bed by defining the variables x_n' and f_c:

$$\frac{\mu_s}{\epsilon} \frac{\partial x_n'}{\partial Z} + \frac{\partial x_n'}{\partial t} + \frac{f_c(1 - \epsilon) Q_n}{C_n^f(\epsilon)} \frac{\partial y_n}{\partial t} = 0 \qquad \text{(III-76)}$$

where

f_c = volume of cation resin/total resin volume

$x_n' = C_n/C_n^f$

$q_n = y_n \cdot Q_n$

The variable x_n' is commonly based on the total bulk phase solution concentration. However, this concentration is not constant through a mixed bed due to the neutralization reaction.

Dimensionless distance and time coordinates used to simplify Equation III-76 are as defined by Kataoka (44):

$$\xi = \frac{k_1(1 - \epsilon)}{\mu} \frac{Z}{d_p} \qquad \text{(III-77)}$$

and

$$\tau = \frac{k_1 C_i^f}{d_p Q} \left(t - \frac{Z\epsilon}{\mu}\right) \qquad \text{(III-78)}$$

The variables k_1, d_p, and Q have different values for the cation and anion resin. Either the cation or anion resin must be selected as a basis for the dimensionless variables so that common increments of Z and t will be used in the

integration of Equation III-76 for the two resins. The cation resin and sodium inlet concentration were selected as the basis in this development. Values corresponding to the cation and anion resins will be shown with superscripts of 1 and 2, respectively. The relationship between ξ and τ for the two resins is given by Equations III-79 and III-80.

$$\xi^1 = \frac{k_1^1 \, d_p^2}{k_1^2 \, d_p^1} \cdot \xi^2 \tag{III-79}$$

$$\tau^1 = \frac{k_1^1 \, d_p^2 \, Q^2}{k_1^2 \, d_p^1 \, Q^1} \, \tau^2 \tag{III-80}$$

To simplify Equation III-76, each of the partials are written in terms of ξ and τ for the cation resin:

$$\frac{\partial x_n'}{\partial Z} = \frac{\partial x_n'}{\partial \xi^1} \frac{k_1^1(1-\epsilon)}{\mu \, d_p^1} - \frac{\partial x_n'}{\partial \tau^1} \frac{k_1^1 \, C_n^f \, \epsilon}{d_p^1 \, Q^1 \, \mu} \tag{III-81}$$

$$\frac{\partial x_n'}{\partial t} = \frac{\partial x_n'}{\partial \xi^1}(o) + \frac{\partial x_n'}{\partial \tau^1} \frac{k_1^1 \, C_n^f}{d_p^1 \, Q^1} \tag{III-82}$$

$$\frac{\partial y_n}{\partial t} = \frac{\partial y_n}{\partial \xi^1}(o) + \frac{\partial y_n}{\partial \tau^1} \frac{k_1^1 \, C_n^f}{d_p^1 \, Q^1} \tag{III-83}$$

Substituting Equations III-81 through III-83 into Equation III-76 yields the final material balance for the cation resin:

$$\frac{\partial x_n}{\partial \xi^1} + f_c \frac{\partial y_n}{\partial \tau^1} = 0 \qquad\qquad \text{(III-84)}$$

The rate of exchange is also expressed in terms of τ by the combination of Equations III-36 and III-83.

$$\frac{\partial y_n}{\partial \tau^1} = 6 \cdot R_i^1 \ (C_n^o/C_n^f - C_n^*/C_n^f) \qquad\qquad \text{(III-85)}$$

A similar development for the anion resin, again based on ξ^1 and τ^1, leads to Equations III-86 and III-87.

$$\frac{\partial x_c}{\partial \xi^1} + (1 - f_c) \frac{Q^2}{Q^1} \frac{\partial y_c}{\partial \tau^1} = 0 \qquad\qquad \text{(III-86)}$$

and

$$\frac{\partial y_c}{\partial \tau^1} = \left\{ \frac{k_1^2}{k_1^1} \frac{d_p^1}{d_p^2} \frac{Q^1}{Q^2} \right\} \cdot 6 \cdot R_i^2 \ (C_c^o/C_n^f - C_c^*/C_n^f) \qquad\qquad \text{(III-87)}$$

With the use of Equations III-79 and III-80, Equations III-86 and III-87 directly reduce to the same form as Equations III-84 and III-85 with ξ^1, τ^1, and f_c, respectively, replaced by ξ^2, τ^2, and $(1 - f_c)$.

The operation of a mixed bed column is now simulated by a calculation mesh, as shown in Figure 8 with Z and $T_p \cdot Z$ replaced by ξ and τ, respectively. Equations III-84 through III-87 are simultaneously integrated along characteristic lines of constant ξ and constant τ. Material balance and rate expression equations of this form may be simultaneously integrated for as many different types of resins or

different resin sizes as desired. For different resin sizes, f_c will represent the volume fraction of any one particular size of resin. This method of separate resin treatment enables mathematical studies more closely simulating actual column operating conditions and variables. One example of this includes imperfect resin separation before regeneration. A column can readily be modeled in which possibly two percent of the cation resin is regenerated with the anion resin. This resin would be modeled as a third resin and would release sodium ions during the initial phases of exchange. Other possible studies include modeling the effects of feed concentration surges, various cation to anion resin ratios, multiple particle sizes, improper resin mixing, or incomplete resin regenerations.

CHAPTER IV

RESULTS AND DISCUSSION

Bulk Phase Neutralization Model

This model was developed to account for neutralization in the bulk phase. The inclusion of the neutralization reaction only affected the bulk phase boundary conditions and not the diffusion equations. Thus, this model is also good for nonreactive ion exchange. The derived flux expressions were found to be independent of the number of coions in the film. In the model development for the cation resin, all chloride and hydroxide ion effects cancelled out of the flux relationships. Thus, the addition of coions to a single resin system will only influence the exchange rate through effects on the boundary conditions unless the coions are involved in chemical reactions or are dissociation products of the exchanging ions. This independence of coion effects is of little value for mixed bed systems, since the coions for one of the resin types (cation or anion) are the exchanging ions for the opposite type of resin.

The general results for the bulk phase neutralization model are given in terms of an effective system diffusivity (D_e) by Equation III-35. For presentation, these results are transformed into R_i factors (ratio of the electrolyte to

nonelectrolyte mass transfer coefficients) with the use of Equation II-30. From Equation III-35, the R_i factor depends upon the ratio of the exiting to entering ion diffusivity (α), the entering ion diffusivity (D_i), the resin selectivity coefficient ($K_{B/A}$), the equivalent fraction of the entering ion in the resin phase (y_i), and the ratio of the exiting to entering bulk phase ion concentration (γ). The system variables, α, D_i, and $K_{B/A}$ are fixed for a particular ion exchange system, but these values vary widely from one system to another and they have a large impact upon the rate of exchange. The general effects of α, D_B, $K_{B/A}$, and y_B on R_i for the sodium/ hydrogen and chloride/hydroxide exchange systems at a constant bulk phase concentration ratio are shown in Figures 13 through 16. These results are comparable to published results for single particle system studies using solutions of infinite dilution (38,87).

The R_i values increase monotonically with progression of exchange for systems in which the slower of the exchanging ions is entering the resin (Figures 13 and 14). The R_i values monotonically decrease for systems in which the slower of the exchanging ions is exiting from the resin (Figures 15 and 16). This effect is a direct influence of the potential gradient which is established during the exchange process. Before an ion can leave the exchanger, it must be replaced by an ion entering the exchanger. When the slower of the exchanging ions is diffusing towards the exchanger, the effect of the electric potential is to
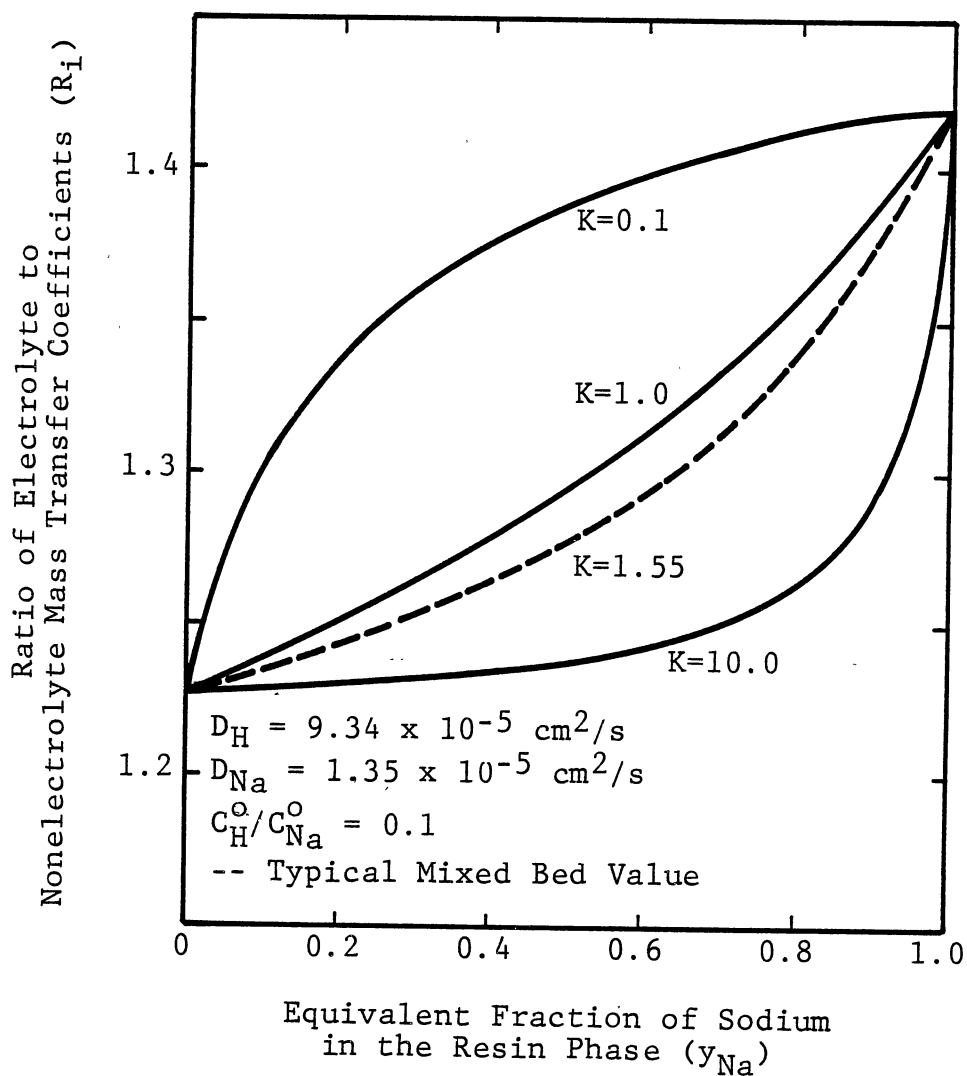
Figure 13. Variation of R_i with y_{Na} and $K_{Na/H}$ for Forward Cation Exchange (Bulk Phase Neutralization Model)
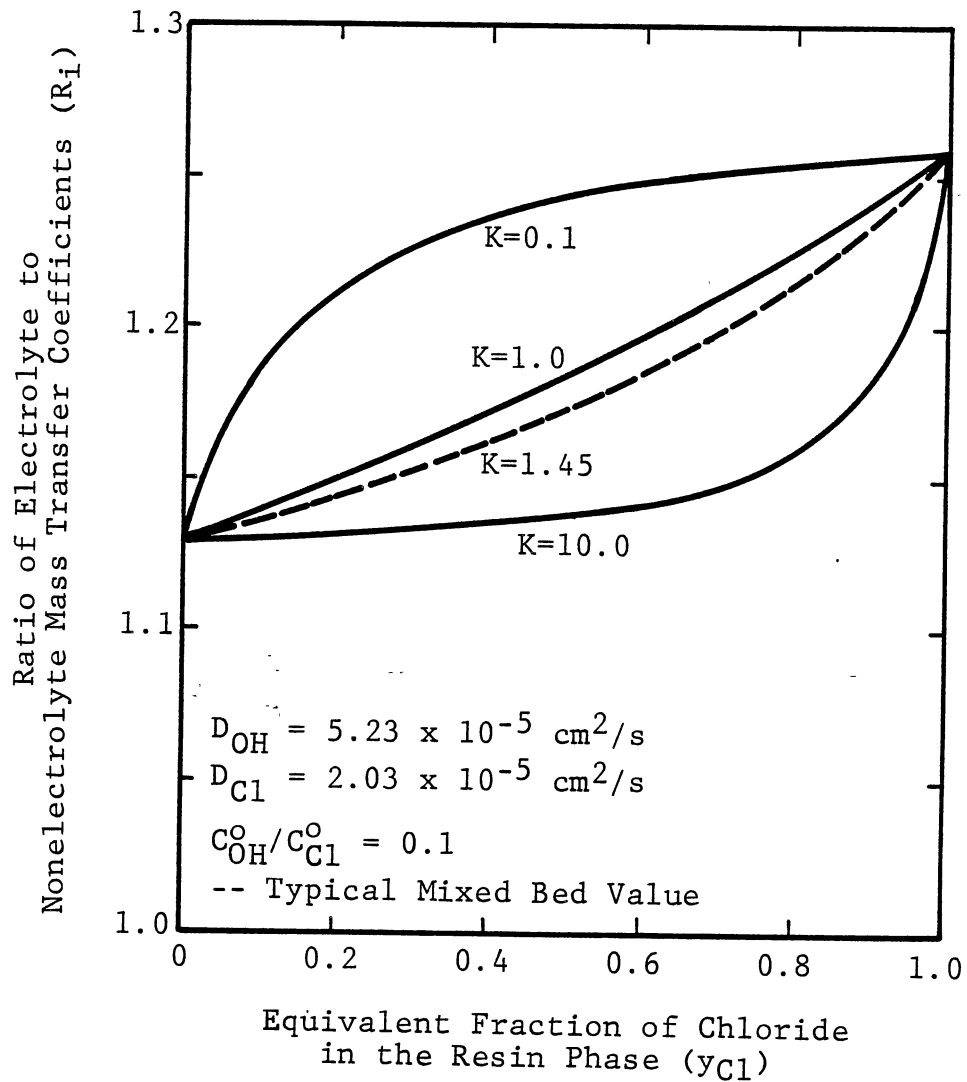
Figure 14.   Variation of R_i with y_{Cl} and $K_{Cl/OH}$ for Forward Anion Exchange (Bulk Phase Neutralization Model)
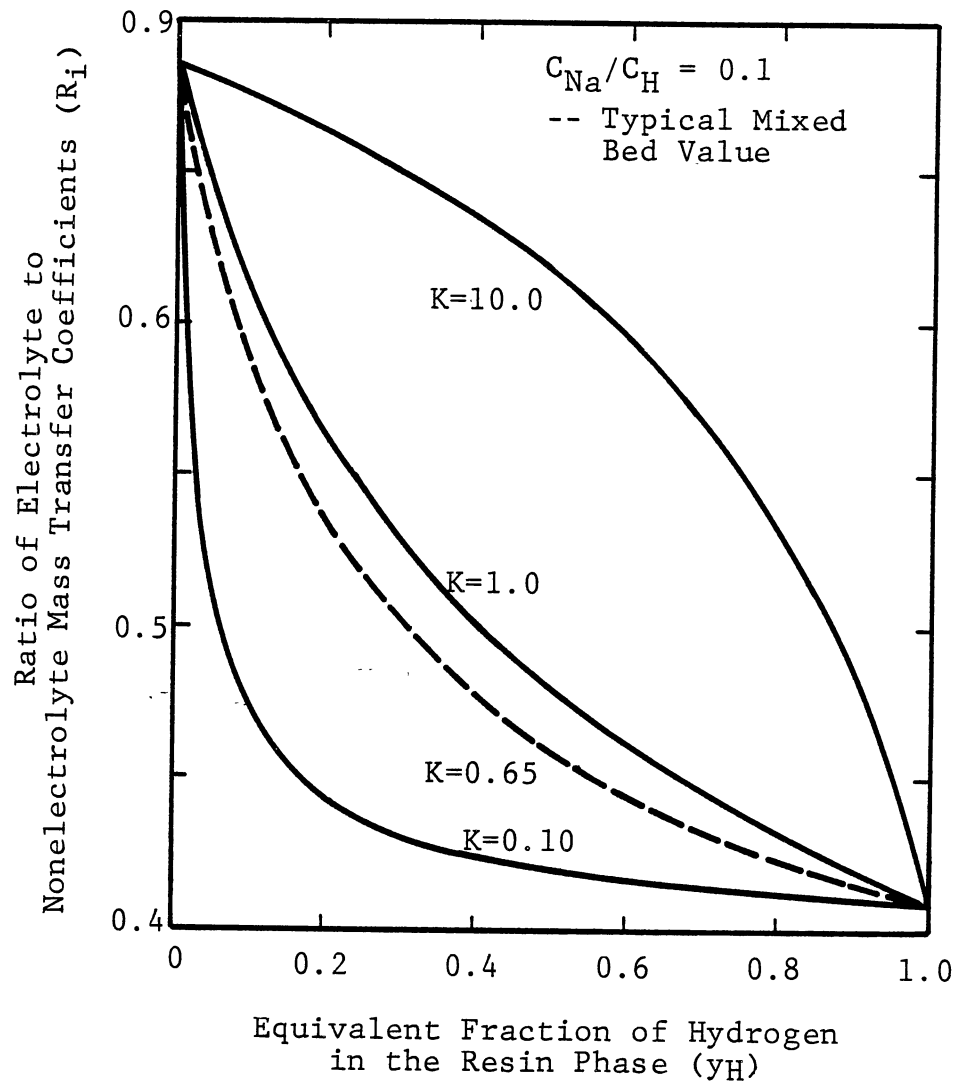
Figure 15. Variation of R_i with y_H and $K_{H/Na}$ for Reverse Cation Exchange (Bulk Phase Neutralization Model)
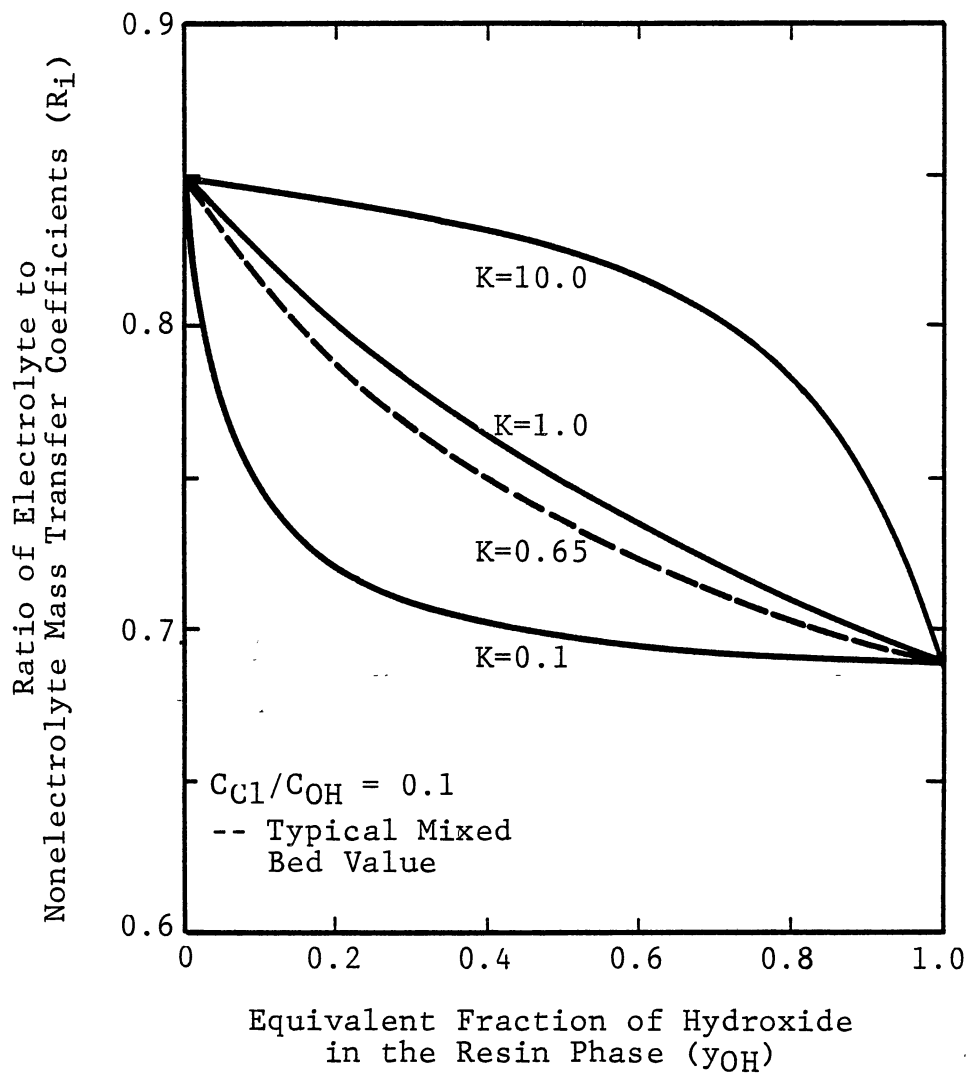
Figure 16.   Variation of R_i with y_{OH} and $K_{OH/Cl}$ for Reverse Anion Exchange (Bulk Phase Neutralization Model)

increase the rate of diffusion of this ion into the exchanger. For the opposite case, the slower ion is exiting the resin. The entering ions have a higher diffusivity and will be repelled as they approach the exchanger. This exchange will be slower than that for a neutral species.

The resin selectivity coefficient has a strong influence on the shape of the R_i versus y_B curves. Typical cation and anion resin selectivity coefficients are 1.5 and 1.45, respectively. The R_i values corresponding to these selectivity coefficients are shown by the dashed lines. The R_i curves are concave and approximately constant at the beginning of exchange for highly favorable forward exchange ($K_{B/A} >> 1$, Figures 13 and 14). For the reverse exchange (Figures 15 and 16), the R_i curves for favorable exchange are convex and are again most nearly constant during the early stages of exchange. For unfavorable exchange ($K_{A/B} << 1$), Figures 13 through 16 show that R_i will strongly affect the exchange rate, even during the initial stages of exchange.

The effect of the ratio of the exiting to entering ion diffusivities (α) on R_i is seen by comparing the figures for cation exchange with those for anion exchange. The larger this ratio (cation exchange), the stronger the effects of the potential gradient on the exchange rate will be. This is shown by the increased magnitude of the R_i values. The variation of the potential effects with progression of

exchange also increases with increasing α, as shown by the larger range in R_i values.

The effects of the concentration ratio in the bulk phase on R_i are investigated in Figures 17 through 19. The R_i curves for γ equal to zero are given by Kataoka's equation (38) for systems in which the concentration of the ion exiting from the exchanger is equal to zero in the bulk phase. For systems with γ less than 0.01, the R_i values are all within 0.5 percent of those values for the same system at infinite dilution. This is true for all values of the selectivity coefficient, since all of the R_i curves at a given γ have common beginning and ending points and the curves for a given selectivity coefficient all have the same curvature. The effect of γ on R_i are again diminished for the anion system (Figure 18), in which α is less than that for the cation system. Similar results are also found for the reverse exchange (Figure 19).

The impact of electric effects, as designated by R_i, on the rate of exchange for a typical cation system is shown in Figures 20 and 21. The exchange rates and nonionic mass transfer coefficient were calculated using Equations III-36 and III-25, respectively. The rates of exchange, excluding electric potential effects, are shown in Figure 20. The rates of exchange for the same systems, but including the R_i factor, are given in Figure 21. As shown in these two figures, the shape of the exchange rate curve is determined by the selectivity coefficient. The overall effect of the
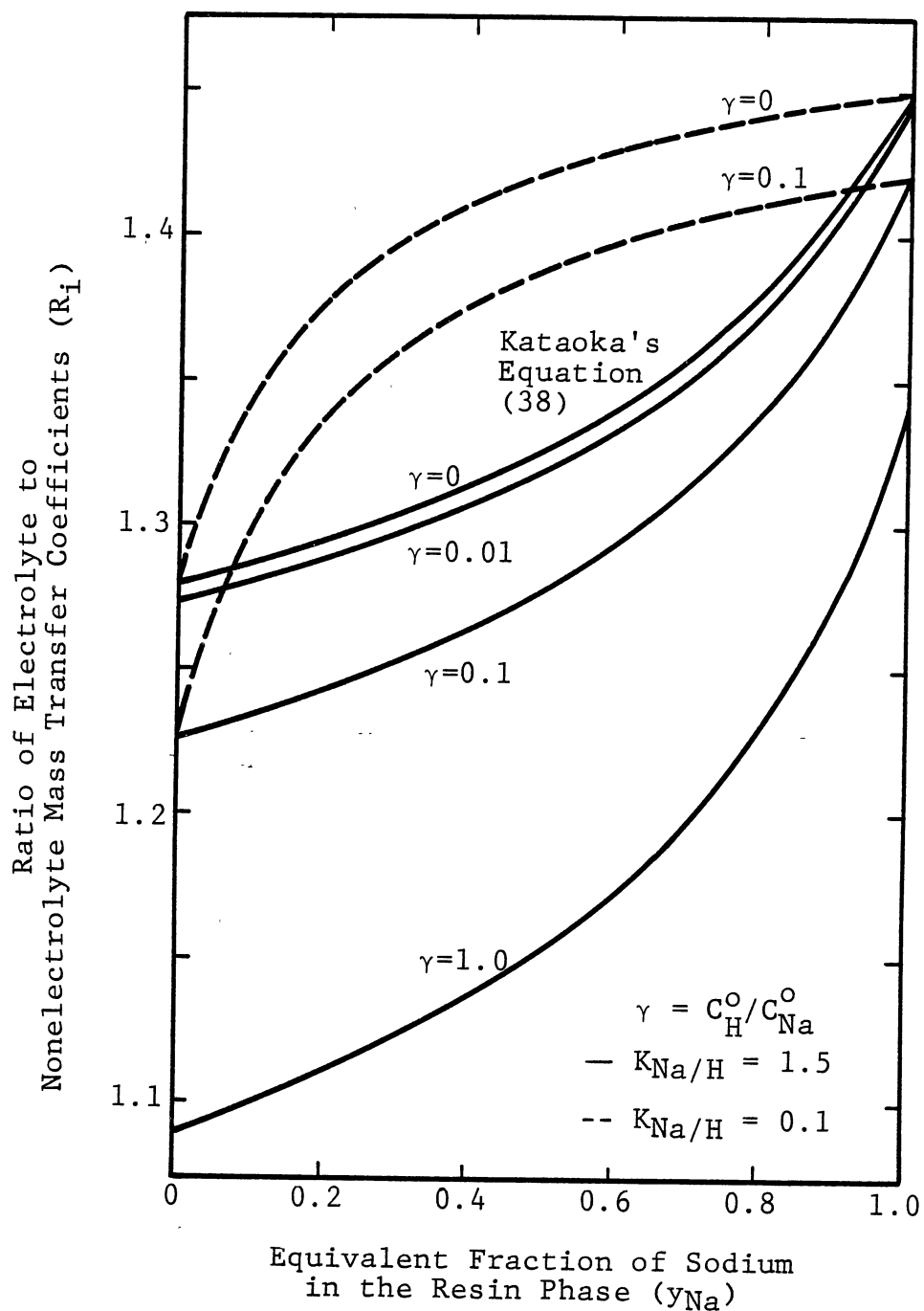
Figure 17. Variation of R_i with Bulk Phase
Concentration for Forward
Cation Exchange (Bulk Phase
Neutralization Model)
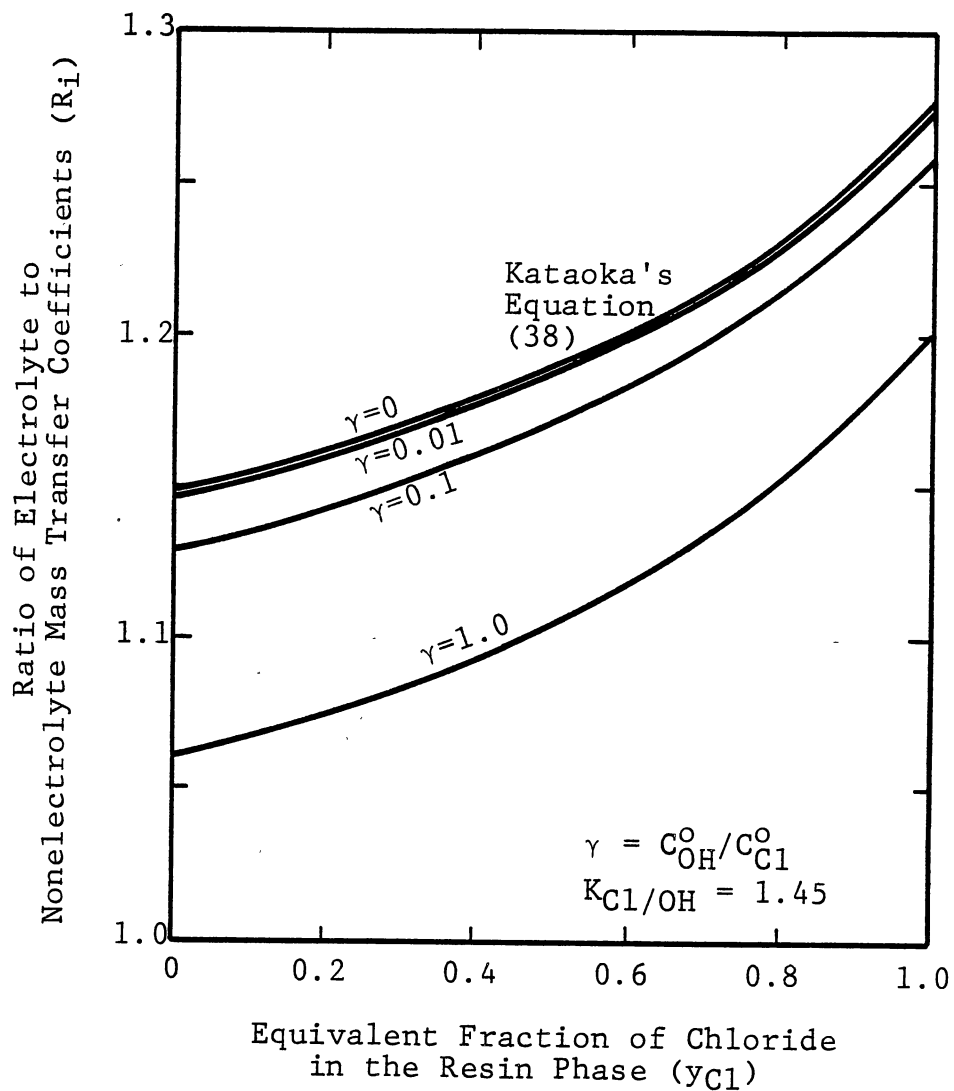
Figure 18. Variation of R_i with Bulk Phase
Concentration for Forward
Anion Exchange (Bulk Phase
Neutralization Model)
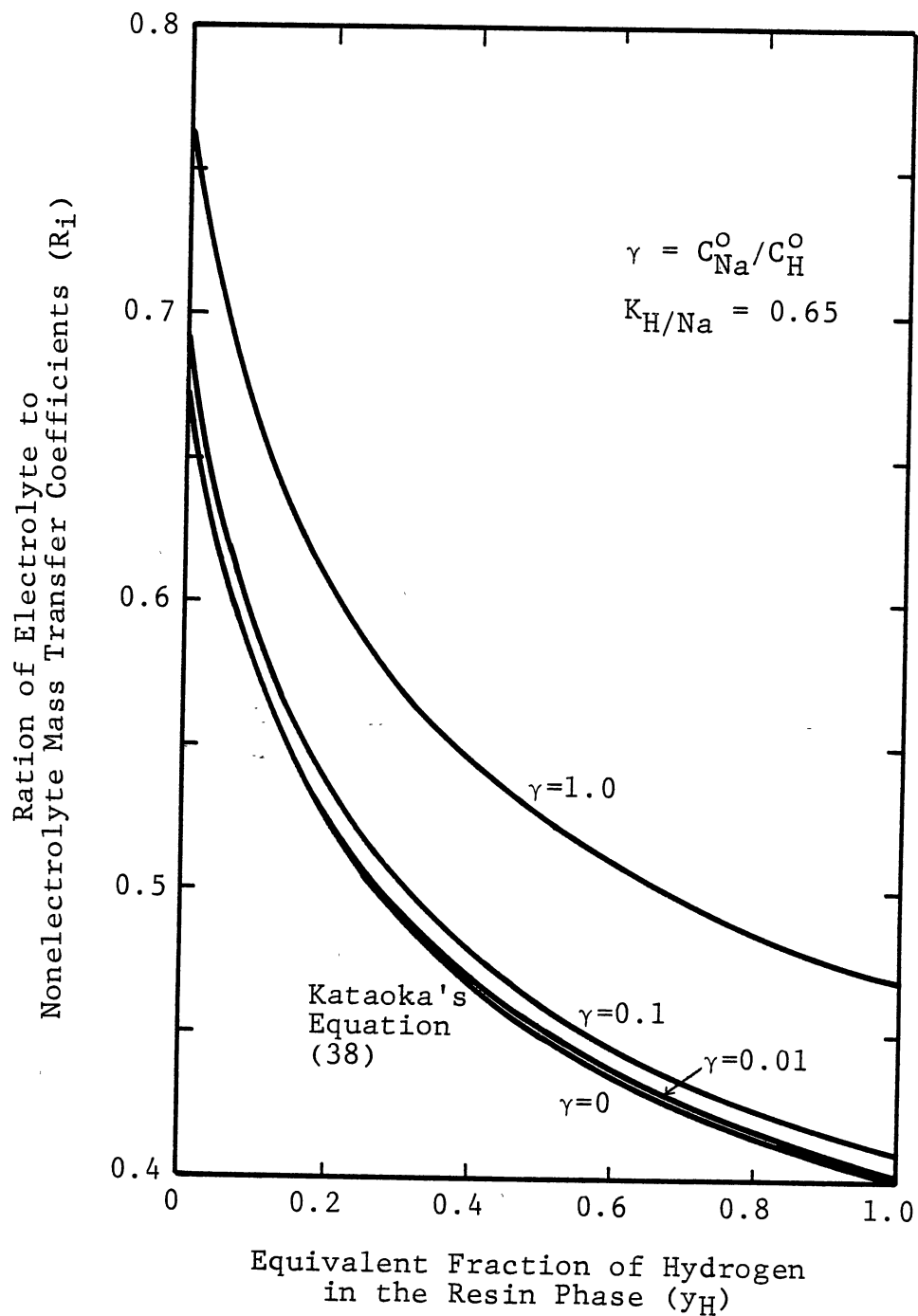
Figure 19. Variation of R_i with Bulk Phase
Concentration for Reverse
Cation Exchange (Bulk Phase
Neutralization Model)
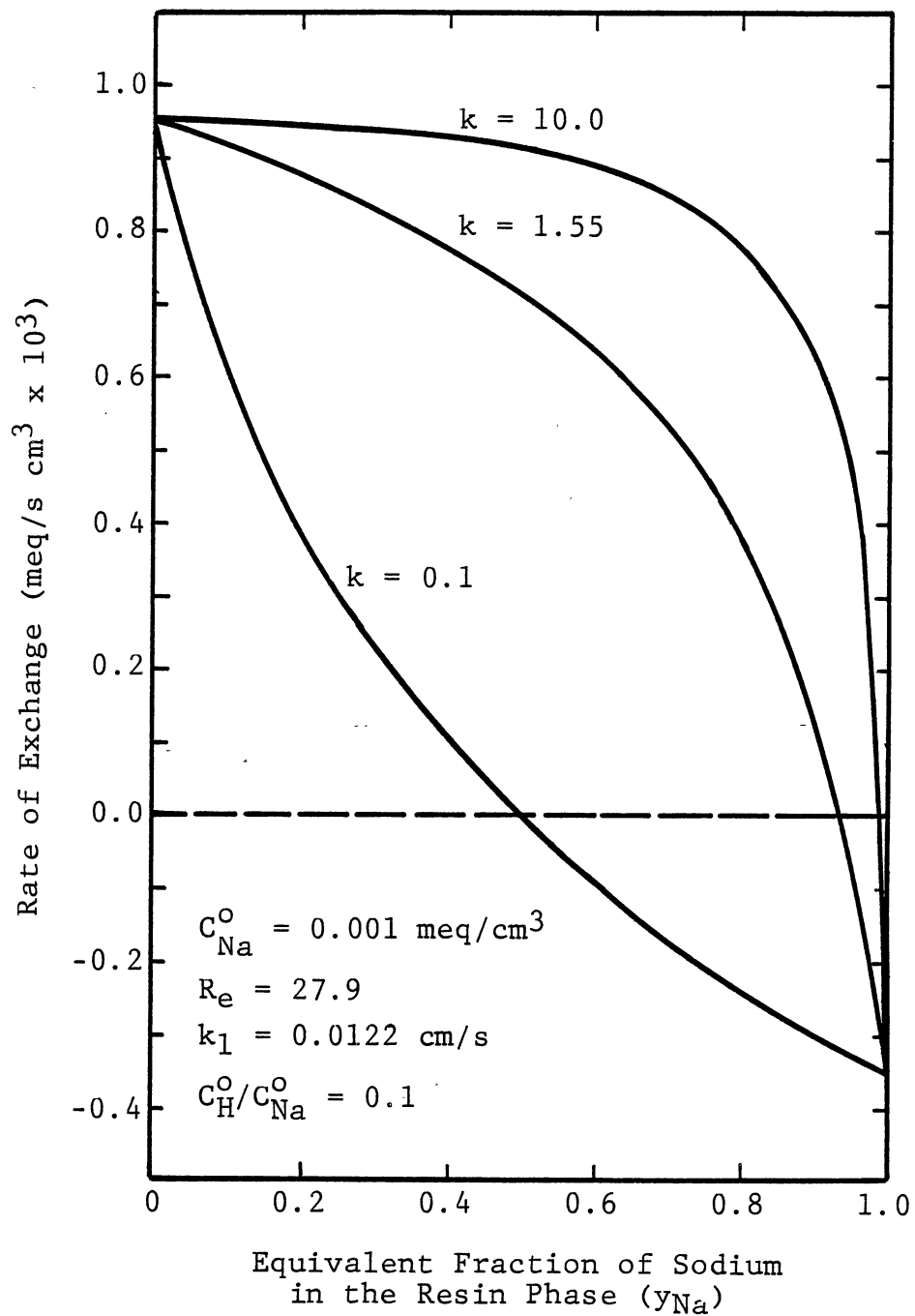
Figure 20. Variation of Exchange Rate with
y_{Na} and $K_{Na/H}$ for Forward
Cation Exchange with a
Constant Mass Transfer
Coefficient

Figure 20. Variation of Exchange Rate with
y_{Na} and $K_{Na/H}$ for Forward
Cation Exchange with a
Constant Mass Transfer
Coefficient
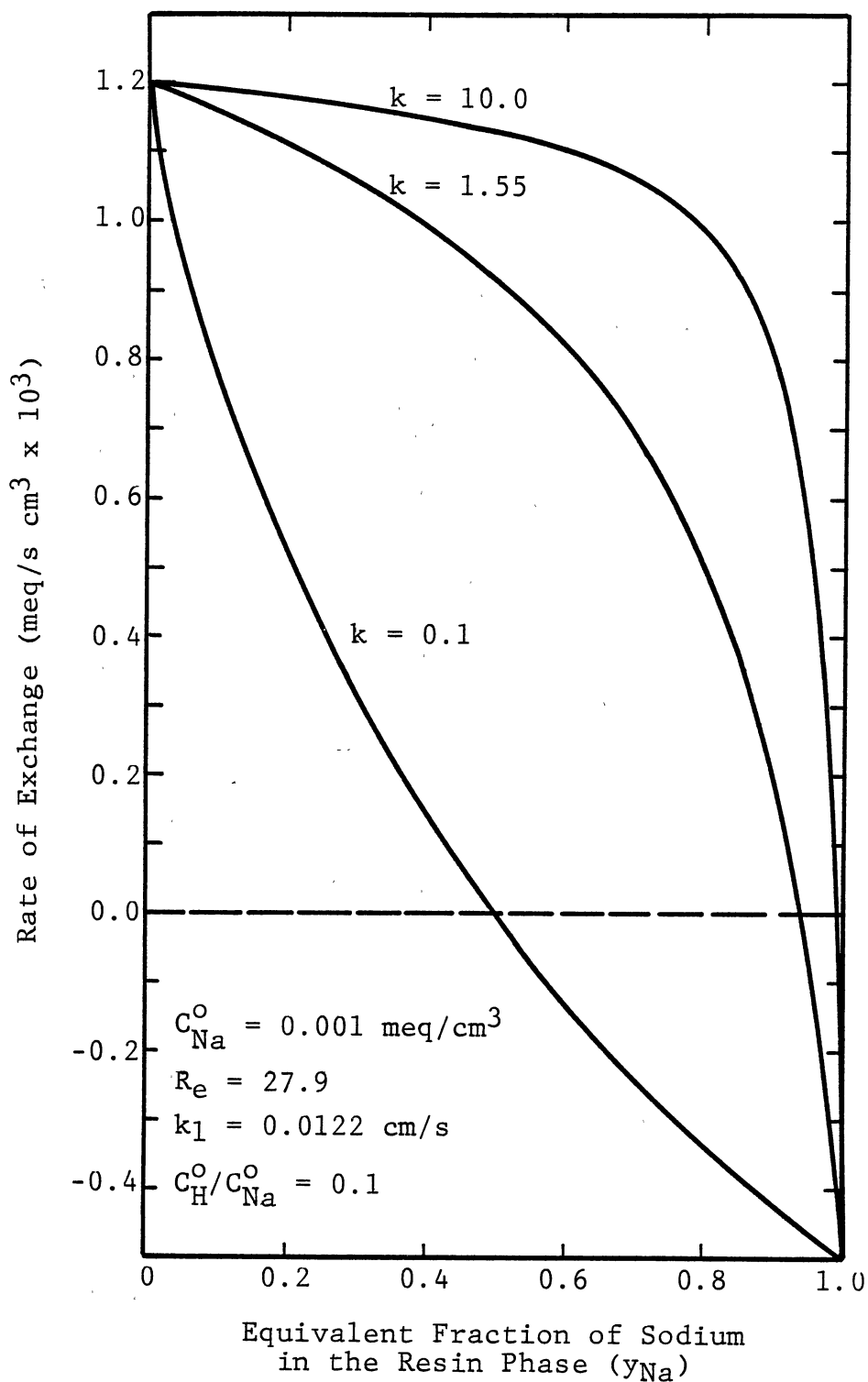
Figure 21. Variation of Exchange Rate with y_{Na} and $K_{Na/H}$ for Forward Cation Exchange Including Electric Potential Effects

electric potential is to increase the magnitude of the exchange rate. The electric effects are shown to have the greatest effect on the exchange rate during the early stages of exchange, even though the R_i factors have the largest variation toward the end of exchange. As the exchange resin approaches equilibrium, the concentration driving force goes to zero, and the rates shown in Figures 20 and 21 are equal. Similar effects are observed for the reverse exchange, except the overall effect of the electric potential is to decrease the magnitude of the exchange rate, as indicated by the R_i factors shown in Figure 15, 16, and 19.

It should be noted that the R_i curves presented thus far and in the remainder of this chapter are extended beyond the equilibrium value of y_i corresponding to the set bulk phase concentration ratio and selectivity coefficient. This is shown by the exchange rate curves given in Figures 20 and 21. The exchange rates are equal to zero at the y_{Na} values corresponding to equilibrium between the ions in solution and those in the exchange resin. The exchange rates are negative, or the reverse exchange is occurring for resin saturations higher than the equilibrium value. When the system reaches equilibrium, the interface concentrations are equal to the bulk solution concentrations, and the equilibrium value for y_{Na} is calculated using Equation III-33. In a column application, the concentration ratio in the bulk phase is constantly changing. As the solution concentration changes, the resin phase equilibrium capacity also changes

as dictated by the resin selectivity coefficient. It is quite possible in this application for a solution to contact a resin which is saturated above the equilibrium value corresponding to that particular solution concentration. Thus, the entire R_i curve may be required in column modeling.

Film Reaction Model

The derived flux expressions for the film reaction model, unlike those for the bulk phase neutralization model, are not independent of the number of coions in the film. The addition of each coion increases the complexity of the problem. This can be seen by comparing the model development of Kataoka (42) with the developments made in Chapter III. This complexity stems from the diffusion of coions, such as hydrogen for the anion resin, to the reaction front. Since the diffusion of one coion is coupled to the remaining coions, the fluxes of all ionic species must be considered.

The rigorous and simplified film reaction models impact the exchange rate equation in their ability to predict R_i values based on calculated hydrogen and chloride concentration profiles from the bulk phase to the reaction front in the film. The number of steps required in the differentiation and integration routines using the Runge-Kutta and Simpon's methods, respectively, was first investigated. The anion exchange system with a high chloride concentration

(0.1 M) and γ (C_h^o/C_c^o) in the range of 0.1-1.0 was used to determine the number of calculation steps required. This system has concentration gradients across the liquid film which are much larger than those in normal mixed bed systems. Thus, this system also requires more accurate integration. Integration and differentiation results using 5-40 increments were compared together. Recall that the concentration profiles are first established using the Runge-Kutta routine, and then the integration involved in determining R_i is performed based on the previously calculated concentrations. For all cases, increasing the number of integration increments above one-half the number of increments used in the differentiation yielded no increase in accuracy. The results using ten differentiation steps were within 0.1 percent of those using 20 and 40 steps. As γ is decreased, the results using different step sizes rapidly converge. For γ equal to 0.1, the results using 10 differentiation steps were within 0.01 percent of those using 40 steps. Thus, respective differentiation and integration increments of ten and five steps were used in all subsequent studies.

Results for the rigorous and simplified film reaction models were compared using the anion exchange system. R_i curves were calculated for chloride concentrations ranging from 0.1 M to 4.0×10^{-7} M, with γ(C_h^o/C_c^o) ranging from 1.0 - 1.0×10^{-4}. Note that the bulk phase hydrogen concentration (C_h^o) cannot be less than 1.0×10^7 M or the

neutralization reaction would no longer be occurring in the liquid film surrounding the anion resin. Instead, the bulk phase would be basic with the neutralization reaction occurring in the liquid film surrounding the cation resin, and the exchange rate for the anion resin would be given by the bulk phase neutralization model. Typical R_i results for the rigorous and simplified film reaction models are tabulated in Appendix C. The R_i values determined using the simplified model vary from those calculated using the rigorous model by less than 0.1 percent for all concentrations with γ less than or equal to 0.1. In mixed bed applications, γ will not be greater than 0.1 until the chloride or sodium concentration is less than 1.0×10^{-6} M. Concentrations of this small magnitude will only be found towards the bottom of the bed where the solution is contacted with resin of the lowest saturation. For concentrations of this order and γ approaching 1.0, the difference between the two models is still less than 0.3 percent for values corresponding to low resin saturation. For this study, only the front part of the breakthrough curve is of interest, since the exchange resistance due to particle diffusion has not been included in the model development. Thus, the simplified film reaction model is used in the current study. It should be noted here that the use of the simplified model does not neglect the effects of the hydrogen and hydroxide concentrations on the diffusion rates after the reaction plane, but only the effects due to

the fluxes of these ions are ignored since these fluxes are assumed to be equal to zero.

The position of the reaction plan during exchange is affected by the concentration ratio in the bulk phase, the bulk phase concentration, and the resin selectivity coefficient. Figures 22-24 show the effects of the concentration ratio in the bulk phase and the resin selectivity coefficient on the position of the reaction plane with the progression of exchange. These figures were calculated using Equation III-69 at a constant bulk phase chloride concentration of 0.01 M. The reaction plane position was found to be independent of the chloride concentration and to only depend on the concentration ratio in the bulk phase for solution concentrations greater than 1.0×10^{-4} M. The results shown in Figures 22-24 were duplicated using Kataoka's (42) film reaction model in which the concentrations of hydrogen and hydroxide are assumed to be equal to zero after the reaction plane.

The concentration ratio in the bulk phase has the largest effect on the position of the reaction plane during exchange. As γ approaches 1.0, the reaction plane moves to the particle-fluid interface (h=0). For γ less than 0.001, the neutralization reaction essentially occurs in the bulk phase (h=1) throughout the entire exchange process. The resin selectivity coefficient more strongly affects the shapes of the calculated curves rather than the total magnitudes. For favorable exchange (Figures 22 and 23), the
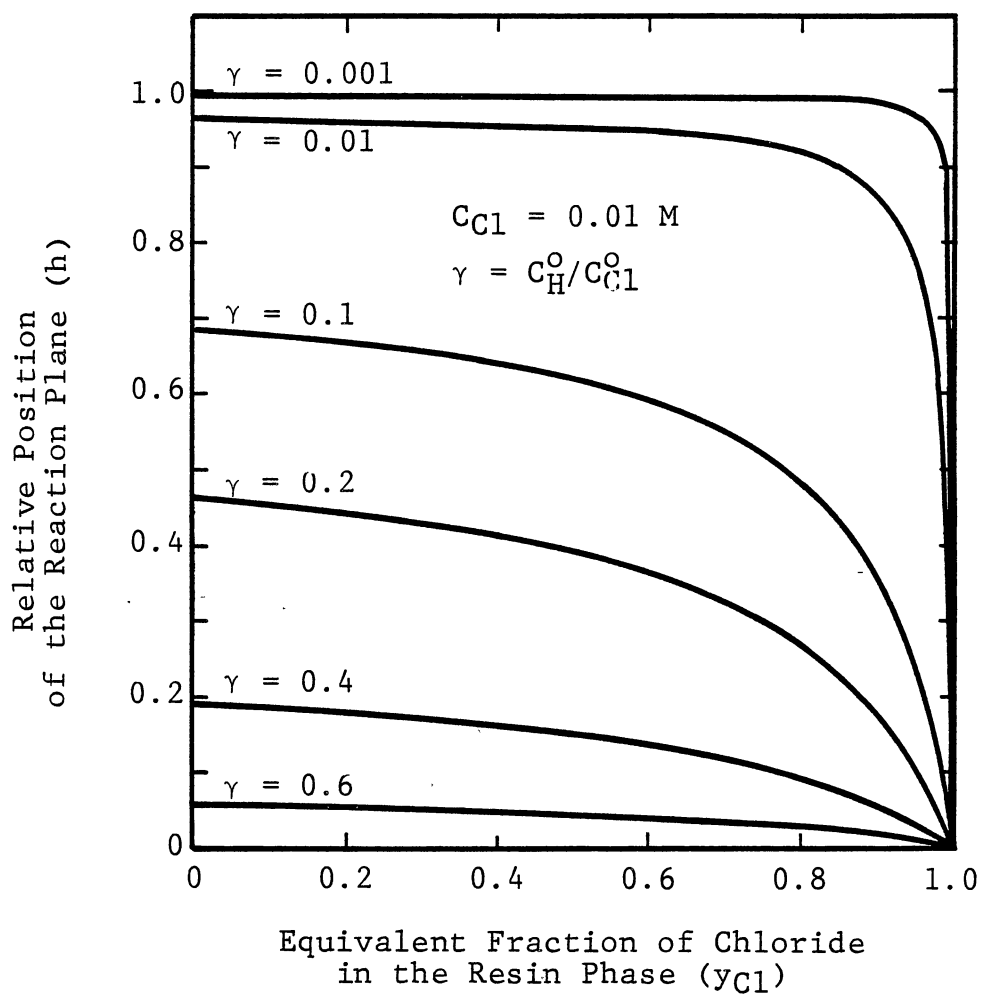
Figure 22. Variation of the Reaction Plane Position with Progression of Ion Exchange for High Solution Concentrations and $\bar{K}_{Cl/OH} = 1.45$
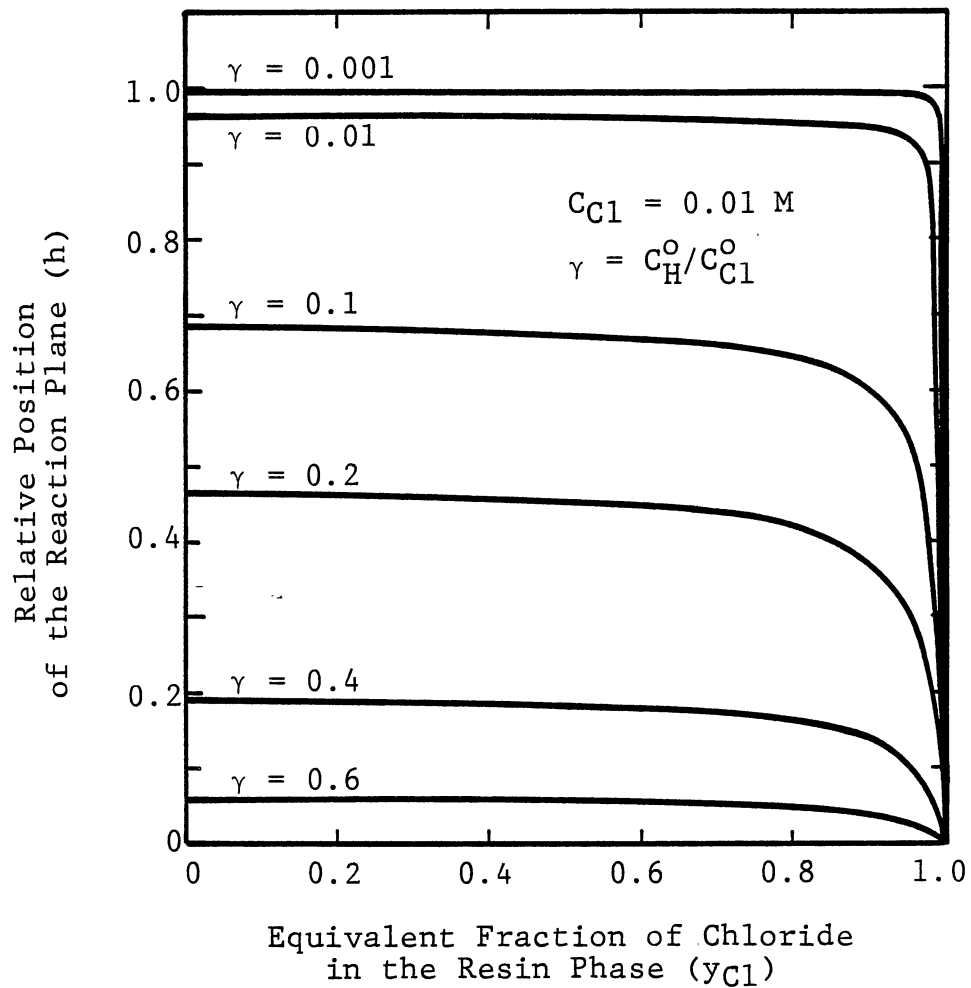
Figure 23. Variation of the Reaction Plane
            Position with Progression of
            Ion Exchange for High Solution
            Concentrations and $K_{Cl/OH}$ =
            10.0
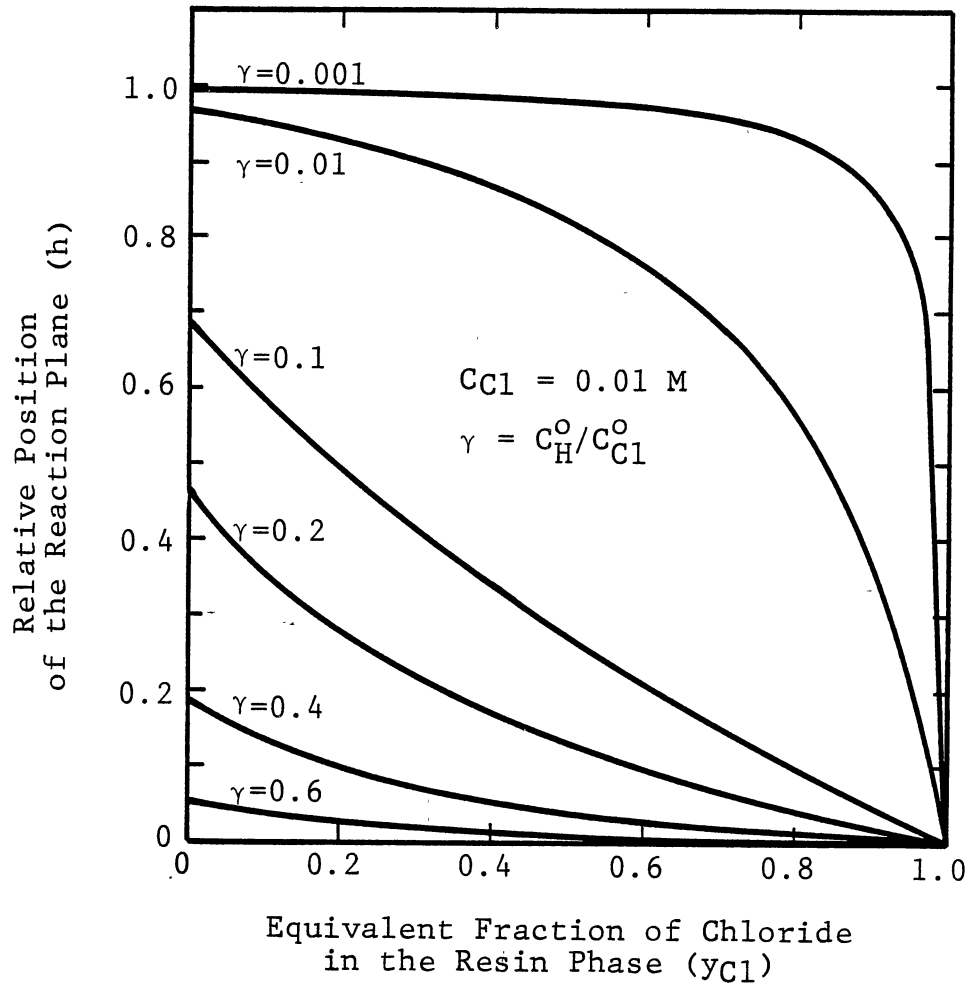
Figure 24. Variation of the Reaction Plane Position with Progression of Ion Exchange for High Solution Concentration and $K_{Cl/OH} = 0.1$

position of the reaction plane remains fairly constant until the exchange is almost complete. For unfavorable exchange (Figure 24), the reaction plane rapidly moves toward the particle-fluid interface with the progression of exchange. As the exchange resin becomes exhausted, the reaction plane moves to the particle-fluid interface for all cases.

The effects of the hydrogen and chloride ion concentrations on the position of the reaction plane rapidly increase for solution concentrations below 1.0×10^{-4} M. These effects are illustrated in Figure 25 for systems having γ equal to 0.2. The curve for a bulk solution concentration equal to 1.0×10^{-4} M is the same as presented in Figure 22. For a constant hydrogen to chloride ion ratio in the bulk phase, the reaction plane moves away from the particle-fluid interface as the solution concentration in the bulk phase decreases. Concurrent with this, the reaction plane moves to the particle-fluid interface at an equilibrium resin phase equivalent fraction which is less than one.

From the above results, there are two major effects in mixed bed units which are not accounted for by Kataoka's (42) film reaction model. In Kataoka's development, the position of the reaction plane is independent of the solution concentration and depends only upon γ. The results shown in Figure 25 indicate that this assumption may lead to serious errors in the prediction of exchange rates for systems with concentrations less than 1.0×10^{-4} M. The second major assumption in Kataoka's development is that the
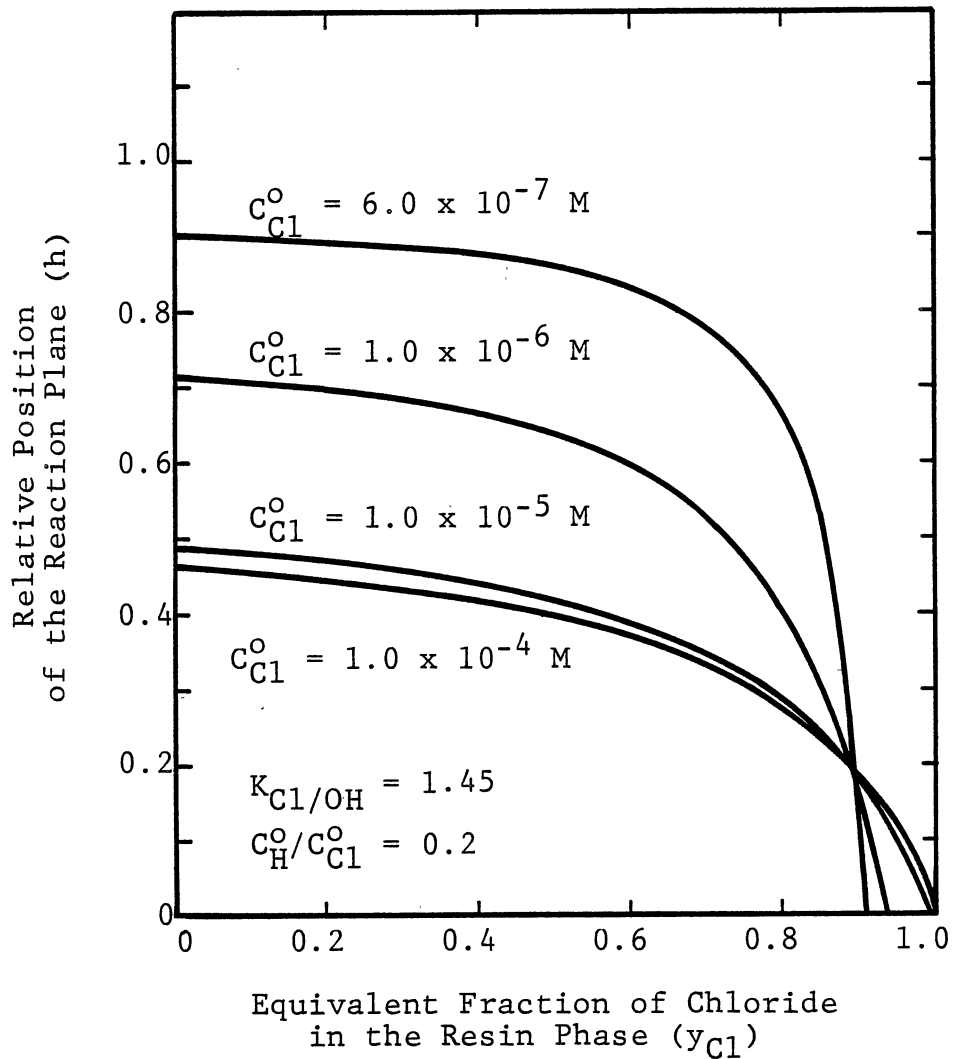
Figure 25. Variation of the Reaction Plane
Position with Progression of
Ion Exchange and Bulk Phase
Concentration for Low Solution
Concentrations

position of the reaction plane never reaches the particle-fluid interface until the exchange resin is completely saturated. Particularly important at low concentrations, the resin and solution phases may reach equilibrium and the reaction plane approach the particle-fluid interface well before the equivalent fraction of the ion entering the resin phase is equal to one.

The effects of the various system parameters on the position of the reaction plane, as previously discussed, are directly associated with the effects of these same parameters on the calculated R_i factors. The variations of R_i with y_{Cl} and γ for solution concentrations greater than 1.0×10^{-4} M are shown in Figure 26. These curves are again independent of the solution concentration and match those given by Kataoka's (42) film reaction model. These curves approach the bulk phase neutralization model or Kataoka's (38) solution for systems at infinite dilution when γ is less than 0.01. As γ approaches 1.0, the R_i factor becomes constant, as predicted by Helfferich (33) for strong acid or base reactive systems.

The effects of the bulk phase concentration on the R_i factor for solution concentrations less than 1.0×10^{-4} M are shown in Figure 27. The R_i curve corresponding to a bulk phase solution concentration of 1.0×10^{-4} M is the same curve as given in Figure 26 for γ equal to 0.2. As the solution concentration approaches 1.0×10^{-7} M, the R_i values calculated using the film reaction model converge to
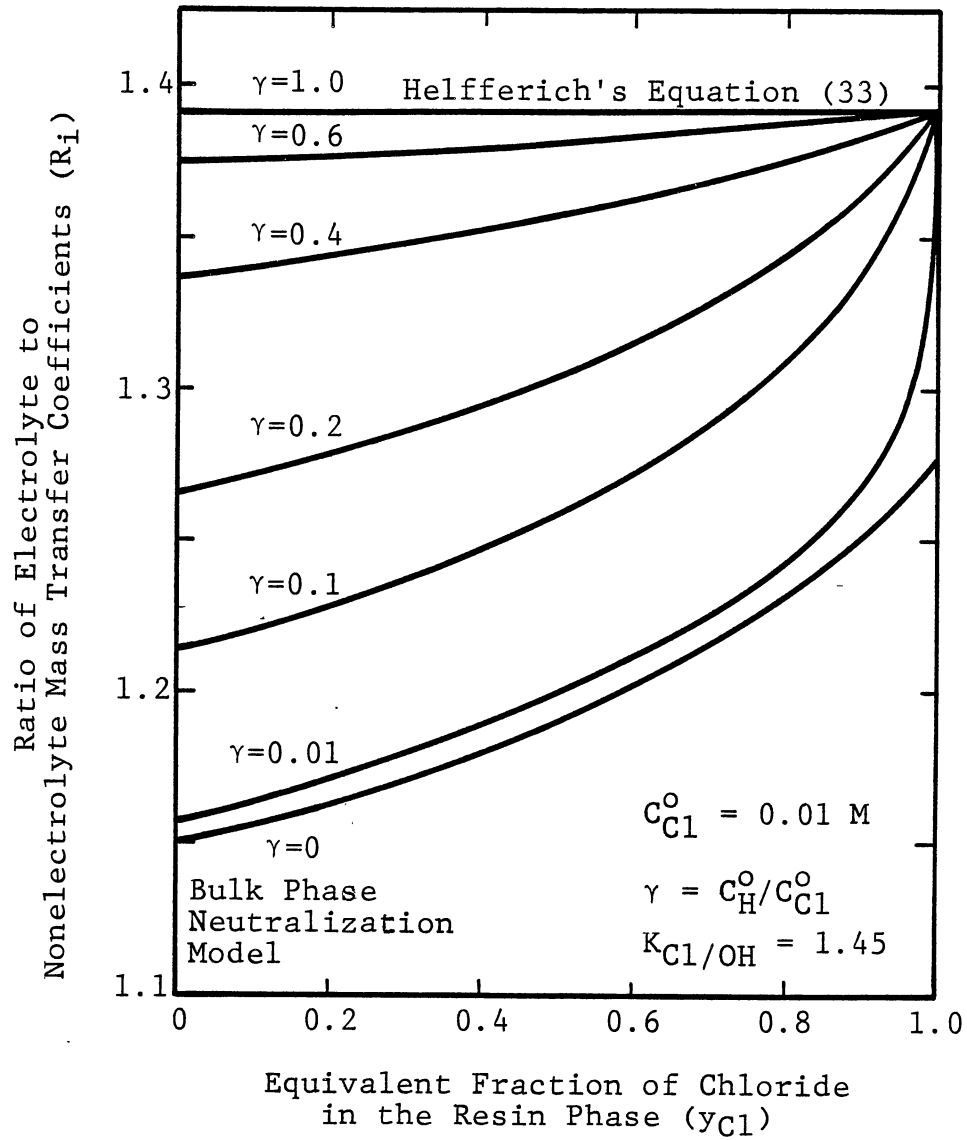
Figure 26. Variation of R_i with Bulk Phase
Concentration and Progression
of Ion Exchange for High
Solution Concentrations
(Film Reaction Model)
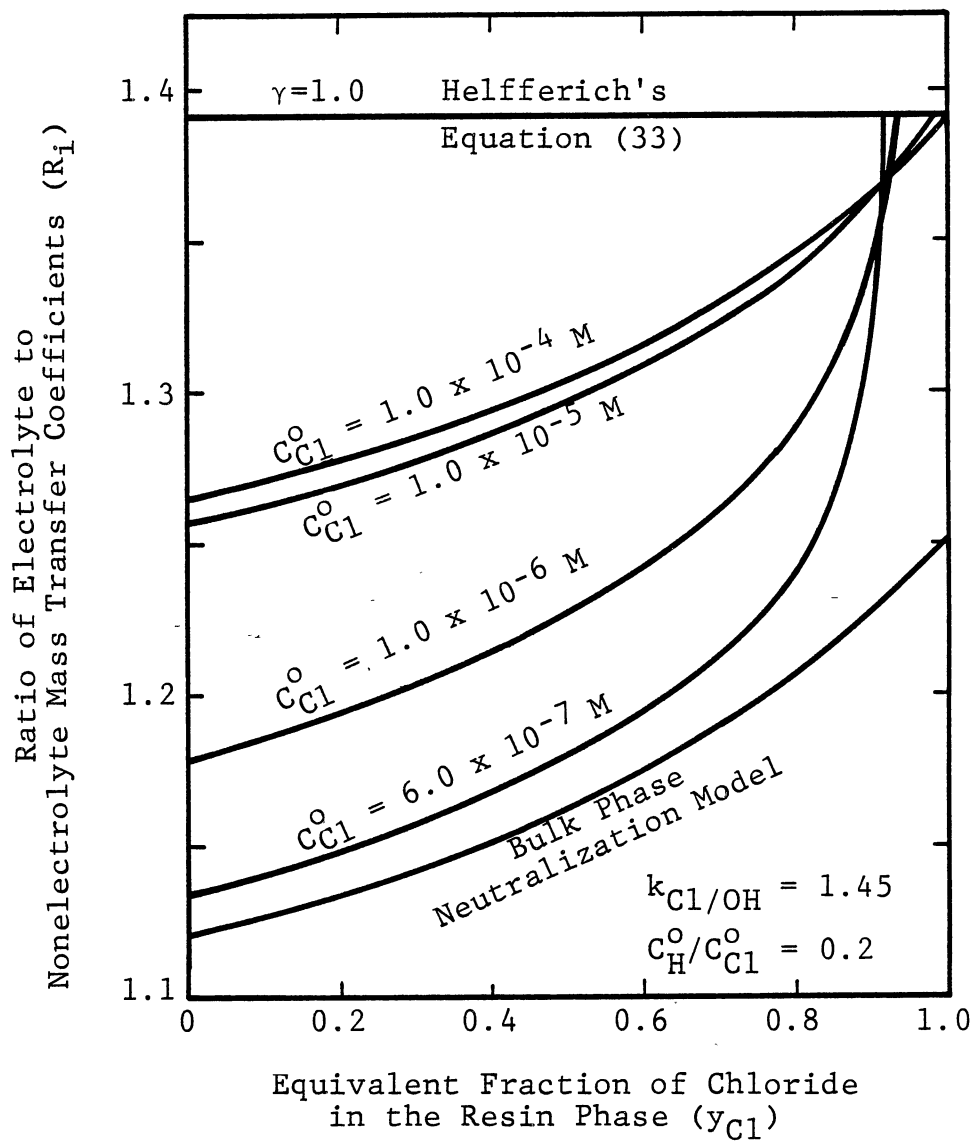
Figure 27. Variation of R_i with Bulk Phase
Concentration and Progression
of Ion Exchange for Low
Solution Concentrations
(Film Reaction Model)

values calculated with the bulk phase neutralization model. As the exchange resin approaches equilibrium, the R_i values approach those suggested by Helfferich (33). Helfferich's derivation was based on the assumption that neutralization takes place at the particle-fluid interface.

Prior to the establishment of equilibrium, the position of the reaction plane will reach the particle-solution interface due to the decreasing rate of exchange. As discussed earlier, this may even occur during the initial stages of the exchange process, depending on the ion ratios in the bulk phase. The exchange process with neutralization occurring at the particle-solution interface will be well simulated by the film reaction model as long as the hydrogen and chloride ion concentrations are equal to 1.0×10^{-7} M at the reaction plane. These concentrations are used as boundary conditions in the numerical methods used to solve for the ion concentration profiles between the bulk phase and the reaction plane.

When equilibrium is obtained, the ion concentrations at the particle-solution interface equal those in the bulk phase. Thus, there must be a short period near the establishment of equilibrium in which the concentration gradients level out as the interface neutralization reaction diminishes. This period of exchange is not accounted for in the film reaction model developed in this study nor in any previous reactive-ion exchange theories. Not accounting for this period of exchange results in a finite rate of exchange
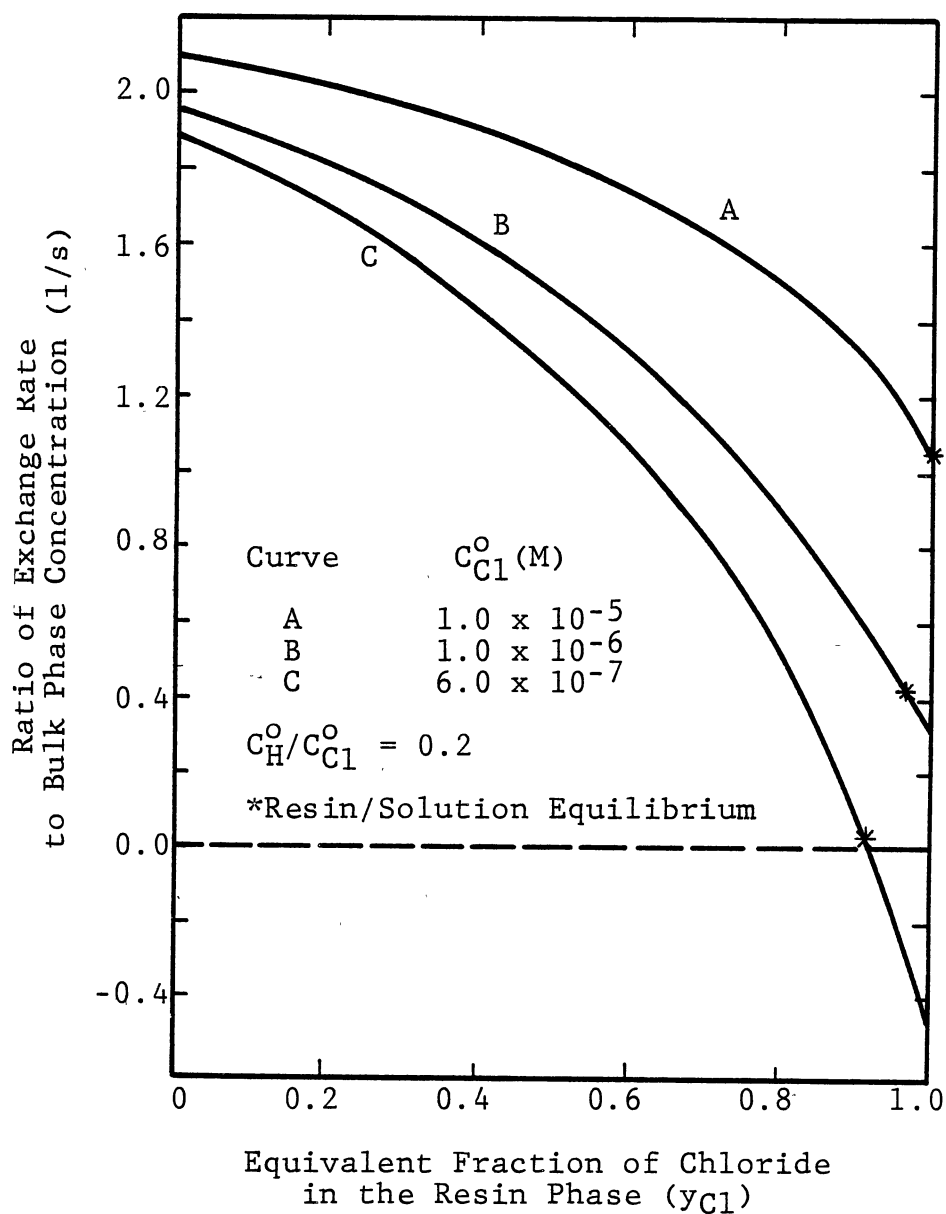
Figure 28. Variation of Exchange Rate
with Bulk Phase Concentra-
tion and Progression of
Ion Exchange (Film Reaction
Model)

at equilibrium as shown in Figure 28. As the bulk phase concentrations approach 1.0×10^{-7} M, the predicted rates of exchange at equilibrium approach zero.

Kataoka's (42) reactive exchange model duplicates curve A in Figure 28. Recall that his solution is independent of the bulk phase concentration. Kataoka does not give rate curves in his publication nor address the fact that his model predicts a finite rate of exchange at equilibrium. Helfferich (33) assumes that this period of exchange is negligible and sets the exchange rate equal to zero after equilibrium is obtained. The chloride ion mole fractions in the resin phase at equilibrium for solution concentrations corresponding to curves A, B, and C in Figure 28 are 0.9996, 0.967, and 0.912, respectively (Equation III-33). From Figure 25, the reaction plane position corresponding to each of these solution concentrations does not reach the particle-solution interface until the chloride ion mole fractions in the resin phase are 0.98, 0.94, and 0.91, respectively. The boundary conditions used in the film reaction model along with the predicted exchange rates are at least valid up to these resin saturation values. Thus, the exchange rate curves in Figure 28 should rapidly decrease to zero within the last two-hundredths of the chloride ion mole fraction in the resin before the equilibrium value is reached.

From Figure 28, the use of the exchange rate, as predicted by the film reaction model, with an instantaneous

decrease to zero at equilibrium will closely simulate the actual exchange rate curve. The predicted exchange rate will also be bounded by the bulk phase neutralization model and the published developments of Helfferich and Kataoka. For resin saturations above the equilibrium value, the reverse exchange will occur and the film reaction model is not representative of the actual exchange process in this region. The simulation of this region of exchange requires solving the same flux equations as solved for the film reaction model but with different boundary conditions and system restraints.

Mixed Bed Applications

The column material balance and exchange rate expressions, as previously developed, were used to simulate sodium-chloride mixed bed systems. A source listing of the simulation program, along with the required input data, and a general program description are given in Appendix D. The material balances for the cation and anion resins (Equations III-84 through III-87) are simultaneously integrated along characteristic lines of constant τ and ξ. The concentration profiles down the column at a constant τ are first determined by integrating the material balances with respect to ξ using the improved Euler technique. This results in a horizontal sweep across the calculational matrix. The equations are then integrated with respect to τ using the backward finite difference method and another horizontal

sweep is made. With this approach, the calculations are continued until the ion concentrations in the column effluent reach a predetermined fraction of the concentrations in the feed solution.

The integration increments for τ and ξ were based on the physical properties of the cation resin. Respective dimensionless increments of 0.04 and 0.01 were used in the column simulations. The ξ increment corresponds to approximately 0.25 cm, depending on the resin properties. The time increment represented by τ is inversely proportional to the feed solution concentration (Equation III-78). The τ increment of 0.04 corresponds to approximately twelve minutes for feed concentrations of 0.001 M. For feed concentrations below 0.0001 M, τ was decreased to 0.004. For a given feed concentration, column integrations were relatively insensitive to the magnitude of τ. The error in predicted concentration profiles gradually increased as τ was made larger. Column results were very sensitive to variations in the size of the ξ increments. Predicted concentrations were in error by several percent for ξ increments of 0.02, and this error rapidly increased for larger increment sizes. These sensitivities can be explained by the concentration profiles within the column. Solution concentrations are quickly reduced with progression through the exchange bed. However, the solution concentrations at a given distance from the column inlet are

relatively stable with time as the active ion exchange zone moves slowly down the column.

At each calculational mesh point, the rate of exchange for the two resins is calculated by either the bulk phase neutralization or film reaction models. The film reaction model is used for the cation and anion resins when the bulk phase hydrogen concentration is less than 0.5×10^{-8} M and greater than 1.5×10^{-7} M, respectively. Otherwise, the bulk phase neutralization model is used. From the above conditions, the bulk phase neutralization model is used for both resins when the hydrogen concentration is in the range of $(0.5-1.5) \times 10^{-7}$ M.

Column simulations were performed for laboratory scale mixed bed units. For parameter studies, a column length of 40 cm was used. The processing time and the corresponding computer cost were very sensitive to the column length due to the small magnitude of ξ increments required for computational accuracy. Approximately 70 seconds of processing time was required on an IBM 3081D computer system to obtain the full breakthrough curve. This time will vary somewhat, depending on the inlet concentration and other system parameters. Plant scale units are normally 1.5-2.5 meters in length with fluid linear velocities similar to those used in this study. Thus, a plant scale simulation may require as much as ten minutes of comparable computing time. Because of this excessive processing time, a more elaborate method of integration with respect to distance down the

column (ξ) should be implemented so that larger increments may be used without sacrificing accuracy of results. A four point Milne predictor-corrector method may be one such possibility.

Program storage requirements were kept to a minimum level so that the program could be readily run on a micro-computer. The concentration profiles through the column are stored for only four consecutive time (τ) increments. With the current method of integration, only the concentration profile from the preceding time increment is required at a given calculation point. More elaborate integration methods, as previously suggested, may require all four of these consecutive profiles. Because of this storage approach, the concentration profiles or breakthrough curve must be printed during the calculation iterations. Using double precision, the simulation program requires approximately 400K of storage space. This can be readily reduced by only storing two consecutive concentration profiles if more elaborate integration techniques are not used.

The utility of this model development and a typical program application are demonstrated by calculating break-through curves for a sodium-chloride mixed bed unit with varying cation to anion resin ratios. Typical cation to anion resin ratios used in industrial practice range from 1:1 to 2:1. The sodium and chloride breakthrough curves are shown in Figures 29 and 30, respectively. A feed
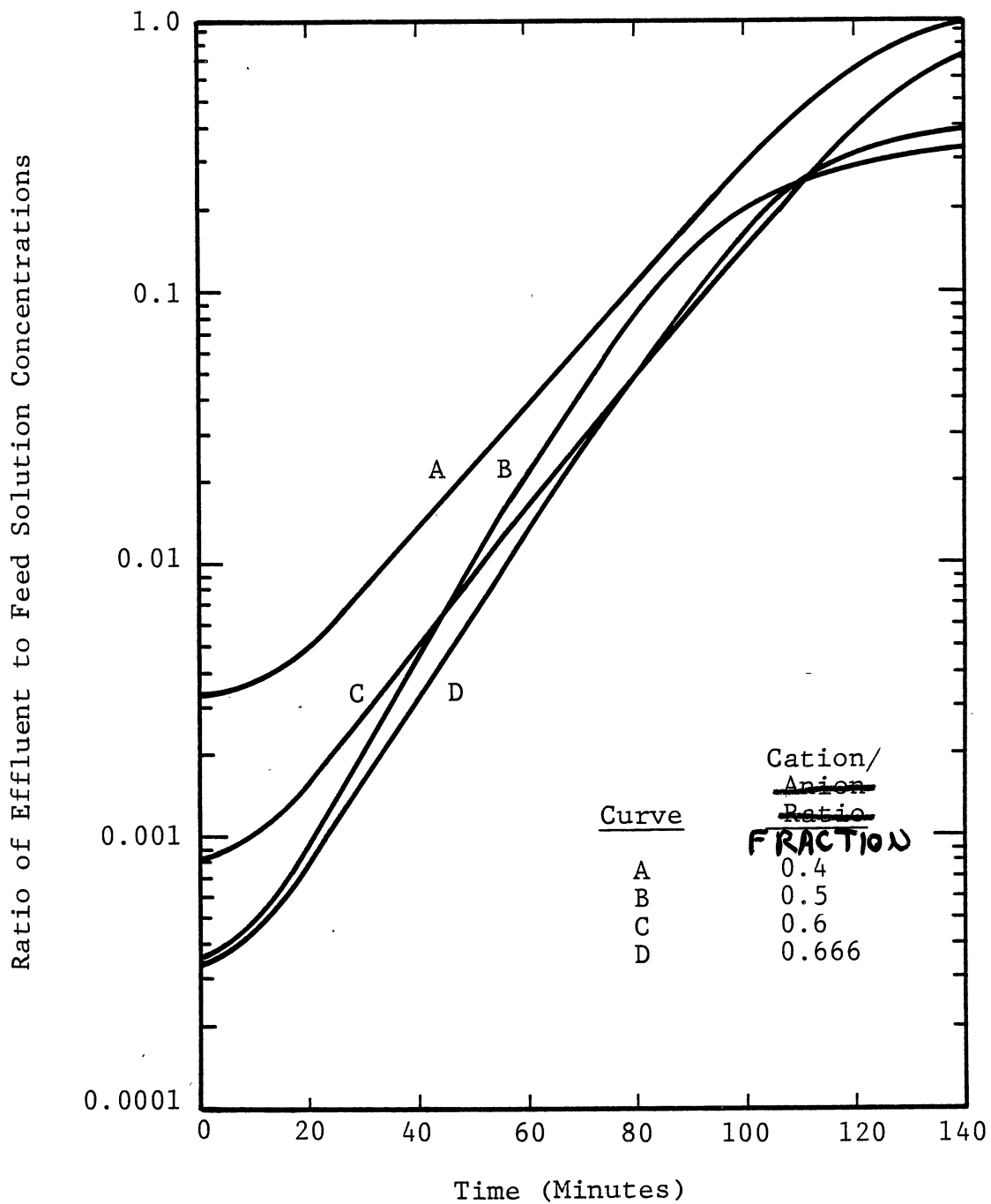
Figure 29. Sodium Breakthrough Curves for Mixed Bed Simulations with Varying Cation to Anion Resin Ratios
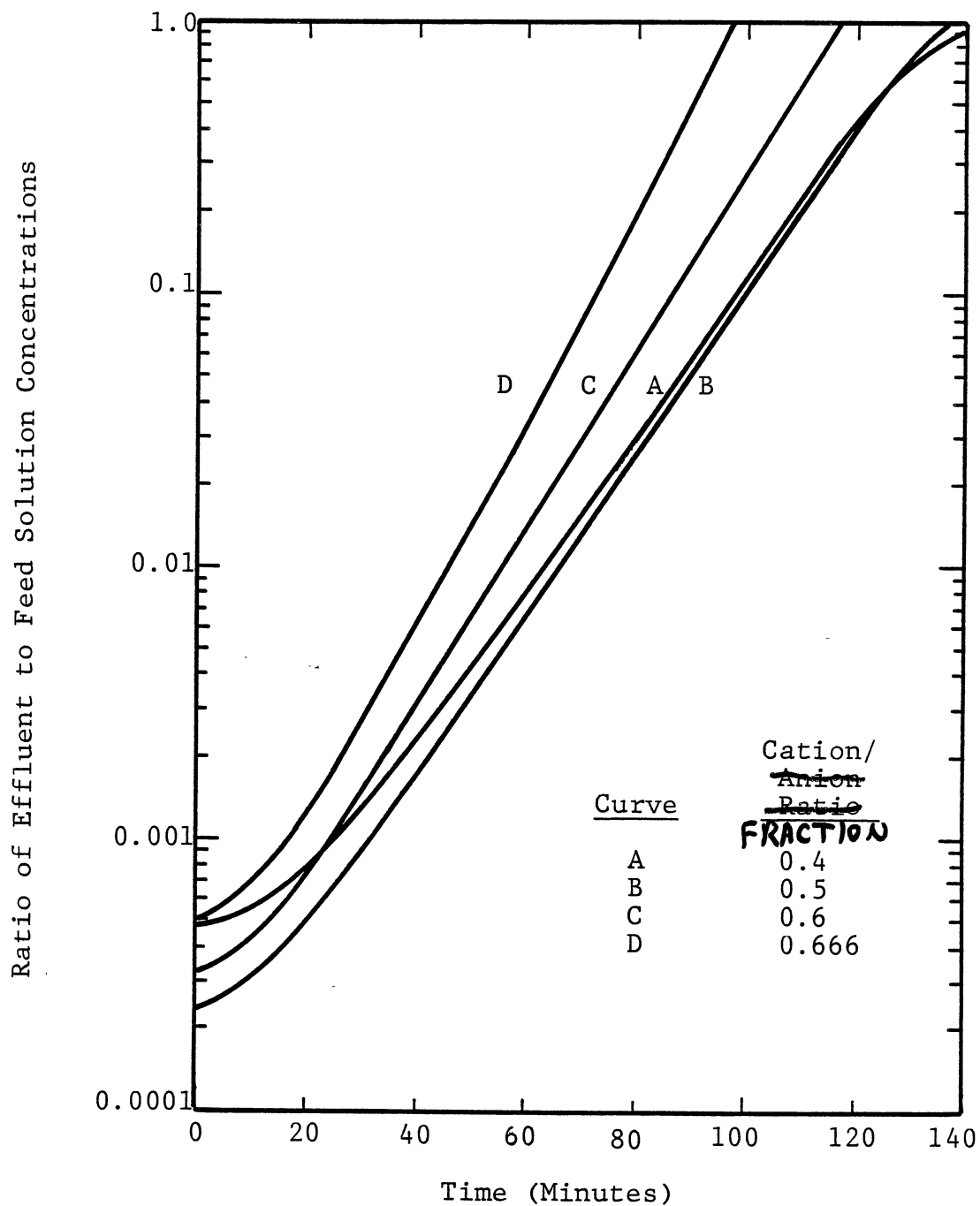
Figure 30. Chloride Breakthrough Curves for
            Mixed Bed Simulations with
            Varying Cation to Anion Resin
            Ratios

concentration of 0.002 M and a column length of 40 cm was used in these simulations. The other system parameters are typical of mixed bed units and are listed in Appendix E. The breakthrough curves are shown as a ratio of the effluent to feed solution concentrations. The dimensionless time has been converted to minutes based on the elapsed time beginning with the discharge of feed solution from the column. As shown in Figures 29 and 30, the ratio of exchange resins in the unit effects the overall capacity of the exchange bed as well as the lower concentration limits in the effluent solution. The lowest total effluent concentration was obtained for a cation to anion ratio of 1.5:1 (Case C). This corresponds well with the industry practice.

Figure 31 shows the sodium and chloride concentration profiles within the mixed bed for Case C of Figures 29 and 30. These profiles show the cause of the large deviations between the sodium and chloride breakthrough curves as the resins approach equilibrium with the feed solution. As the resins become saturated, the anion resin capacity is first exhausted. This results in an acidic solution wave as the cation resin continues to exchange hydrogen for sodium ions. The cation resin in this wave is simulated with the bulk phase neutralization model. When the acidic wave reaches the active anion exchange zone, the neutralization reaction occurs in the film surrounding the anion resin. The effects of the film neutralization reaction are to increase the
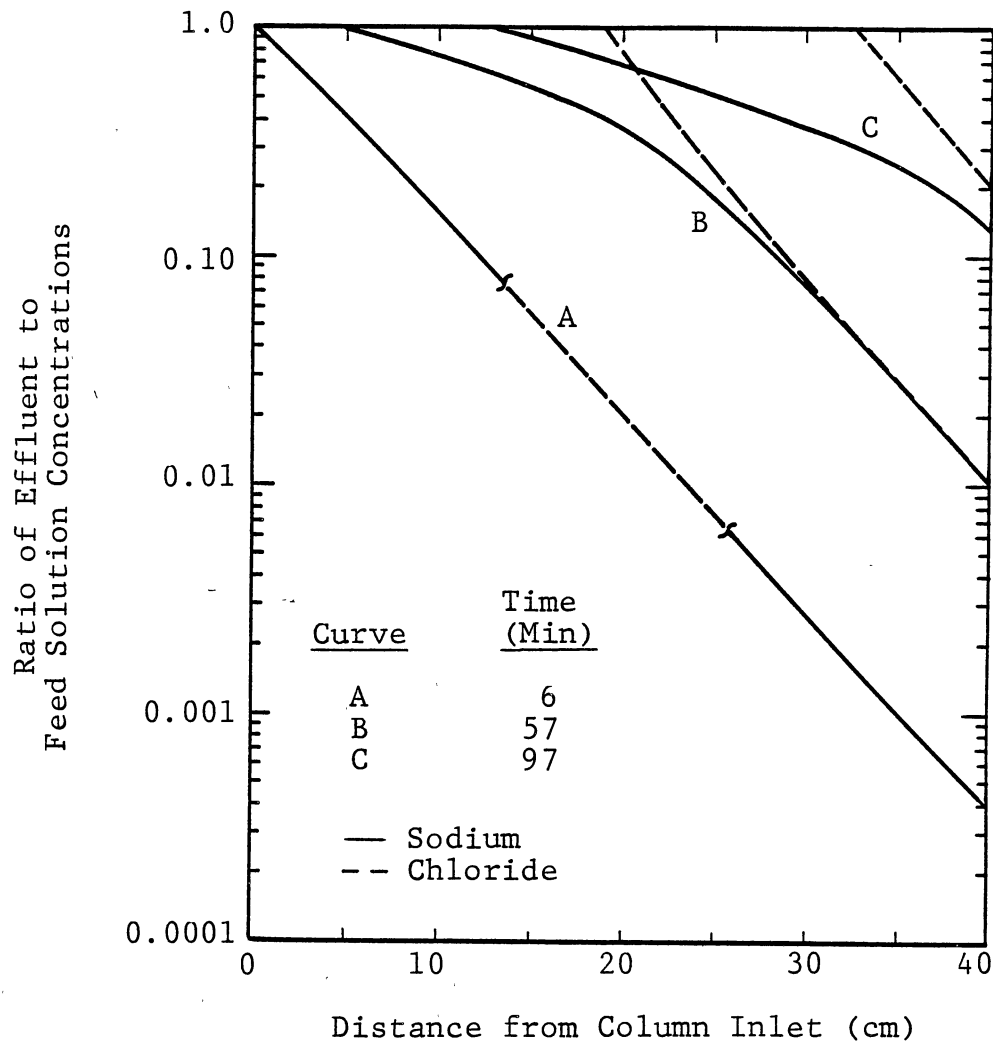
Figure 31.   Variation of Sodium and Chloride
             Concentration Profiles with
             Time and Distance (Cation/
             Anion Ratio = 0.6)

anion exchange rate, equalize the sodium and chloride concentrations, and neutralize the acidic wave. The sharp approach of the chloride concentration profiles to the equilibrium values is due to the finite rate of exchange at equilibrium as predicted by the film reaction model.

Detailed mathematical studies of mixed bed parameters, such as the resin ratio, exchange capacities, and particle sizes have not been possible with previous models for mixed bed exchange. Besides the study of the above parameters, this model predicts the lower limit for mixed bed exchange. In the example application, initial effluent concentrations less than 1.0×10^{-6} M were predicted. Mathematical studies of the lower exchange limit have not been made before due to the lack of rate models which are applicable at these concentration levels.

Suitable experimental data for confirming the reactive ion exchange rate expressions and column simulations at concentration levels for which the model was developed were not discovered in the published literature. As previously mentioned, only a very few experimental results of laboratory quality mixed bed studies have been published. The experimental breakthrough curves of these studies were modeled by essentially curve-fitting the data points through adjustment of the film thickness, mass transfer coefficients, or dimensionless quantities in the rate expressions. Complete descriptions of the experimental parameters in these studies were not given, and the results

were not modeled with the current simulation program. For solution concentrations above 1.0×10^{-4} M, the rate equations give results identical to those of Kataoka (42) and Helfferich (33) which have been experimentally confirmed.

CHAPTER V

CONCLUSIONS AND RECOMMENDATIONS

Conclusions

The study reported in this thesis included (a) the development of rate expressions for reactive ion exchange at low solution concentrations and (b) the application of these equations to mixed bed ion exchange. The major points from this study are summarized below:

Bulk Phase Neutralization Model

1. The ion flux expressions for the bulk phase neutralization model are independent of the number of coions in the system. All coion fluxes are equal to zero, and the coion terms in the flux expressions mathematically cancel out. Thus, the addition of coions to a nonreactive system containing a single type of resin (cation or anion) will only influence the exchange rate through effects on the boundary conditions of the exchange system.

2. This model is based on Kataoka's (38) derivation for ion exchange in which the exiting ion concentration is equal to zero in the bulk phase. The derivation is applicable to nonreactive exchange as well as exchange with neutralization in the bulk phase. The most rapid exchange

131

occurs when the exiting ion concentration is equal to zero. Results for this case reduce to those given by Kataoka. As the exiting ion concentration in the bulk phase increases, the exchange rate and electric potential effects decrease.

3. The electric potential effects on the mass transfer coefficient depend upon the exchanging ion diffusivities, selectivity of the resin, fraction of resin exhausted, and ratio of exchanging ion concentrations in the bulk phase. The electric potential effect is independent of the total ion concentrations.

4. For a given resin selectivity, the effects of the electric potential increase with the progression of exchange. This effect is offset by the decreasing concentration driving force as the resin approaches equilibrium with the solution. Thus, the strongest effects of the electric potential on the overall rate of exchange occur during the initial stages of exchange. The equilibrium concentrations are not influenced by the electric potential.

Film Reaction Model

1. The addition of coions to a reactive exchange system increases the complexity of the rate expressions. The rate of exchange in a reactive system may be controlled by the diffusion of coions to the reaction plane as well as the diffusion of the exchanging ions.

2. For exchange systems involving a water neutralization reaction in the solution phase, the neutralization

reaction may be considered irreversible and the concentration of the dissociation products after the reaction equal to zero for solution concentrations as low as 1.0×10^{-4} M. Results for these concentrations reduce to earlier developments of Kataoka (42).

3. For solution concentrations below 1.0×10^{-4} M, the assumptions of irreversible neutralization and negligible concentrations of hydrogen and hydroxide ions after the reaction plane are no longer valid. The ions from water dissociation have an increasingly strong influence on the position of the reaction plane within the film, and the rate of exchange as the solution concentrations are decreased to 1.0×10^{-7} M.

4. The electric potential effects on the mass transfer coefficient and the position of the reaction plane within the film are dependent upon the total ion concentrations in the bulk phase as well as those variables mentioned in the third conclusion for the bulk phase neutralization model. The ion concentration ratio of interest for reactive ion exchange is the ratio of the reacting coion to entering counterion concentrations (γ). The neutralization reaction essentially occurs in the bulk phase throughout the entire exchange process when γ is less than 0.001. The reaction plane again approaches the bulk phase as solution concentrations decrease to 1.0×10^{-7} M.

5. Results of the film reaction model are bounded by earlier solutions of Helfferich (33) and Kataoka (42). The

model is strictly applicable only when the hydrogen and hydroxide ion concentrations at the reaction plane are equal to 1.0 x 10^{-7} M. These values are used as boundary conditions in the numerical methods used to solve the flux equations. Similar to all previously developed reactive ion exchange theories, this results in predictions of a finite rate of exchange at equilibrium. However, this effect is negligible in applications of extremely low concentrations for which this model was developed.

Mixed Bed Applications

1. The film reaction model allows for the separate treatment of cation and anion resins in mixed bed units. This in turn presents a method for systematic mathematical studies of the effects of differing cation and anion resin properties on the operation of mixed bed units. Previous to this development, the cation and anion resins in a mixed bed were most effectively modeled as a single salt removing resin. This model also predicts effluent concentrations on the order of parts per billion while accounting for the effects of a finite exchange rate, dissociation of water molecules, and reversible exchange.

2. For feed solution concentrations of 0.002 M, column integrations using τ and ξ increments of 0.02 and 0.01 predicted results which were within 0.5 percent of those using respective integration increments of 0.001 and 0.005. The integration error is very sensitive to the size of the ξ

increment but relatively insensitive to variations in the τ increments. These sensitivities result from the rapid decrease of impurity concentrations with solution progression through the column but the relatively slow movement of the active exchange zone down the exchange bed.

3. Test simulations were made of a laboratory scale mixed bed column using typical mixed bed parameters with four different cation to anion resin ratios. The lowest impurity levels were predicted for a cation to anion volume ratio of 1.5 to 1. This is consistent with industrial practice.

Recommendations

The rate expressions and mixed bed column simulation developed in this study allow mathematical studies of various resin and column parameter effects which have not been possible with previous reactive ion exchange models. The following recommendations are made concerning extensions of this model and areas of future work.

1. The effects of a third nonreactive exchanging ion on the reactive exchange system should be determined. The flux equations for this case can be readily derived by the inclusion of an additional flux equation for the third ion in the development of Chapter III. The accuracy of this extension depends on the ability to predict equilibrium relationships for the ternary exchange systems. There is a

serious need for further development and research in this area.

2. The effects of a second reactive ion, such as a weak acid or base, on the exchange system should also be investigated. Results of this development will allow simulations of complex industrial mixed bed units. These simulations will again require the ability to predict equilibrium relationships for higher order exchange systems.

3. In this study, a mass action type of equilibrium relationship was employed, as this is most often used in ion exchange rate investigations. The rate expressions could also be solved using Freundlich, Langmuir, or other applicable equilibrium relationships.

4. Kunin (22) suggested that ion exchange rates vary approximately with the absolute temperature raised to the 6.2 power. The simulations made in this study used ionic diffusivities and system parameters evaluated at 25°C. Temperature dependence may be added to the current model by the inclusion of temperature effects on the ionic diffusivities, water dissociation, solution viscosity, and resin equilibrium constants.

5. The inclusion of particle diffusion control in this model will enable the simulation of periods of intermittent service, performance cycles, and continuing operation past breakthrough. Very efficient methods of numerical integration must be used or extremely large computational times will be required.

6. The film reaction model developed in this study is strictly applicable only when the concentrations of the water dissociation products at the plane of reaction are equal to 1.0×10^{-7} M. A model has not been developed to account for the short period of exchange between the times that the interface hydrogen and hydroxide concentrations deviate from 1.0×10^{-7} M and equilibrium is reached. A model developed for this region would also predict exchange rates for resin saturations above the equilibrium value corresponding to the solution concentration.

7. Thorough mathematical investigations of the following variables on mixed bed operation and exchange limits may be made with the model developed in this study.

    a) variations of the cation to anion resin ratio,

    b) variations of the cation and anion resin diameters and size distributions,

    c) incomplete resin regeneration,

    d) incomplete resin separation before regeneration,

    e) variations of the feed concentration and pH.

BIBLIOGRAPHY

1. Abrams, I. M., _Ind._ _Eng._ _Chem._, 48, 1469 (1956).

2. Abrams, I. M. and Wolff, J. J., _A.I.Ch.E._ _Symp._ _Ser._, 78, 112 (1982).

3. Acrivos, A., _Phys._ _Fluids_, 3, 567 (1960).

4. Adamson, A. W. and Grossman, J. J., _J._ _Chem._ _Phys._, 17, 1002 (1949).

5. Amundson, N. R., _Ind._ _Eng._ _Chem._, 26, 35 (1956).

6. Boyd, G. E., Adamson, A. W., Myers, L. S., Jr., _J._ _Am._ _Chem._ _Soc._, 69, 2836 (1947)

7. Bunzl, K., _Isr._ _J._ _Chem._, 11, 1 (1973).

8. Bunzl, K., _Anal._ _Chem._, 50, 258 (1978).

9. Cadell, J. R. and Moison, R. L., _Chem._ _Eng._ _Prog._ _Symp._ _Ser._, 50, No. 14, 1 (1954).

10. Carberry, J. J., _A.I.Ch.E._ _J._, 4, 460 (1960).

11. Coats, J. I. and Glueckauf, E., _J._ _Chem._ _Soc._ _(London)_, 1308 (1947).

12. Danckwerts, P. V., _Ind._ _Eng._ _Chem._, 43, 1960 (1951).

13. Darji, J. D., _Proc._ _Am._ _Power._ _Conf._, 42, 1101 (1980).

14. DeVault, D., _J._ _Am._ _Chem._ _Soc._, 65, 532 (1943).

15. Dow Chemical Company, _A_ _Guide_ _to_ _Condensate_ _Polishing_, From No. 177-1331-79, Midland, Michigan (1979).

16. Down, P. E. and Salem, E., _The_ _Theory_ _and_ _Practice_ _of_ _Ion_ _Exchange_; An International Conference Held at Churchhill College, University of Cambridge, July 25-30, 1976: Society of Chemical Ind., London, 1976, p. 21.1.

17. Dranoff, J. S. and Lapidus, L., _Ind._ _Eng._ _Chem._ _Fund._, 49, 1297 (1957).

18. Dranoff, J. S. and Lapidus, L., _Ind. Eng. Chem. Fund._, 50, 1648 (1958).

19. Dranoff, J. S. and Lapidus, L., _Ind. Eng. Chem._, 53, 71 (1961).

20. Emmett, J. R., _Water Chem. Nucl. React. Syst., Proc. Int. Conf._, Paper No. 4, 1977.

21. Erickson, K. L. and Rase, H. F., _Ind. Eng. Chem. Fund._, 18, 312 (1979).

22 Frisch, N. W. and Kunin, R., _A.I.Ch.E. J._, 6, 640 (1960).

23. Gilliland, E. R. and Baddour, R. F., _Ind. Eng. Chem._, 45, 330 (1953).

24. Glaski, F. A. and Dranoff, J. S., _A.I.Ch.E. J._, 9, 426 (1963).

25. Glueckauf, E., _J. Soc. Chem. Ind. (London)_, 74, 34 (1955).

26. Goldstein, S., _Proc. Roy. Soc. (London)_, A219, 151, 171 (1953).

27. Goldstein, S. and Murray, J. D., _Proc. Roy. Soc. (London)_, A252, 334, 348, 360 (1959).

28. Graham, E. E. and Dranoff, J. S., _Ind. Eng. Chem. Fund._, 21, 360 (1982).

29. Grimshaw, R. W. and Harland, C. E., _Ion Exchange: Introduction to Theory and Practice_, Chem. Soc., London, England, 1975.

30. Helfferich, F. G. and Plesset, M. S., _J. Chem. Phys._, 28, 418 (1958).

31. Helfferich, F. G., _Angew. Chem. Int._, 1, 440 (1962).

32. Helfferich, F. G., _Ion Exchange_, McGraw Hill Book Company, New York, 1962.

33. Helfferich, F. G., _J. Phys. Chem._, 69, 1178 (1965).

34. Helfferich, F. G., in _Ion Exchange_, Vol. 1, J. Marinsky (ed.), p. 65, Marcel-Dekker Inc., New York, 1966.

35. Hiester, H. K. and Vermeulen, T., _Chem. Eng. Prog._, 48, 505 (1952).

36. Holm, L. W., _J. Chem. Phys._, 22, 1132 (1954).

37. Kasten, P. R., Lapidus, L., Amundson, N. R., J. Phys. Chem., 56, 683 (1952).

38. Kataoka, T. et al., J. Chem. Eng. Jap., 1, 38 (1968).

39. Kataoka, T. et al., J. Chem. Eng. Jap., 5, 132 (1972).

40. Kataoka, T. et al., J. Chem. Eng. Jap., 6, 172 (1973).

41. Kataoka, T. et al., J. Chem. Eng. Jap., 9, 74 (1976).

42. Kataoka, T. et al., J. Chem. Eng. Jap., 9, 130 (1976).

43. Kataoka, T. et al., J. Chem. Eng. Jap., 9, 326 (1976).

44. Kataoka, T. et al., J. Chem. Eng. Jap., 9, 383 (1976).

45. Kataoka, T. et al., J. Chem. Eng. Jap., 10, 245 (1977).

46. Kataoka, T. et al., J. Chem. Eng. Jap., 10, 385 (1977).

47. Kataoka, T. et al., J. Chem. Eng. Jap., 13, 328 (1980).

48. Kitchener, J. A., Ion Exchange Resins, Wiley, New York, 1957.

49. Klein, G., Tondeur, D., Vermeulen, T., Ind. Eng. Chem. Fund., 6, 339 (1967).

50. Kunin, R. and McGarvey, F. X., U.S.P. 2,578,937 (1951).

51. Kunin, R., and McGarvey, F. X., Ind. Eng. Chem., 43, 734 (1951).

52. Kunin, R., Elements of Ion Exchange, Reinhold, New York, 1960.

53. Kunin, R., Personal Communication. Houston, Texas, April 28, 1983.

54. Kuo, J. C. W. and David, M. M., A.I.Ch.E. J., 9, 365 (1963).

55. Lagos, A. E. and Kitchener, J. A., Trans. Faraday Soc., 56, 1245 (1960).

56. Lapidus, L., Digital Computation for Chemical Engineers, McGraw-Hill Cook Company, New York, 1962.

57. Lightfoot, E., Massot, C., Ivani, F., _Chem. Eng. Prog. Symp. Ser._, 61, 28 (1966).

58. Mackay, D., _J. Phys. Chem._ 64, 1718 (1960).

59. Mackie, J. S. and Meares, P., _Proc. Roy. Soc. (London)_, A232, 510 (1955).

60. Mayer, S. W. and Tompkins, E. R., _J. Am. Chem. Soc._, 69, 2866 (1947).

61. McGarvey, F. X. and Kunin, R., _Ind. Eng. Chem._, 43, 734 (1951).

62. Monet, G. P., _Chem. Eng. Prog._, 52, 299 (1956).

63. Nelson, F., _J. Polymer Sci._, 40, 563 (1959).

64. Nernst, W., _Z. Physik. Chem._, 47, 52 (1904).

65. Omatete, O. O., Clazie, R. N., Vermeulen, T., _Chem. Eng. J._, 19, 229 (1980).

66. Opler, A. and Hiester, N. K., _Tables for Predicting the Performance of Fixed Bed Ion Exchange and Similar Mass-Transfer Procseses_, Stanford Research Institute, 1954.

67. Pan, S. H. (Unpub. Ph. D. dissertation, Library, University of Washington, Seattle, 1976).

68. Pan, S. H. and David, M. M. (Paper presented at the A.C.S. national meeting, San Francisco, California, August, 1976.), Seattle, Washington: University of Washington, Dept. of Chemical Engineering, 1976.

69. Pan, S. H. and David, M. M., _A.I.Ch.E. Symp. Ser._, 74, 74 (1978).

70. Pepper, K. W., _J. Appl. Chem._, 1, 124 (1951).

71. Pepper, K. W., Paisley, H. M., Young, M. A., _J. Chem. Soc._, 4097 (1953).

72. Perry, J. H., ed., _Chemical Engineer's Handbook_, 5th Edition, Section 16, McGraw-Hill Book Company, New York 1973.

73. Pieroni, L. J. and Dranoff, J. S., _A.I.Ch.E. J._, 9, 42 (1963).

74. Plesset, M. S., Helfferich, F. G., Franklin, J. N., J. Chem. Phys., 29, 1064 (1958).

75. Rao, M. G. and David, M. M., A.I.Ch.E. J., 10, 213 (1964).

76. Reents, A. C. and Kahler, F. H., Ind. Eng. Chem., 43, 730 (1951).

77. Rosen, J. B., J. Chem. Phys., 20, 387 (1952).

78. Schlögl, R. and Helfferich, F. G., J. Chem. Phys., 26, 5 (1957).

79. Smith, T. G. and Dranoff, J. S., Ind. Eng. Chem. Fund., 3, 195 (1964).

80. Strauss, S. D., Power, 122, No. 11, S-14 (1978).

81. Streat, M. and Bringal, W. J., Trans. Inst. Chem. Eng., 48, T151 (1970).

82. Thomas, H. C., J. Am. Chem. Soc., 66, 1664 (1944).

83. Thompson, J., et al., Chem. Eng. Prog., 49, 341, 437 (1953).

84. Tittle, K., Proc. Am. Power Conf., 43, 1126 (1981).

85. Tondeur, D. and Klein, G., Ind. Eng. Chem. Fund., 6, 351 (1967).

86. Tsal, F., J. Phys. Chem., 86, 2339 (1982).

87. Van Brocklin, L. P. and David, M. M., Ind. Eng. Chem. Fund., 11, 91 (1972).

88. Van Brocklin, L. P. and David, M. M., A.I.Ch.E. Symp. Ser., 71, 191 (1975).

89. Vasishth, R. C. and David, M. M., Chem. Eng. Prog. Symp. Ser., 25, 113 (1959).

90. Vermeulen, T., Ind. Eng. Chem., 45, 1664 (1953).

91. Vermeulen, T. and Hiester, N. K., J. Chem. Phys., 22, 96 (1954).

92. Vermeulen, T., Advan. Chem. Eng., 2, 147 (1958).

93. Wagner, J. D. and Dranoff, J. S., _J. of Phys. Chem._,
      71, 4551 (1967).

94. Walter, J. E., _J. Chem. Phys._, 13, 229 (1945).

95. Wheaton, R. M. and Bauman, W. C., _Ind. Eng. Chem._, 43,
      1088 (1951).

96. Wicke, E., _Kolloid Z._, 86, 295 (1939).

APPENDIX A

DERIVATION OF ION FLUX EXPRESSIONS FOR BINARY EXCHANGE HAVING A NEGLIGIBLE EXITING ION CONCENTRATION IN THE BULK PHASE

The following derivation results in analytical flux expressions for each ion in a binary exchange system with a single coion in the solution, as originally derived by Helfferich (33), Kataoka (38), and Smith et al. (79). The concentration profiles for a typical system are shown in Figure 10.

Applying the Nernst-Planck Equation (II-15) for the diffusion of each ion, Equations A-1, A-2, and A-3 are obtained.

$$J_n = -D_n \left\{ \frac{\partial C_n}{\partial r} + \frac{C_n F}{RT} \frac{\partial \phi}{\partial r} \right\} \tag{A-1}$$

$$J_h = -D_h \left\{ \frac{\partial C_h}{\partial r} + \frac{C_h F}{RT} \frac{\partial \phi}{\partial r} \right\} \tag{A-2}$$

$$J_c = -D_c \left\{ \frac{\partial C_c}{\partial r} \oplus \frac{C_c F}{RT} \frac{\partial \phi}{\partial r} \right\} \tag{A-3}$$

The conditions of electroneutrality, no net current flow, and no net coion flux are respectively given by

$$C_n + C_h = C_c \tag{A-4}$$

$$J_n + J_h = J_c \tag{A-5}$$

$$J_c = 0 \tag{A-6}$$

For simplicity, let

$$N = \frac{F}{RT} \tag{A-7}$$

The first step is to eliminate the potential gradient and coion concentration from the diffusing ion flux equations. Equation A-8 is obtained from Equation A-4.

$$\frac{\partial C_n}{\partial r} + \frac{\partial C_h}{\partial r} = \frac{\partial C_c}{\partial r} \tag{A-8}$$

Using Equations A-3, A-4, A-6, and A-8, the potential gradient is expressed in terms of sodium and hydrogen concentrations.

$$\frac{\partial \phi}{\partial r} = \frac{1}{N(C_n + C_h)} \left\{ \frac{\partial C_h}{\partial r} + \frac{\partial C_n}{\partial r} \right\} \tag{A-9}$$

Substituting Equation A-8 into Equations A-1 and A-2 yields flux equations in terms of diffusing ion concentrations and concentration gradients only.

$$J_n = -D_n \left[\frac{\partial C_n}{\partial r} + \frac{C_n}{C_n + C_h} \left\{ \frac{\partial C_n}{\partial r} + \frac{\partial C_h}{\partial r} \right\} \right] \tag{A-10}$$

$$J_h = -D_h \left[\frac{\partial C_h}{\partial r} + \frac{C_h}{C_n + C_h} \left\{ \frac{\partial C_n}{\partial r} + \frac{\partial C_h}{\partial r} \right\} \right] \tag{A-11}$$

To integrate Equations A-10 and A-11, the concentration and concentration gradient relationships between sodium and hydrogen must be determined. Substituting Equations A-10, A-11, and A-6 into Equation A-5, rearranging, and putting the resulting fractions over common denominators gives the following relationships:

$$\frac{\partial C_h}{\partial r} = - \frac{\partial C_n}{\partial r} \left\{ \frac{2 D_n C_n + D_n C_h + D_h C_h}{2 D_h C_h + D_h C_n + D_n C_n} \right\} \tag{A-12}$$

and

$$\frac{\partial C_h}{\partial C_n} = - \left\{ \frac{2 D_n C_n + D_n C_h + D_h C_h}{2 D_h C_h + D_h C_n + D_n C_n} \right\} \tag{A-13}$$

The relationship between sodium and hydrogen concentration gradients is given by Equation A-12. The relationship between n and h concentrations is determined by integrating Equation A-13. With proper factoring, Equation A-13 can be written in the following form:

$$(\frac{D_h}{D_n} C_h + C_n)(dC_h + dC_n) + (C_h + C_n)(\frac{D_h}{D_n} dC_h + dC_n) = 0 \tag{A-14}$$

Since D_h and D_n are constant, this form is equivalent to

$$(\frac{D_h}{D_n} C_h + C_n)d(C_h + C_n) + (C_h + C_n)d(\frac{D_h}{D_n} C_h + C_n) = 0 \tag{A-15}$$

Letting

$$x = \frac{D_h}{D_n} C_h + C_n \tag{A-15}$$

and

$$y = C_h + C_n \tag{A-16}$$

Equation A-15 becomes

$$x \, dy + y \, dx = 0 \tag{A-17}$$

or

$$\frac{dx}{x} = -\frac{dy}{y} \tag{A-18}$$

The boundary conditions for this system are:

$$C_h = C_h', \quad C_n = C_n \quad \text{at } r_o \leq r < r_o + \delta \tag{A-19}$$

$$C_h = 0, \quad C_n = C_n^o \quad \text{at } r = r_o + \delta \tag{A-20}$$

Integration of Equation A-18 with the above boundary conditions gives the concentration relationship between sodium and hydrogen in the film to that in the bulk phase.

$$(\frac{D_h}{D_n} C_h + C_n)(C_h + C_n) = (C_n^o)^2 \tag{A-21}$$

The information required to integrate Equations A-10 and A-11 is now available. Using Equation A-12 to eliminate $\partial C_h / \partial r$ from Equation A-10, the following expression for J_n is obtained after rearrangement, proper factoring, and cancellation of common factors.

$$J_n = -\frac{\partial C_n}{\partial r} \left\{ \frac{2 \, D_h D_n (C_h + C_n)}{D_n C_n + D_h C_n + 2 \, C_h D_h} \right\} \tag{A-22}$$

The concentration of hydrogen is expressed in terms of sodium by using Equation A-21 and the quadratic formula. Equation A-21 is first written:

$$D_h(C_h)^2 + (D_h C_n + D_n C_n)C_h + [D_n(C_n)^2 - D_n(C_n^o)^2] = 0 \quad (A-23)$$

Solving for C_h yields the following expression:

$$C_h = \left\{ - C_n(D_h + D_n) \pm [(C_n)^2 ((D_h)^2 - 2 D_h D_n + (D_n)^2) + \right.$$
$$\left. 4 D_h D_n(C_n^o)^2]^{1/2} \right\} / 2 D_h \quad (A-24)$$

Assuming pseudo-steady state exchange ($\partial J_n/\partial r = 0$), and integrating with respect to radial distance, Equation A-25 is obtained.

$$J_n = K' \quad (A-25)$$

where

$$K' = \text{constant of integration}$$

Substituting Equation A-22 for J_n yields

$$dC_n \left\{ \frac{2 D_h D_n(C_h + C_n)}{D_n C_n + D_h C_n + 2 C_h D_h} \right\} = - K' \, dr \quad (A-26)$$

Substituting Equation A-24 into Equation A-26 to eliminate C_h and rearranging gives

$$dC_n \left\{ \frac{K_1 C_n}{(K_2(C_n)^2 + K_3)^{1/2}} + D_n \right\} = - K' \, dr \quad (A-27)$$

where

$$K_1 = D_n(D_h - D_n)$$

$$K_2 = (D_h)^2 - 2 D_h D_n + (D_n)^2$$

$$K_3 = 4 D_h D_n (C_n^o)^2$$

Since K_1, K_2, and K_3 are constant, Equation A-27 can be readily integrated.

$$\int \frac{xdx}{(a + bx^2)^{1/2}} = \frac{1}{b}(a + bx^2)^{1/2} \tag{A-28}$$

Equation A-31 is obtained after integrating Equation A-27 with the following boundary conditions.

$$C_n = C_n^*, \quad r = r_o \tag{A-29}$$

$$C_n = C_n^o, \quad r = r_o + \delta \tag{A-30}$$

$$\frac{D_n}{D_h - D_n}[(D_h + D_n)(C_n^o)] + D_n C_n^o - \frac{D_n}{D_h - D_n}[4 D_h D_n (C_n^o)^2 +$$

$$((D_h)^2 - 2 D_h D_n + (D_n)^2)(C_n^*)^2]^{1/2} - D_n C_n^* = -K'(\delta) \tag{A-31}$$

If Equation A-21 is written in terms of interfacial concentrations,

$$(\frac{D_h}{D_n} C_h^* + C_n^*)(C_h^* + C_n^*) = (C_n^o)^2 \tag{A-32}$$

and substituted for $(C_n^o)^2$ in Equation A-31, the radical term in Equation A-31 may be written as follows once it is properly factored:

$$[D_h(2 \ C_h^* + C_n^*) + D_n C_n^*]^2 \qquad \text{(A-33)}$$

With this simplification, Equation A-31 may be manipulated to give the final expression for the sodium flux as given by Kataoka (38) and Smith et al. (79).

$$J_n = K' = \frac{2 \ D_h D_n (C_n^o - C_n^* - C_h^*)}{(D_n - D_h)\delta} \qquad \text{(A-34)}$$

A similar expression for J_h may be obtained by starting after Equation A-21, but eliminating C_n instead of C_h. The expression for J_h is determined much easier by noting from Equations A-5 and A-6 that

$$J_h = - \ J_n \qquad \text{(A-35)}$$

Thus,

$$J_h = \frac{2 \ D_h D_n (C_n^o - C_n^* - C_h^*)}{(D_h - D_n)\delta} \qquad \text{(A-36)}$$

APPENDIX B

DERIVATION OF ION FLUX EXPRESSIONS FOR THE
RIGOROUS FILM REACTION MODEL BETWEEN
THE REACTION PLANE AND BULK PHASE

The following derivation results in flux expressions
and concentration relationships, in terms of concentration
gradients, for diffusing ions between the plane of reaction
and bulk fluid phase, as shown in Figure 12. The assumption
of negligible hydroxide ion flux after the plan of reaction
is not made in this derivation. The ionic diffusion
relationships are obtained using the flux expressions of
Equations III-5 through III-8 along with the
electroneutrality and system restraints given by Equations
III-39, III-40, III-43, and III-44.

The potential gradient is first expressed in terms of
diffusing ion concentrations by eliminating all nondiffusing
ion (sodium) terms. Using Equations III-6, III-39, and
III-44, the potential gradient is expressed as

$$\frac{\partial \phi}{\partial r} = - \frac{RT}{FC_n} \partial (C_c + C_o + C_h)/\partial r \qquad (B-1)$$

Using the water dissociation relationships (Equations III-12
and III-13) along with Equation B-1, the flux expressions

151

for the diffusing ions may be written in terms of the concentration gradients of chloride and hydrogen ions only.

$$J_c = -D_c \frac{\partial C_c}{\partial r} - \frac{D_c C_c}{C_n} \left[\frac{\partial C_c}{\partial r} - \frac{\partial C_h}{\partial r} \left\{ \frac{10^{-14}}{(C_h)^2} + 1 \right\} \right] \quad (B-2)$$

$$J_o = \frac{D_o \, 10^{-14}}{(C_h)^2} \frac{\partial C_h}{\partial r} - \frac{D_o \, 10^{-14}}{C_n C_h} \left[\frac{\partial C_c}{\partial r} - \frac{\partial C_h}{\partial r} \left\{ \frac{10^{-14}}{(C_h)^2} + 1 \right\} \right] \quad (B-3)$$

$$J_h = -D_h \frac{\partial C_h}{\partial r} + \frac{D_h C_h}{C_n} \left[\frac{\partial C_c}{\partial r} - \frac{\partial C_h}{\partial r} \left\{ \frac{10^{-14}}{(C_h)^2} + 1 \right\} \right] \quad (B-4)$$

The concentration relationship between hydrogen and chloride may now be determined by eliminating the sodium concentration using Equations III-12 and III-39 and substituting Equations B-1, B-2, and B-3 into Equation III-40.

$$\frac{\partial C_h}{\partial r} = \frac{(A)(C_h)^2}{(B)} \frac{\partial C_c}{\partial r} \quad (B-5)$$

where

$$A = D_h (C_h)^2 - D_c (C_h)^2 + 2 D_c C_c C_h + D_o \, 10^{-14} + D_c \, 10^{-14}$$

and

$$B = D_h C_c (C_h)^3 + 2 D_h \, 10^{-14} \, (C_h)^2 + D_o C_c C_h \, 10^{-14} +$$

$$2 D_o \, 10^{-28} + D_c C_c C_h \, 10^{-14} + D_c C_c (C_h)^3$$

The final flux expressions are obtained by substituting Equation B-5 into Equations B-2 and B-4 to respectively eliminate the hydrogen and chloride ion concentration gradients;

$$J_c = -D_c \frac{\partial C_c}{\partial t} \left\{ \frac{C_n(B) + C_c(B) - C_c 10^{-14}(A) - C_c(A)(C_h)^2}{C_n(B)} \right\} \quad (B-6)$$

$$J_h = -D_h \frac{\partial C_h}{\partial r} \left\{ \frac{C_n(A)C_h - (B) + (A) 10^{-14} + (A)(C_h)^2}{C_n(A)C_n} \right\} \quad (B-7)$$

where (A) and (B) are as defined in Equation B-5. The hydroxide ion flux is directly obtained with the use of Equation III-40.

APPENDIX C

COMPARISON OF R_i VALUES CALCULATED

WITH THE RIGOROUS AND SIMPLIFIED

FILM REACTION MODELS

The following R_i values were calculated for a chloride/ hydroxide anion exchange system using the rigorous (R_i^r) and simplified (R_i^s) reaction film models as developed in Chapter III. The calculations for each case were terminated when y_{Cl} was equal to one or the reaction plane position reached the particle-fluid interface. The system parameters were defined as follows:

$$K_{Cl/OH} = 1.45$$
$$D_H = 9.34 \times 10^{15} \ cm^2/s$$
$$D_{OH} = 5.23 \times 10^{-5} \ cm^2/s$$
$$D_{Cl} = 2.03 \times 10^{-5} \ cm^2/s$$
$$\gamma = C_H^o/C_{Cl}^o \ (\text{o superscript signifies bulk phase})$$

TABLE I

VARIATION OF R_i WITH BULK PHASE CONCENTRATION
AND PROGRESSION OF EXCHANGE AS CALCULATED
BY THE RIGOROUS AND SIMPLIFIED FILM
REACTION MODELS

y_{Cl}	R_i^s	R_i^r
For $C_{Cl}^o = 0.10$ and $\gamma = 0.6$		
0.00	1.3749	1.3783
0.20	1.3773	1.3801
0.40	1.3802	1.3823
0.60	1.3836	1.3849
0.80	1.3873	1.3879
0.84	1.3887	1.3836
0.88	1.3896	1.3893
0.92	1.3906	1.3900
0.96	1.3915	1.3907
0.98	1.3920	1.3910
1.00	1.3925	1.3914
For $C_{Cl}^o = 0.10$ and $\gamma = 0.1$		
0.00	1.2139	1.2144
0.20	1.2284	1.2289
0.40	1.2470	1.2474
0.60	1.2719	1.2722
0.80	1.3091	1.3092
0.84	1.3194	1.3195
0.88	1.3314	1.3314
0.92	1.3461	1.3459
0.94	1.3549	1.3546
0.96	1.3651	1.3646
0.98	1.3773	1.3765
1.00	1.3925	1.3914
For $C_{Cl}^o = 0.10$ and $\gamma = 0.01$		
0.00	1.1565	1.1565
0.20	1.1705	1.1705
0.40	1.1881	1.1881
0.60	1.2110	1.2110
0.80	1.2435	1.2435
0.84	1.2522	1.2522
0.88	1.2622	1.2622
0.92	1.2749	1.2749

TABLE I (CONTINUED)

y_{C1}	R_i^s	R_i^r
0.94	1.2833	1.2833
0.96	1.2949	1.2948
0.98	1.3154	1.3153
1.00	1.3926	1.3918

For C_{C1}^o = 0.10 and γ = 0.001

0.00	1.1501	1.1501
0.20	1.1639	1.1639
0.40	1.1811	1.1811
0.60	1.2032	1.2032
0.80	1.2333	1.2333
0.84	1.2408	1.2408
0.88	1.2489	1.2489
0.92	1.2580	1.2581
0.94	1.2632	1.2632
0.96	1.2690	1.2690
0.98	1.2770	1.2770
1.00	1.3930	1.3922

For C_{C1}^o = 1.0 x 10^{-3} and γ = 0.6

0.00	1.3748	1.3760
0.20	1.3772	1.3782
0.40	1.3801	1.3808
0.60	1.3836	1.3839
0.80	1.3877	1.3876
0.84	1.3886	1.3884
0.88	1.3896	1.3892
0.92	1.3905	1.3900
0.94	1.3910	1.3905
0.96	1.3915	1.3909
0.98	1.3920	1.3913
1.00	1.3927	1.3919

For C_{C1}^o = 1.0 x 10^{-3} and γ = 0.1

0.00	1.2138	1.2139
0.20	1.2283	1.2285
0.40	1.2469	1.2470
0.60	1.2718	1.2719
0.80	1.3090	1.3090
0.84	1.3193	1.3192
0.88	1.3314	1.3312
0.92	1.3461	1.3458

TABLE I (CONTINUED)

y_{C1}	R_i^s	R_i^r
0.94	1.3549	1.3546
0.96	1.3651	1.3647
0.98	1.3773	1.3768
1.00	1.3932	1.3924

For $C_{C1}^o = 1.0 \times 10^{-3}$ and $\gamma = 0.01$

0.00	1.1554	1.1554
0.20	1.1704	1.1704
0.40	1.1880	1.1880
0.60	1.2109	1.2109
0.80	1.2434	1.2434
0.84	1.2520	1.2520
0.88	1.2621	1.2621
0.92	1.2748	1.2748
0.94	1.2831	1.2831
0.96	1.2947	1.2946
0.98	1.3152	1.3151
1.00	1.3986	1.3976

For $C_{C1}^o = 1.0 \times 10^{-5}$ and $\gamma = 0.8$

0.00	1.3802	1.3822
0.20	1.3815	1.3833
0.40	1.3830	1.3846
0.60	1.3848	1.3862
0.80	1.3883	1.3903

For $C_{C1}^o = 1.0 \times 10^{-5}$ and $\gamma = 0.1$

0.00	1.2045	1.2064
0.20	1.2193	1.2211
0.40	1.2382	1.2398
0.60	1.2637	1.2649
0.80	1.3025	1.3027
0.84	1.3135	1.3133
0.88	1.3266	1.3258
0.92	1.3430	1.3413
0.94	1.3531	1.3507
0.96	1.3653	1.3618
0.98	1.3804	1.3754
1.00	1.4683	1.4566

TABLE I (CONTINUED)

y_{C1}	R_i^s	R_i^r
For $C_{C1}^o = 1.0 \times 10^{-7}$ and $\gamma = 0.8$		
0.00	1.2389	1.2348
0.20	1.2526	1.2465
0.40	1.2698	1.2609
0.60	1.3177	1.3399
For $C_{C1}^o = 1.0 \times 10^{-7}$ and $\gamma = 0.4$		
0.00	1.1574	1.1595
0.20	1.1740	1.1751
0.40	1.1959	1.1952
0.60	1.2276	1.2231
0.80	1.2904	1.3258

APPENDIX D

DESCRIPTION AND FORTRAN SOURCE LISTING

OF THE MIXED BED BINARY EXCHANGE

SIMULATION PROGRAM

The main scheme of this program is the simultaneous integration of cation and anion column material balances and rate expressions as presented in Equations III-84 through III-87. Depending on the ion concentrations in the bulk phase, the rate expressions at each calculation point are evaluated by the subroutines film or bulk. These subroutines correspond to the film reaction and bulk phase neutralization models, respectively. A fortran source listing of the simulation program is given in Table II following the description of the required input parameters.

The input parameters for the column program are inserted in data statements between lines 500-680. The input parameters are listed below under the same headings and of the same order as they are listed in the program:

Print Control (1 = Print, 0 = No Print):

KPBK: The effluent breakthrough curve is printed if this value is equal to one.

KPPR,TIME: If KPPR is equal to one, then the concentration profiles for all ionic species in

the column are printed during the first program iteration in which the time elapsed from feed introduction exceeds the value of TIME in minutes.

State of Regeneration:

YCO: Initial equivalent fraction of chloride in the anion resin.

YNO: Initial equivalent fraction of sodium in the cation resin.

Resin Characteristics:

PDC: Cation resin particle diameter (cm)

PDA   Anion resin particle diameter (cm)

VD: Bed void fraction

FCR: Cation resin volume fraction (cation resin/total resin)

Bed and System Variables:

CF: Feed solution concentration (meq/cm^3)

FR: Volumetric flow rate (cm^3/s)

DIA: Column diameter (cm)

CHT: Height of packed resin (cm)

Resin Constants:

QC: Cation resin capacity (meq/cm^3)

QA: Anion resin capacity (meq/cm^3)

TKCO: Selectivity coefficient for chloride-hydroxide exchange

N

TKHH: Selectivity coefficient for sodium-hydrogen exchange

Ionic Constants:

DH: Hydrogen diffusivity (cm^2/s)

DN: Sodium diffusivity (cm^2/s)

DO: Hydroxide diffusivity (cm^2/s)

DC: Chloride diffusivity (cm^2/s)

Integration Increments:

XK: Number of increments used for the Runge-Kutta Routine

XS: Number of half increments used in the Simpson's integration method

TAU: Dimensionless time increment (Equation III-77)

XI: Dimensionless distance increment (Equation III-78)

Fluid Properties:

CP: Solution viscosity (cp)

DEN: Solution density (g/cm)

Program Limits:

TMAX: Time limit for column operation (min)

XNMAX: Effluent sodium concentration limit (C_n/C_n^f)

TABLE II

FORTRAN SOURCE LISTING FOR THE
MIXED BED SIMULATION PROGRAM

```
$JOB            ,TIME=(0,40)                                      00000050
    10 FORMAT ('1MIXED BED SYSTEM PARAMETERS:')                   00000060
    11 FORMAT ('0')                                               00000070
    12 FORMAT ('ORESIN REGENERATION',7X,': YCO=',F5.3,8X,'YNO=',F5.3)  00000080
    13 FORMAT ('ORESIN PROPERTIES',9X,': PDC=',F6.4,6X,'PDA=',F6.4,6X, 00000090
      A'VD =',F6.4,6X,'FCR =',F6.3)                               00000100
    14 FORMAT ('ORESIN CONSTANTS',10X,': QC =',E10.4,'  QA =',E10.4,   00000110
      A2X,'TKCO=',F6.4,'     TKNH=',F6.4)                         00000120
    15 FORMAT ('OCOLUMN PARAMETERS',8X,': CF =',E10.4,'  FR =',F7.3,5X 00000130
      A,'DIA =',F5.2,7X,'CHT =',F5.1)                             00000140
    16 FORMAT ('OIONIC CONSTANTS',10X,': DH =',E10.4,'  DN =',E10.4,   00000150
      A2X,'DO =',E10.4,'  DC =',E10.4)                            00000160
    17 FORMAT ('OFLUID PROPERTIES',9X,': CP =',F7.5,5X,'DEN=',F6.4)    00000170
    18 FORMAT ('0')                                               00000180
    19 FORMAT ('OCALCULATED PARAMETERS')                          00000190
    20 FORMAT ('0')                                               00000200
    21 FORMAT ('OINTEGRATION INCREMENTS    : TAU=',F7.5,5X,'XI =',F7.5,5 00000210
      AX,'NT  =',I6)                                              00000220
    22 FORMAT ('OTRANSFER COEFFICIENTS     : REC=',E10.4,'  REA=',E10.4 00000230
      A,'  KLC =',E10.4,'  KLA=',E10.4)                           00000240
    23 FORMAT ('OSUPERFICIAL VELOCITY      : VS =',F7.3)          00000250
    24 FORMAT ('1')                                               00000260
    25 FORMAT ('OBREAKTHROUGH CURVE RESULTS:')                    00000270
    26 FORMAT ('0')                                               00000280
    27 FORMAT ('0',6X,'T(MIN)',9X,'XNC',11X,'XCA',11X,'XHC',11X,'XOA', 00000290
      A11X,'YNC',11X,'YCA')                                       00000300
    28 FORMAT ('0')                                               00000310
    29 FORMAT ('0',7(2X,E12.5))                                   00000320
    30 FORMAT ('1')                                               00000330
    31 FORMAT ('OCONCENTRATION PROFILES AFTER ',F5.0,' MINUTES')  00000340
    32 FORMAT ('0')                                               00000350
    33 FORMAT ('0',9X,'Z',11X,'XNC',11X,'XCA',11X,'XHC',11X,'XOA', 00000360
      A11X,'YNC',11X,'YCA')                                       00000370
    34 FORMAT ('0')                                               00000380
    35 FORMAT ('0',7(2X,E12.5))                                   00000390
       IMPLICIT REAL*8 (A-H,O-Z)                                  00000400
       DIMENSION YCA(4,300),YNC(4,300),XCA(4,300),                00000410
      1XNC(4,300),XOA(4,300),XHC(4,300),XCAD(5),XNCD(5),          00000420
      2RATEC(10),RATEN(10),RATC(4,300),RATN(4,300)                00000430
       REAL KLC,KLA                                               00000440
C                                                                 00000450
C      FUNCTION STATEMENTS                                        00000460
C      CARBERRY'S CORRELATION                                     00000470
       F1(R,S) = 1.15*VS/(VD*(S**(2./3.))*(R**.5))                00000480
C      KATAOKA'S CORRELATION                                      00000490
       F2(R,S) = 1.85*VS*((VD/(1.-VD))**(1./3.))/                 00000500
      A(VD*(S**(2./3.))*(R**(2./3.)))                             00000510
C                                                                 00000520
C      INPUT DATA:                                                00000530
C      PRINT CONTROL (1=PRINT, 0=NOPRINT)                         00000540
       DATA KPBK,KPPR,TIME/1,0,0.0D0/                             00000550
```

TABLE II (CONTINUED)

```
C       SATE OF REGENERATION                                    00000560
        DATA YCO,YNO/0.1D0,0.1D0/                               00000570
C       RESIN CHARACTERISTICS                                   00000580
        DATA PDC,PDA,VD,FCR/.0760D0,.063D0,.445D0,0.600D0/      00000590
C       BED AND SYSTEM VARIABLES                                00000600
        DATA CF,FR,DIA,CHT/2.0D-3,10.32D0,2.54D0,40.0D0/        00000610
C       RESIN CONSTANTS                                         00000620
        DATA QC,QA,TKCO,TKNH/3.0728D0,2.4334D0,1.45D0,1.55D0/   00000630
C       IONIC CONSTANTS                                         00000640
        DATA DH,DN,DO,DC/9.35D-5,1.35D-5,5.23D-5,2.03D-5/       00000650
C       INTEGRATION INCREMENTS                                  00000660
        DATA XK,XS,TAU,XI/10.0D0,10.0D0,0.04D0,0.01D0/          00000670
C       FLUID PROPERTIES                                        00000680
        DATA CP,DEN/1.0D0,1.0D0/                                00000690
C       PROGRAM LIMITS                                          00000700
        DATA TMAX,XNMAX/8000.0D0,0.95D0/                        00000710
C                                                               00000720
C       PRINT SYSTEM PARAMETERS                                 00000730
        WRITE (6,10)                                            00000740
        WRITE (6,11)                                            00000750
        WRITE (6,12) YCO,YNO                                    00000760
        WRITE (6,13) PDC,PDA,VD,FCR                             00000770
        WRITE (6,14) QC,QA,TKCO,TKNH                            00000780
        WRITE (6,15) CF,FR,DIA,CHT                              00000790
        WRITE (6,16) DH,DN,DO,DC                                00000800
        WRITE (6,17) CP,DEN                                     00000810
C                                                               00000820
C       CALCULATION OF NONIONIC MASS TRANSFER COEFFICIENTS      00000830
        A = 1./4.*3.14159*(DIA**2)                              00000840
        VS = FR/A                                               00000850
        RE = 100.*VS*DEN/((1.-VD)*CP)                           00000860
        REC = PDC*RE                                            00000870
        REA = PDA*RE                                            00000880
        SC = (CP/100.)/DEN                                      00000890
        SCC = SC/DN                                             00000900
        SCA = SC/DC                                             00000910
        IF (REC.LT.20.) THEN                                    00000920
        KLC = F2(REC,SCC)                                       00000930
        ELSE                                                    00000940
        KLC = F1(REC,SCC)                                       00000950
        ENDIF                                                   00000960
        IF (REA.LT.20.) THEN                                    00000970
        KLA = F2(REA,SCA)                                       00000980
        ELSE                                                    00000990
        KLA = F1(REA,SCA)                                       00001000
        ENDIF                                                   00001010
C                                                               00001020
C       INITIALIZE TAU AND XI INCREMENTS BASED ON BED DIMENSIONS 00001030
C                                                               00001040
C       SET MATRIX DIMENSIONS BASED ON TAU AND XI               00001050
        CHTD = KLC*(1.-VD)*CHT/(VS*PDC)                         00001060
        NT = CHTD/XI                                            00001070
C                                                               00001080
C       PRINT CALCULATED PARAMETERS                             00001090
        WRITE (6,18)                                            00001100
        WRITE (6,19)                                            00001110
```

TABLE II (CONTINUED)

```
      WRITE (6,20)                                           00001120
      WRITE (6,21) TAU,XI,NT                                 00001130
      WRITE (6,22) REC,REA,KLC,KLA                           00001140
      WRITE (6,23) VS                                        00001150
C                                                            00001160
C     PRINT BREAKTHROUGH CURVE HEADINGS                      00001170
      IF (KPBK.NE.1) GO TO 50                                00001180
      WRITE (6,24)                                           00001190
      WRITE (6,25)                                           00001200
      WRITE (6,26)                                           00001210
      WRITE (6,27)                                           00001220
      WRITE (6,28)                                           00001230
   50 CONTINUE                                               00001240
C                                                            00001250
C     PRINT CONCENTRATION PROFILE HEADINGS                   00001260
      T = 0.                                                 00001270
      TAUPR = KLC*CF*(TIME*60.)/(PDC*QC)                     00001280
      IF (KPPR.NE.1) GO TO 60                                00001290
      WRITE (6,30)                                           00001300
      WRITE (6,31) TIME                                      00001310
      WRITE (6,32)                                           00001320
      WRITE (6,33)                                           00001330
      WRITE (6,34)                                           00001340
   60 CONTINUE                                               00001350
C                                                            00001360
C     SET INITIAL COLUMN CONDITIONS                          00001370
      MT = NT + 1                                            00001380
      DO 100 M=1,MT                                          00001390
      YCA(1,M)=YCO                                           00001400
      YNC(1,M)=YNO                                           00001410
  100 CONTINUE                                               00001420
C                                                            00001430
C     CALCULATE DIMENSIONLESS PROGRAM TIME LIMIT BASED ON    00001440
C     INLET CONDITIONS (Z=0)                                 00001450
      TAUMAX = KLC*CF*(TMAX*60.)/(PDC*QC)                    00001460
C                                                            00001470
C     INITIALZE VALUES                                       00001480
      J = 1                                                  00001490
      JK = 1                                                 00001500
      TAUTOT = 0.                                            00001510
      JFLAG = 0                                              00001520
      XNC(JK,NT) = 0.                                        00001530
C                                                            00001540
C     LOOP TO INCREMENT TIME AND CHECK PROGRAM RESTRAINTS    00001550
      WHILE (TAUTOT.LT.TAUMAX.AND.XNC(JK,NT).LT.XNMAX)       00001560
      IF (J.EQ.4) THEN                                       00001570
      JD = 1                                                 00001580
      ELSE                                                   00001590
      JD = J + 1                                             00001600
      ENDIF                                                  00001610
C                                                            00001620
C     SET COLUMN INLET CONDITIONS                            00001630
      XCA(J,1) = 1.                                          00001640
      XNC(J,1) = 1.                                          00001650
      XOA(J,1) = 1.0E-7/CF                                   00001660
      XHC(J,1) = XOA(J,1)                                    00001670
```

TABLE II (CONTINUED)

```
C                                                                   00001680
C        LOOP TO INCREMENT DISTANCE                                 00001690
         DO 400 K=1,NT                                              00001700
C        DEFINE BULK PHASE CONCENTRATIONS FOR SUBROUTINES           00001710
         CCO = XCA(J,K)*CF                                          00001720
         COO = XOA(J,K)*CF                                          00001730
         CHO = XHC(J,K)*CF                                          00001740
         CNO = XNC(J,K)*CF                                          00001750
         YC = YCA(J,K)                                              00001760
         YN = YNC(J,K)                                              00001770
C                                                                   00001780
C        INTEGRATE X USING IMPROVED EULER METHOD                    00001790
         DO 300 L=1,2                                               00001800
C                                                                   00001810
C        CALL ROUTINES TO CALCULATE RIA XCI, RIC, AND XNI           00001820
         IF (YC.LT.1.0) THEN                                        00001830
         IF (CHO.LT.1.5E-7) THEN                                    00001840
         CALL BULK(TKCO,COO,CCO,YC,DO,DC,RIA,XCI)                   00001850
         ELSE                                                       00001860
         CALL FILM(TKCO,XK,XS,DH,DC,DO,CCO,CHO,YC,RIA,XCI,H,T)      00001870
         ENDIF                                                      00001880
         ELSE                                                       00001890
         XCI = 1.0                                                  00001900
         ENDIF                                                      00001910
         IF (YN.LT.1.0) THEN                                        00001920
         IF (CHO.GT.5.0E-8) THEN                                    00001930
         CALL BULK(TKNH,CHO,CNO,YN,DH,DN,RIC,XNI)                   00001940
         ELSE                                                       00001950
         CALL FILM(TKNH,XK,XS,DO,DN,DH,CNO,COO,YN,RIC,XNI,H,T)      00001960
         ENDIF                                                      00001970
         ELSE                                                       00001980
         XNI = 1.0                                                  00001990
         ENDIF                                                      00002000
C                                                                   00002010
C        CHANGE CALCULATED INTERFACE CONCENTRATIONS TO FEED BASIS   00002020
         XCAD(1) = XCA(J,K)                                         00002030
         XNCD(1) = XNC(J,K)                                         00002040
         XCI = XCI * XCAD(L)                                        00002050
         XNI = XNI * XNCD(L)                                        00002060
C                                                                   00002070
         RATEN(L) = 6.*RIC*((XNC(J,K)) - XNI)                       00002080
         RATEC(L) = 6.*RIA*((XCA(J,K)) - XCI)*PDC*KLA/(PDA*KLC)     00002090
         IF (L.EQ.2) GO TO 310                                      00002100
         IF (K.EQ.1) THEN                                           00002110
         RATN(J,1) = RATEN(1)                                       00002120
         RATC(J,1) = RATEC(1)                                       00002130
         YNC(JD,1) = YNC(J,1)+TAU*RATN(J,1)                         00002140
         YCA(JD,1) = YCA(J,1)+TAU*RATC(J,1)*QC/QA                   00002150
         IF (YNC(JD,1).GT.1.0) YNC(JD,1) = 1.0                      00002160
         IF (YCA(JD,1).GT.1.0) YCA(JD,1) = 1.0                      00002170
         ENDIF                                                      00002180
         XN2 = XNC(J,K) - XI*RATEN(L)*FCR                           00002190
         XC2 =XCA(J,K) - XI*RATEC(L)*(1.-FCR)                       00002200
         XCAD(2) = XC2                                              00002210
         XNCD(2) = XN2                                              00002220
         CNO2 = XN2 * CF                                            00002230
```

```
      CCO2 = XC2 * CF                                             00002240
C                                                                 00002250
C     MATERIAL BALANCE FOR H2 AND OH CONCENTRATIONS               00002260
      BZ = CNO2 - CCO2                                            00002270
      CHO = (-BZ + (BZ**2 + 4.0E-14)**0.5) / 2.0                 00002280
      COO = 1.0E-14/CHO                                           00002290
C                                                                 00002300
C     REDEFINE BULK PHASE CONCENTRATIONS FOR SUBROUTINES          00002310
      CCO = CCO2                                                  00002320
      CNO = CNO2                                                  00002330
      YC = YCA(J,K+1)                                             00002340
      YN = YNC(J,K+1)                                             00002350
  300 CONTINUE                                                    00002360
  310 CONTINUE                                                    00002370
      XNC(J,K+1) = XNC(J,K) - (XI/2.)*(RATEN(1) + RATEN(2))*FCR   00002380
      XCA(J,K+1) = XCA(J,K) - (XI/2.)*(RATEC(1) + RATEC(2))*(1.-FCR) 00002390
      CCO = XCA(J,K+1) * CF                                       00002400
      CNO = XNC(J,K+1) * CF                                       00002410
      BZ2 = CNO - CCO                                             00002420
      CHO = (-BZ2 + (BZ2**2 + 4.0E-14)**0.5) / 2.0               00002430
      XHC(J,K+1) = CHO / CF                                       00002440
      COO = 1.0E-14/CHO                                           00002450
      XOA(J,K+1) = COO/CF                                         00002460
      IF (YC.LT.1.0) THEN                                         00002470
      IF (CHO.LT.1.5E-7) THEN                                     00002480
      CALL BULK(TKCO,COO,CCO,YC,DO,DC,RIA,XCI)                    00002490
      ELSE                                                        00002500
      CALL FILM(TKCO,XK,XS,DH,DC,DO,CCO,CHO,YC,RIA,XCI,H,T)       00002510
      ENDIF                                                       00002520
      ELSE                                                        00002530
      XCI = 1.0                                                   00002540
      ENDIF                                                       00002550
      IF (YN.LT.1.0) THEN                                         00002560
      IF (CHO.GT.5.0E-8) THEN                                     00002570
      CALL BULK(TKNH,CHO,CNO,YN,DH,DN,RIC,XNI)                    00002580
      ELSE                                                        00002590
      CALL FILM(TKNH,XK,XS,DO,DN,DH,CNO,COO,YN,RIC,XNI,H,T)       00002600
      ENDIF                                                       00002610
      ELSE                                                        00002620
      XNI = 1.0                                                   00002630
      ENDIF                                                       00002640
      XCI = XCI*XCA(J,K+1)                                        00002650
      XNI = XNI*XNC(J,K+1)                                        00002660
      RATN(J,K+1) = 6.*RIC*((XNC(J,K+1)) - XNI)                   00002670
      RATC(J,K+1) = 6.*RIA*((XCA(J,K+1)) - XCI)*PDC*KLA/(PDA*KLC) 00002680
C                                                                 00002690
C     INTEGRATE Y USING BACKWARD DIFFERENCE                       00002700
      YNC(JD,K+1) = YNC(J,K+1) + TAU*RATN(J,K+1)                  00002710
      YCA(JD,K+1) = YCA(J,K+1) + TAU*RATC(J,K+1)*QC/QA            00002720
      IF (YNC(JD,K+1).GT.1.0) YNC(JD,K+1) = 1.0                   00002730
      IF (YCA(JD,K+1).GT.1.0) YCA(JD,K+1) = 1.0                   00002740
C                                                                 00002750
C     PRINT CONCENTRATION PROFILES                                00002760
      IF (KPPR.NE.1) GO TO 350                                    00002770
      IF (TAUTOT.LT.TAUPR) GO TO 350                              00002780
      JFLAG = 1                                                   00002790
```

TABLE II (CONTINUED)

```
        ZA = NT                                                       00002800
        ZB = K-1                                                      00002810
        Z = ZB*CHT/ZA                                                 00002820
        WRITE (6,35) Z,XNC(J,K),XCA(J,K),XHC(J,K),XOA(J,K),YNC(J,K)   00002830
     A,YCA(J,K)                                                       00002840
  350 CONTINUE                                                        00002850
  400 CONTINUE                                                        00002860
C                                                                     00002870
C       PRINT BREAKTHROUGH CURVES                                     00002880
        IF (KPBK.NE.1) GO TO 450                                      00002890
        TAUTIM = TAUTOT*PDC*QC/(KLC*CF*60.)                           00002900
        T = TAUTIM                                                    00002910
        WRITE (6,29) TAUTIM,XNC(J,NT),XCA(J,NT),XHC(J,NT),XOA(J,NT),  00002920
     AYNC(J,NT),YCA(J,NT)                                             00002930
  450 CONTINUE                                                        00002940
        JK = J                                                        00002950
        IF (J.EQ.4) THEN                                              00002960
        J = 1                                                         00002970
        ELSE                                                          00002980
        J = J+1                                                       00002990
        ENDIF                                                         00003000
        IF (JFLAG.EQ.1) QUIT                                          00003010
        TAUTOT = TAUTOT + TAU                                         00003020
        ENDWHILE                                                      00003030
C                                                                     00003040
        STOP                                                          00003050
        END                                                          00003060
C                                                                     00003070
C                                                                     00003080
C       SUBROUTINE TO CALCULATE RI AND THE INTERFACE CONCENTRATION    00003090
C       USING THE FILM REACTION MODEL                                 00003100
        SUBROUTINE FILM(TKCO,XK,XS,DH,DC,DO,CCO,CHO,YC,RIA,XCI,H,T)   00003110
        IMPLICIT REAL*8 (A-H,O-Z)                                     00003120
        DIMENSION AC(50),AH(50),AII(50)                              00003130
        CALL KUTTA(CHO,CCO,DH,DC,XK,AC,AH,CCR)                        00003140
        CALL SIMP(CCR,CCO,AC,AH,DH,DC,XS,XK,AI,AII)                   00003150
        ALP = DO/DC                                                   00003160
        A = (ALP*1.0E-7/CCO + CCR/CCO) * (1.0E-7/CCO + CCR/CCO)       00003170
        Y1 = (1.0-YC)*TKCO + YC                                       00003180
        Y2 = ALP*(1.-YC)*TKCO + YC                                    00003190
        Y = (A**.5)*((Y1/Y2)**.5)                                     00003200
        R1 = YC*(A**.5)                                               00003210
        XCI = R1/((Y2*Y1)**.5)                                        00003220
        H1 = 2.*DO*DC*CCO*(1.E-7/CCO + CCR/CCO - Y)                   00003230
        H2 = AI*(DO-DC)                                               00003240
        H = H1/(H2 + H1)                                              00003250
        IF (H.LT.0.) THEN                                             00003260
        DE = 2.*DH*DC/(DH + DC)                                       00003270
        ELSE                                                          00003280
        DE = AI/((1.-H)*CCO*(1.-XCI))                                 00003290
        ENDIF                                                         00003300
        RIA = (DE/DC)**(2./3.)                                        00003310
        RETURN                                                        00003320
```

```
         END                                                      00003330
C                                                                 00003340
C                                                                 00003350
C        SUBROUTINE KUTTA: SOLVES FOR CH AND CC CONCENTRATION     00003360
C        RELATIONSHIP IN THE LIQUID FILM USING THE RUNGE-KUTTA METHOD  00003370
         SUBROUTINE KUTTA(CHO,CCO,DH,DC,XK,AC,AH,CCR)             00003380
         IMPLICIT REAL*8 (A-H,O-Z)                                00003390
         DIMENSION AC(50),AH(50)                                  00003400
         REAL K1,K2,K3,K4                                         00003410
         FD(CH,CC) = 2.*DC*1.E-14 + 2.*DC*CC*CH - DC*CH**2 + DH*CH**2  00003420
         F(CH,CC) = (2.*DH*1.E-14 + DH*CC*CH + DC*CC*CH)/FD(CH,CC)  00003430
         CHR = 1.0E-7                                             00003440
         W = (CHO-CHR)/XK                                         00003450
         CH = CHO                                                 00003460
         CC = CCO                                                 00003470
         N = XK                                                   00003480
         AH(N+1) = CHO                                            00003490
         AC(N+1) = CCO                                            00003500
         DO 100 K=1,N                                             00003510
         K1 = W*F(CH,CC)                                          00003520
         K2 = W*F(CH-W/2.,CC-K1/2.)                               00003530
         K3 = W*F(CH-W/2.,CC-K2/2.)                               00003540
         K4 = W*F(CH-W,CC-K3)                                     00003550
         CC = CC - (K1 + 2.*K2 + 2.*K3 + K4)/6.                   00003560
         CH = CH-W                                                00003570
         I = N+1-K                                                00003580
         AC(I) = CC                                               00003590
         AH(I) = CH                                               00003600
     100 CONTINUE                                                 00003610
         CCR = CC                                                 00003620
         RETURN                                                   00003630
         END                                                      00003640
C                                                                 00003650
C                                                                 00003660
C        SUBROUTINE SIMP: USES SIMPSONS RULE TO INTEGRATE THE CC  00003670
C        CONCENTRATION INTEGRAL FROM THE REACTION PLANE TO THE BULK PHASE  00003680
         SUBROUTINE SIMP(CCR,CCO,AC,AH,DH,DC,XS,XK,AI,AII)        00003690
         IMPLICIT REAL*8 (A-H,O-Z)                                00003700
         DIMENSION AC(50),AH(50),AII(50)                          00003710
         FD(CH,CC) = 2.*DH*1.E-14 + DH*CC*CH + DC*CC*CH           00003720
         F(CH,CC) = (2.*DC*DH*(CC*CH + 1.E-14))/FD(CH,CC)         00003730
         W = (CCO-CCR)/XS                                         00003740
         NS = XS/2.                                               00003750
         AI = 0.                                                  00003760
         AII(1) = 0.                                              00003770
         DO 100 J=1,NS                                            00003780
         G = J                                                    00003790
         XLC = 2.*(G-1.)*W + CCR                                  00003800
         XRC = 2.*G*W + CCR                                       00003810
         XMC = (XLC + XRC)/2.                                     00003820
         CALL CONC(XLC,XRC,XMC,AC,AH,XK,XLH,XRH,XMH)              00003830
         AI = (W/3.) * (F(XLH,XLC) + 4.*F(XMH,XMC) + F(XRH,XRC)) + AI  00003840
         AII(J+1) = AI                                            00003850
     100 CONTINUE                                                 00003860
         RETURN                                                   00003870
         END                                                      00003880
```

TABLE II (CONTINUED)

```
C                                                                 00003890
C                                                                 00003900
C      SUBROUTINE CONC: CALLED BY SUBROUTINE SIMP TO INTERPOLATE  00003910
C      BETWEEN CONCENTRATION PROFILE POINTS CALCULATED BY         00003920
C      SUBROUTINE KUTTA                                           00003930
       SUBROUTINE CONC(XLC,XRC,XMC,AC,AH,XK,XLH,XMH,XRH)          00003940
       IMPLICIT REAL*8 (A-H,O-Z)            .                     00003950
       DIMENSION AC(50),AH(50)                                    00003960
       NK1 = XK + 1.001                                           00003970
       M = 1                                                      00003980
       WHILE ((XLC.GE.AC(M)).AND.(M.LT.NK1))                      00003990
       M = M+1                                                    00004000
       ENDWHILE                                                   00004010
       N = M-1                                                    00004020
       H = AH(M) - AH(N)                                          00004030
       XLH = AH(N) + ((XLC - AC(N))/(AC(M) - AC(N))) * H          00004040
       WHILE ((XMC.GE.AC(M)).AND.(M.LT.NK1))                      00004050
        M = M+1                                                   00004060
       ENDWHILE                                                   00004070
       N = M-1                                                    00004080
       XMH = AH(N) + ((XMC-AC(N))/(AC(M)-AC(N))) * H              00004090
       WHILE ((XRC.GE.AC(M)).AND.(M.LT.NK1))                      00004100
       M = M+1                                                    00004110
       ENDWHILE                                                   00004120
       N = M-1                                                    00004130
       XRH = AH(N) + ((XRC-AC(N))/(AC(M)-AC(N))) * H              00004140
       RETURN                                                     00004150
       END                                                        00004160
C                                                                 00004170
C                                                                 00004180
C      SUBROUTINE TO CALCULATE RI AND THE INTERFACE CONCENTRATION 00004190
C      USING THE BULK PHASE NEUTRALIZATION MODEL                  00004200
       SUBROUTINE BULK(TKNH,CHO,CNO,YN,DH,DN,RIC,XNI)             00004210
       IMPLICIT REAL*8 (A-H,O-Z)                                  00004220
       A = DH/DN                                                  00004230
       Y = CHO/CNO                                                00004240
       IF (YN.GT.1.0) YN = 1.0                                    00004250
       IF (YN.LT.0.0001) THEN                                     00004260
       YP = ((CHO/CNO + 1./A) * (CHO/CNO + 1.))**0.5              00004270
       DE = 2.*A*DN*(YP - CHO/CNO - 1.) / (1.-A)                  00004280
       XNI = 0.0                                                  00004290
       ELSE                                                       00004300
       S = TKNH*(1. - YN)/YN                                      00004310
       XNI = (((A*Y+1.)*(Y+1.))/((A*S+1.)*(S+1.)))**0.5           00004320
       DE = 2.*A*DN*(S*XNI+XNI-Y-1.)/((1.-A)*(1.-XNI))            00004330
       ENDIF                                                      00004340
       RIC = (DE/DN)**(2./3.)                                     00004350
       RETURN                                                     00004360
       END                                                        00004370
                                                                  00004380
                                                                  00004390
```

APPENDIX E

SYSTEM PARAMETERS FOR MIXED
BED SIMULATIONS

The following input parameters were used to generate the column breakthrough curves shown in Figures 29 and 30. Only the value for the cation resin volume fraction (FCR) was changed to produce the different curves. Unit dimensions and descriptions for the following input parameters are given in Appendix D:

KPBK,KPPR,TIME: 1,0,0

YCO,YNO: -   0.1,0.1

PDC,PDA,VD,FCR: 0.076,0.063,0.445,*

CF,FR,DIA,CHT: 0.002,10.32,2.54,40.0

QC,QA,TKCO,TKHH: 3.0728,2.4334,1.45,1.55

DH,DH,DO,DC: 9.35×10^{-5}, 1.35×10^{-5}, 5.23×10^{-5},

2.03×1^{-5}

XK,XS,TAU,XI: 10,10,0.04,0.01

CP,DEN: 1.0,1.0

TMAX,XNMAX: 300,0.95

*Values of 0.4, 0.5, 0.6, and 0.666 were used.

VITA 𝒜

Carl Eugene Haub

Candidate for the Degree of

Master of Science

Thesis: MODEL DEVELOPMENT FOR LIQUID RESISTANCE-CONTROLLED
          REACTIVE ION EXCHANGE AT LOW SOLUTION CONCENTRA-
          TIONS WITH APPLICATION TO MIXED BED ION EXCHANGE

Major Field: Chemical Engineering

Biographical:

    Personal Data: Born in Ponca City, Oklahoma,
        September 2, 1960, the son of Mr. and Mrs. F. C.
        Haub. Married to R. Rene' Haffner, June 26, 1982.

    Education: Graduated from Ponca City High School,
        Ponca City, Oklahoma, in May, 1978; received
        Bachelor of Science in Chemical Engineering degree
        from Oklahoma State University in May, 1982;
        completed requirements for the Master of Science
        degree at Oklahoma State University in May, 1984.

    Professional Experience: Employed as a summer engineer
        for Conoco, Inc., 1979-82; employed as a research
        assistant with Oklahoma State University, 1980-81;
        employed as a permanent engineer for Conoco, Inc.,
        September, 1983.